

RCA REVIEW

a technical journal

RADIO AND ELECTRONICS
RESEARCH • ENGINEERING

VOLUME X

DECEMBER 1949

NO. 4

RCA REVIEW

GEORGE M. K. BAKER
Manager

CHAR. C. FOSTER, JR.
Business Manager

SUBSCRIPTIONS:

United States, Canada, and Postal Union: One Year \$2.00, Two Years \$3.50, Three Years \$4.50
Other Countries: One Year \$2.40, Two Years \$4.30, Three Years \$5.70

SINGLE COPIES:

United States: \$.75 each. Other Countries: \$.85 each

Copyright, 1949, by Radio Corporation of America, RCA Laboratories Division

Published quarterly in March, June, September, and December by Radio Corporation of America, RCA Laboratories Division, 30 Rockefeller Plaza, New York 20, N. Y.

Editorial and General Offices: RCA Review, Radio Corporation of America,
RCA Laboratories Division, Princeton, New Jersey

Entered as second class matter April 3, 1946, at the Post
Office at New York, New York, under the act of March 3, 1879

RADIO CORPORATION OF AMERICA

DAVID SARNOFF, *Chairman of the Board*

FRANK M. FOLSOM, *President*

LEWIS MACCONNACH, *Secretary*

ERNEST B. GORIN, *Treasurer*

PRINTED IN U.S.A.

RCA REVIEW

a technical journal

RADIO AND ELECTRONICS
RESEARCH • ENGINEERING

Published quarterly by
RADIO CORPORATION OF AMERICA
RCA LABORATORIES DIVISION
in cooperation with

RCA VICTOR DIVISION

RADIOMARINE CORPORATION OF AMERICA

RCA INTERNATIONAL DIVISION

RCA COMMUNICATIONS, INC.

NATIONAL BROADCASTING COMPANY, INC.

RCA INSTITUTES, INC.

VOLUME X

DECEMBER 1949

NUMBER 4

CONTENTS

	PAGE
Counter Circuits Using Transistors	459
E. EBERHARD, R. O. ENDRES AND R. P. MOORE	
Artificial Lines for Video Distribution and Delay	477
A. H. TURNER	
Duo-Cone Loud Speaker	490
H. F. OLSON, J. PRESTON AND D. H. CUNNINGHAM	
Six-Megacycle Compatible High-Definition Color Television System ...	504
Photomultipliers for Scintillation Counting	525
G. A. MORTON	
Direct-Reading Electronic Timer	554
R. R. FREAS	
A New Direct-Reading Loran Indicator for Marine Service	567
F. E. SPAULDING, JR. AND R. L. ROD	
A New Image Orthicon	586
R. B. JANES, R. E. JOHNSON AND R. R. HANDEL	
The Evaluation of Chromium-Iron Alloys for Metal Kinescope Cones ..	593
A. S. ROSE AND J. C. TURNBULL	
The Provisional Frequency Board	600
P. F. SILING	
RCA Technical Papers	608
Authors	610
Index, Volume X (1949)	613

RCA Review is regularly abstracted and indexed by *Industrial Arts Index*, *Science Abstracts* (I.E.E.-Brit.), *Engineering Index*, *Electronic Engineering Master Index*, *Abstracts and References* (Wireless Engineer-Brit. and Proc. I.E.E.) and *Digest-Index Bulletin*.

RCA REVIEW

BOARD OF EDITORS

Chairman

C. B. JOLLIFFE

RCA Laboratories Division

M. C. BATSEL
RCA Victor Division

G. L. BEERS
RCA Victor Division

H. H. BEVERAGE
RCA Laboratories Division

I. F. BYRNES
Radiomarine Corporation of America

D. D. COLE
RCA Victor Division

O. E. DUNLAP, JR.
Radio Corporation of America

E. W. ENGSTROM
RCA Laboratories Division

A. N. GOLDSMITH
Consulting Engineer, RCA

O. B. HANSON
National Broadcasting Company, Inc.

E. A. LAPORT
RCA International Division

C. W. LATIMER
RCA Communications, Inc.

H. B. MARTIN

Radiomarine Corporation of America

H. F. OLSON
RCA Laboratories Division

D. F. SCHMIT
RCA Victor Division

S. W. SEELEY
RCA Laboratories Division

G. R. SHAW
RCA Victor Division

R. E. SHELBY
National Broadcasting Company, Inc.

S. M. THOMAS
RCA Communications, Inc.

G. L. VAN DEUSEN
RCA Institutes, Inc.

A. F. VAN DYCK
RCA Laboratories Division

I. WOLFF
RCA Laboratories Division

V. K. ZWORYKIN
RCA Laboratories Division

Secretary

GEORGE M. K. BAKER

RCA Laboratories Division

REPUBLICATION AND TRANSLATION

Original papers published herein may be referenced or abstracted without further authorization provided proper notation concerning authors and source is included. All rights of republication, including translation into foreign languages, are reserved by RCA Review. Requests for republication and translation privileges should be addressed to *The Manager*.

COUNTER CIRCUITS USING TRANSISTORS*

By

E. EBERHARD, R. O. ENDRES AND R. P. MOORE

Engineering Products Department, RCA Victor Division,
Camden, N. J.

Summary—Several transistor multivibrator circuits are described that are capable of performing all the functions required by a decade counter composed of bistable stages, or by a frequency divider. Their basic design features are given and their limitations are pointed out. An analysis of a bistable circuit using a single transistor is given to show how its operation may be correlated with the commonly known transistor constants. Finally, a brief description of two counters built for demonstration purposes, with appropriate wave forms, is presented. It may be concluded that as soon as transistors with stable and more nearly uniform characteristics become available they will be widely used in counter circuits.

INTRODUCTION

SINCE the public announcement of the transistor in July of 1948, there has been much speculation as to the fields of usefulness which this device is almost certain to have. Potentially the application of transistors to electronic circuits can result in considerable saving both in size of equipment and power consumption. However, the transistors available through the summer of 1949 have several serious limitations which prevent, for the present, their wide application. Their power output is low, their internal noise level is high, and it is difficult to build transistor amplifiers for frequencies much higher than five megacycles. These limitations seriously restrict the usefulness of transistors as amplifiers; however, they do not present as serious a limitation to the use of transistors in pulse-counting types of circuits.

In counter circuits the power level can be kept within the capabilities of the transistor; and, while the frequency limitation does apply, it appears that such a counter should be operable to frequencies of the order of one megacycle. Thus, it would seem that counter circuits present a field for the application of transistors having the noise level and power limitations of present units. In order to explore the possibilities of using transistors in counter circuits a development program has been carried out.

* Decimal Classification: R282.12.

This paper describes the circuits that were developed and discusses their operational limitations. It is divided into three sections; one on "bistable" circuits (circuits having two stable states), one on relaxation oscillator circuits, and one describing briefly two experimental counters that were built as demonstration models.

BISTABLE TRANSISTOR CIRCUITS

Bistable Multivibrator Using Two Transistors

The first transistor multivibrators to be described are analogous to the basic Eccles-Jordan type of circuit using vacuum tubes. In fact, if the assumption is made that the base of the transistor corresponds to the grid of the tube and that the emitter of the transistor corresponds to the cathode of the tube, the circuit is seen to be quite similar to the Eccles-Jordan multivibrator (See Figure 1). In operation, if transistor #1 is conducting heavily its collector potential will be near

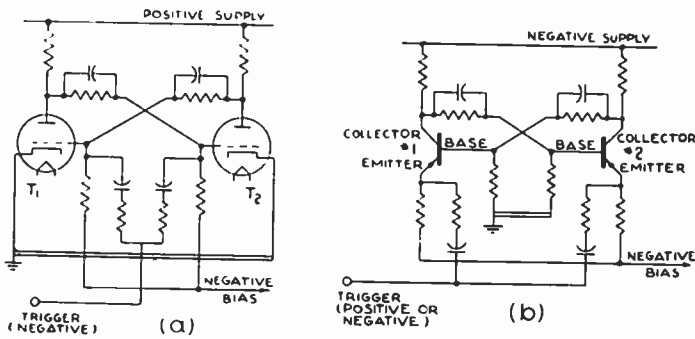


Fig. 1—Comparison of transistor bistable multivibrator (b) with Eccles-Jordan circuit (a).

ground, thus holding #2 in a state of low conduction by making its base potential positive with respect to its emitter. The application of a trigger pulse to both emitters will cause the circuit to revert to its other stable state with transistor #1 in low conduction and transistor #2 in high conduction. This operation will be clear from an analysis of the feedback loops.

However, the analogy with the Eccles-Jordan circuit is not nearly as close as might be expected from a superficial examination. There are two fundamental characteristics of transistors which make the circuit of Figure 1b differ from the vacuum tube circuit of Figure 1a. One of these differences arises from the odd shape of the transistor gain function. Figure 2 shows how the current gain changes with emitter current. A family of curves has been plotted to show also the variation of current gain with changes in collector current. (I_{c3} is the largest collector current and I_{c1} , the smallest.) In a quiescent condition one transistor of the multivibrator will be in high conduc-

tion, operating on the right-hand portion of the curves in Figure 2. The other transistor will be in low conduction and operating on the left-hand portion of the curves near zero emitter current. (This assumes that the current gain curves of units 1 and 2 are similar to those of Figure 2.)

Since the high gain region lies to the left of the operating point of one transistor and to the right of the operating point of the other, the circuit can be triggered into operation with either positive or negative trigger pulses on the emitters. This action may be explained as follows. In order to trigger with positive pulses it is necessary for these pulses to have a greater effect on the transistor that is in low conduction than they have on the unit that is in high conduction. Conversely, to trigger with negative pulses the greater effect must be on the unit that is in high conduction. An examination of Figure 2 shows that this will be the case if both transistors have characteristics similar to those shown. The curves also indicate that negative input pulses are preferable since the current gain curves decrease much more rapidly on the negative side. In the experimental circuits this was found to be true.

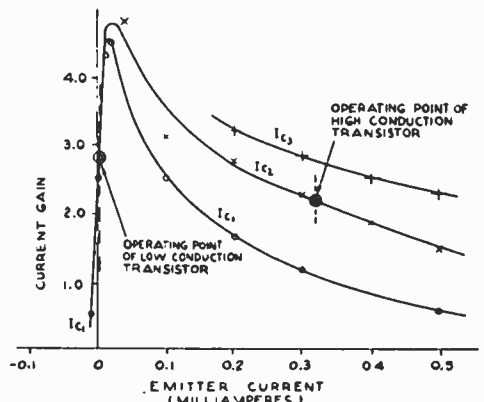


Fig. 2 — Transistor current gain as a function of emitter current. Curves for three values of collector current are shown.

Another difference between the transistor and the Eccles-Jordan multivibrator is that the resistor between base and ground, analogous to the grid resistor in the vacuum tube circuit, produces regeneration in each transistor. (As will be discussed later, each transistor may in fact have two stable states without reference to the other.) This regeneration may assist in the operation of the circuit but it often produces undesirable oscillations involving only one of the units. For this reason, the base return resistances must usually be kept less than 10,000 ohms. Hence, while the circuits seem to be identical, their operation involves somewhat different principles.

Practical values of constants for this circuit using a supply voltage of 45 volts are:

Collector Resistance	5,000-25,000 ohms
Base Resistance	3,000-10,000 ohms
Feedback Resistance	15,000-50,000 ohms
Emitter Resistance	500- 1,500 ohms

Capacitors may be used in parallel with the feedback resistors to increase the feedback at high frequencies.

Figure 3 is a variation of the circuit in Figure 1b which departs even more from the Eccles-Jordan multivibrator. Here, coupling C_2 has been added between the emitters of the two units and triggering may be accomplished by the application of positive or negative pulses to the base of the first transistor only. Briefly the action is as follows: With #1 in high conduction and #2 in low conduction, a positive trigger pulse at the input decreases the current in #1. The resulting regenerative action through the coupling resistor and the second transistor causes #1 to go into low conduction and #2 to go into high conduction. On the following input pulse the change back to the original condition is accomplished by a combination of a positive pulse coupled to the collector of #2 and a negative pulse on the emitter of #2 derived by differentiation of the trigger pulse in C_2 . Since differentiation is required, this part of the cycle must start at the trailing edge of the input trigger. Operation may consequently depend to some extent on the shape of the trigger pulses.

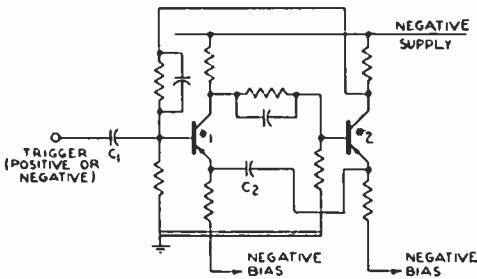


Fig. 3 — Variation of the basic transistor bistable multivibrator.

From a practical standpoint, however, this limitation is not severe and in several applications the modified circuit of Figure 3 has been found somewhat more stable than the circuit of Figure 1. Typical values using a supply voltage of 45 volts for this circuit are:

Collector Resistance	5,000-25,000 ohms
Feedback Resistance	10,000-50,000 ohms
Base Resistance	2,000-10,000 ohms
Emitter Resistance	500- 5,000 ohms

General Design Considerations

The multivibrator circuits that have been discussed above depend to a large extent on the direct-current characteristics of the transistors. Since these characteristics vary considerably between transistors, the circuits may often be asymmetrical for best operation. Both the circuits described are quite critical with respect to the values of the base resistors and emitter biases. However, once the proper constants are obtained and the circuit is operated from a single power supply, stability with respect to the supply voltage and the trigger amplitude is comparatively good. Variations of ± 10 to 20 per cent in supply

voltage, and of several hundred per cent in trigger amplitude are usually permissible. Good operation can usually be obtained with trigger voltages as low as $\frac{1}{2}$ volt.

The speed of transition from one state to the other varies considerably with different transistors. For units having good high-frequency response, the transition period (one direction only) may be between $\frac{1}{4}$ and $\frac{1}{10}$ microsecond while other transistors may give transition times as large as 2 microseconds. The circuit of Figure 1b was operated as a bistable counter up to about one megacycle. The operation at 500 kilocycles appeared to be quite satisfactory although the wave shape at one megacycle was hardly good enough to be differentiated into usable output pulses. However, by choosing transistors carefully it appears quite possible to build a circuit of this type to operate at frequencies up to one megacycle.

The transistor circuits shown in Figure 1 and Figure 3 were designed to operate at 45 volts. The current required is usually five to seven milliamperes resulting in a power drain of close to 250 milliwatts per stage. However, it is believed that this figure can be cut by a factor of two to four if lower supply voltages are used.

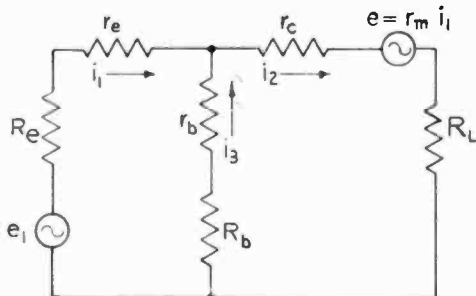


Fig. 4—Schematic showing transistor equivalent T network with resistors in base and collector and a voltage generator in the emitter circuit.

Bistable Multivibrator Using One Transistor

As mentioned above, it is possible to devise a bistable multivibrator using only one transistor. This circuit is of particular interest in that it differs considerably from those possible with vacuum tubes. In order to show clearly how this multivibrator can have two stable states the equivalent circuit approach, combined with measured curves of the transistor constants, will be used. It should be pointed out that although this analysis makes use of "small signal" or alternating-current transistor constants it is valid since these constants are measured over the entire range being explored and are only applied point by point to predict stability.

Figure 4 is a schematic using the T network, alternating-current equivalent circuit and showing a transistor with constants r_e , r_b , r_c and r_m connected to a load resistance R_L , a base resistance R_b and an emitter resistance R_e . A source of driving voltage e_1 is shown in the emitter circuit. The application of Kirchhoff's laws to this network

yields three independent equations whose solution gives the three currents. The output current i_2 can be shown to be:

$$i_2 = e_1 \frac{r_m + r_b + R_b}{(r_e + R_e)(r_c + R_L + r_b + R_b) + (r_b + R_b)(r_c + R_L - r_m)}. \quad (1)$$

Substituting r_b' for $r_b + R_b$ and r_e' for $r_e + R_e$

$$i_2 = e_1 \frac{r_m + r_b'}{r_e'(r_c + R_L + r_b') + r_b'(r_c + R_L - r_m)}. \quad (2)$$

A point of instability obviously occurs when $i_2 \rightarrow \infty$ (with e_1 finite) or when

$$r_e'(r_c + R_L + r_b') + r_b'(r_c + R_L - r_m) = 0, \quad (3)$$

from which

$$r_m = \frac{(r_e' + r_b')(r_c + R_L)}{r_b'} + r_e'. \quad (4)$$

This point is reached when the second term of Equation (3) becomes negative and equal to the first term. For this to occur, r_m must be greater than $r_c + R_L$ and either r_b' or the difference between r_m and $r_c + R_L$ must be large. Note that both r_e' and R_L are positive terms and hence tend to preserve stability.

In the multivibrator circuit to be described, all circuit elements may be pure resistances, and a circuit identical with that of Figure 4 is obtained except that $e_1 = 0$. If R_b is made large enough and R_L and R_e small enough the conditions of Equation (3) can be satisfied in most cases so that the circuit becomes unstable. Both emitter and collector currents now tend to increase rapidly and would reach very high values if there were no limiting action. However, several factors limit this increase. The positive resistances in both emitter and collector and the normal variation of r_m are all limiting factors. Referring to Figure 5, r_m (the solid curve) is shown to start low at negative values of emitter current, build up rapidly to a peak, (which occurs here at an emitter current of approximately 25 microamperes) and then decrease again as emitter current is increased still more. Curves for higher values of collector current would lie above the curve shown but will have approximately the same shape (see the current gain curves of Figure 2). Even at high collector currents the value of r_m falls quite low for high emitter currents. Consequently, the regenerative

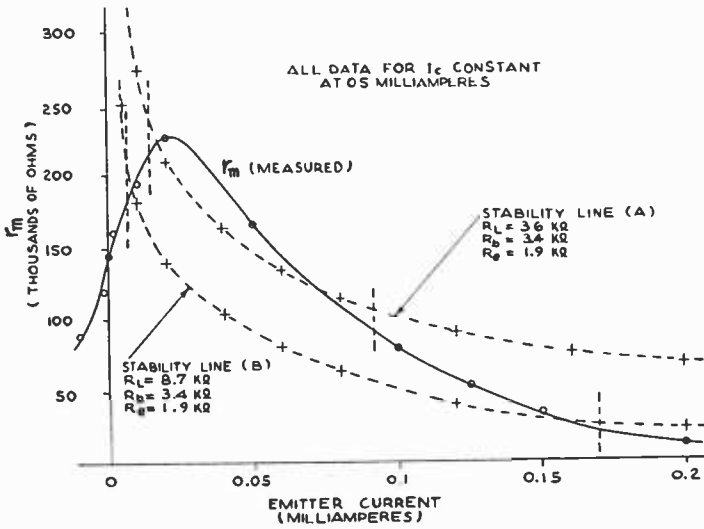


Fig. 5—Curve showing r_m as a function of I_e and indicating stability limits for two values of R_L .

process proceeds until the transistor is operating on the right-hand portion of its curve at higher emitter and collector currents.

The curves of Figure 5 and Figure 6 have been plotted to show how the several factors combine to permit two stable states of operation. In Figure 5 the heavy curve is a plot of measured values of r_m for a certain transistor operated as indicated. Figure 6 shows the measured values of r_c and r_e for the same transistor over the same operating range. These values were obtained with very small alternating currents. The dotted curves of Figure 5 were plotted from the solution of Equation (4), hence they represent the values of r_m at the edge of stability. All r_m values higher than these indicate unstable conditions and lower values represent stable conditions. The point at which the actual r_m curve crosses the dotted curves determines where the transition from one stable state to the other would be expected to start. Note that the dotted curves at low values of emitter current are controlled largely by the rapidly changing values of r_e , while at the right on the plot r_c is essentially the only remaining variable.

Experimental checks have been made of the transition points with the circuit constants of lines A and B. These points are indicated in Figure 5 by the short, vertical, dotted lines. Note that in every case the points occurred on the stable side of the

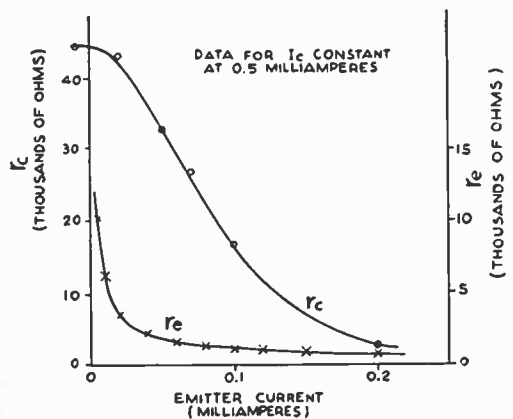


Fig. 6—Plot of r_e and r_c as functions of I_e for the transistor of Figure 5.

predicted transition value. This discrepancy is very probably due to inherent transistor noise which causes the circuit to "trigger" over into the unstable region slightly before the conditions of Equation (3) are satisfied. As would be expected, the agreement between the actual transition point and the predicted transition point is better on the low current side since the two curves intersect at a much steeper angle.

Thus, it has been shown that the existence of the two stable states and the transition from one to the other may be predicted with reasonable accuracy by the application of equivalent circuit theory and experimental measurements of the transistor constants. Although an analysis of a given bistable circuit by this method requires rather complete knowledge of the transistor characteristics it should nevertheless furnish valuable correlation between the commonly known transistor constants and this type of circuit operation.

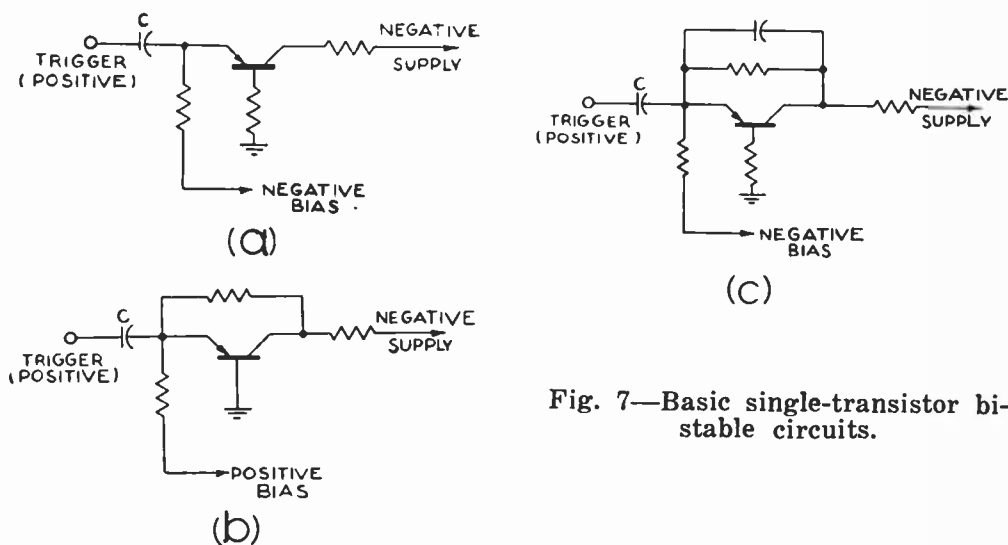


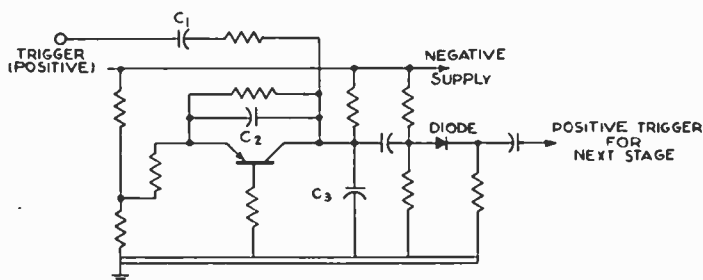
Fig. 7—Basic single-transistor bistable circuits.

Not all transistors have the high peak of r_m at low emitter currents as shown in Figure 5. As a result, not all transistors exhibit bistable operation in the circuits to be described. As indicated by Equation (4) the condition of instability is satisfied with a minimum value of r_m when R_L and R_e are both zero. Even under these conditions, transistors having r_m curves without the peak of Figure 5 do not exhibit two stable states.

Figure 7a shows the basic circuit suggested by the mathematical analysis. Figure 7b shows another circuit which is capable of two stable states by virtue of the positive feedback directly from collector to emitter. Those familiar with the transistor field will recognize that the addition of this feedback path is very similar to increasing the r_b of the transistor equivalent circuit, therefore, the circuit of Figure 7b

may be analyzed in much the same manner as that of Figure 7a. The former has a disadvantage in that a high impedance collector is coupled back to a low impedance emitter. It has been found that a circuit combining both of these principles is somewhat more stable than either circuit by itself. Such a circuit is shown in Figure 7c. Here a capacitor has been included across the feedback resistor from collector to emitter. This increases the high frequency coupling between emitter and collector and tends to decrease the transition time from one state to the other. In all of these circuits, triggering has been shown on the emitter by means of positive input pulses. It is obvious that this will produce the transition from low conduction to high conduction. However, the change from high conduction to low conduction may only be accomplished by a negative pulse. This is obtained by allowing the input pulse to develop a negative overshoot by differentiation. Hence, in the circuit shown, differentiation must occur in condenser C for the circuit to trigger from high conduction to low conduction. This might seem

Fig. 8—One stage of a pulse counter.



to introduce dependence on input pulse width and shape, however, as in the two-transistor circuits, impedance changes at the emitter tend to aid the desired effect (See the emitter impedance curve of Figure 6) and from a practical viewpoint the circuit has good stability.

Figure 8 shows one complete stage of a decade counter. This is the circuit found most satisfactory as a single-transistor counter stage. The circuit of Figure 7c has been modified slightly by the introduction of the trigger pulses to the collector, the addition of a capacitor from collector to ground, and the addition of a crystal diode which passes a single positive pulse to the next stage. In this case, triggering from high to low conduction is obtained by differentiation of the pulse which appears on the emitter, and integration of the pulse which appears on the collector. The combination of these two effects gives good triggering from high to low conduction and the circuit does not seem to be unduly sensitive to either trigger amplitude or shape.

Operationally, the single-transistor counter stage exhibits somewhat the same characteristics as the two-unit circuit. Constants are quite critical for a given transistor but when the complete circuit is

in operation from a single voltage source good stability with respect to trigger amplitude and supply voltage is again obtained. Typical circuit constants for operation with a 45-volt supply are:

Collector Resistance	10,000-30,000 ohms
Base Resistance	3,000-10,000 ohms
Feedback Resistance	15,000-50,000 ohms
Emitter Resistance	500- 5,000 ohms
C_2	100- 500 micromicrofarads
C_3	100- 800 micromicrofarads

The transition time from low conduction to high conduction is quite rapid. For transistors with good high frequency response it may be 1/10 microsecond. From high conduction to low the transition time is apt to be longer and will of necessity start at the trailing edge of the trigger pulse. This tends to limit the upper frequency of operation. A single stage as shown in Figure 8 (except that the diode circuit has been omitted) was operated successfully up to 250 kilocycles. It appears probable that with a carefully selected transistor such a circuit could be operated at frequencies up to 500 kilocycles.

When operated from a 45-volt source this circuit takes a current of about two milliamperes for a power drain of 90 milliwatts. Here again, a considerable power saving might be effected by reducing the supply voltage. A circuit similar to Figure 7c has been operated as a single-stage counter with a three-volt supply.

OTHER COUNTER CIRCUITS

For many counter applications circuits other than the bistable types, just described, are required. These circuits fall into two general classes, astable and monostable (astable referring to the free-running type, and monostable referring to the type that must be triggered once for each cycle of operation). In general, the circuits to be discussed may be either of these types, depending upon the bias voltages applied. While multivibrators of these types using two transistors have been built, they seem to have no advantage over circuits that use one transistor; consequently only the latter will be discussed here.

These circuits also have the requirements for oscillation stated mathematically in Equation (3). However, in this case, the transition from one stable state of conduction to another is accomplished by incorporating a time constant (either RC or RL) into the circuit. These circuit constants compel the unit to pass into the unstable region (indicated in Figure 5) at regular intervals. When operated in a monostable condition the circuit is so biased as to have one continu-

ously stable state. Triggering pulses must then be provided to drive the unit into the unstable region.

Three basic astable or monostable oscillator circuits are shown in Figure 9. The circuits of Figures 9a and 9b differ from the bistable multivibrator of Figure 7a only by the addition of shunt capacitance in the collector or the emitter. The circuit of Figure 9a functions in much the same manner as a single gas-tube oscillator.¹ When in an astable condition, condenser C alternately charges and discharges. It charges when the transistor is in its low conduction state and discharges when the transistor is in its high conduction state. This action produces a sawtooth collector voltage wave and approximately rectangular pulses at the base and the emitter. Synchronization may be achieved by the introduction of an external pulse somewhat before the

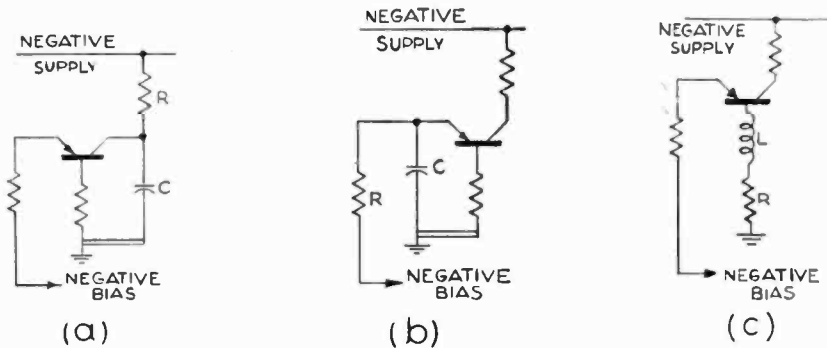


Fig. 9—Three basic relaxation oscillator circuits.

time the circuit would normally reach the transition point. For this purpose, positive pulses may be applied to the emitter, or negative pulses may be applied to the base.

In the circuit of Figure 9b, the time constant is employed in the emitter circuit. However, its operation is similar to that of the circuit of Figure 9a, except that in this case the capacitance charges to its greatest negative voltage while the transistor is in a state of high conduction.

A somewhat different type of operation is characterized by the circuit of Figure 9c. Here an inductance replaces the resistance in the base, and frequency is determined by the time constant afforded by L and the resistance of the transistor and its associated components. Operation is brought about by the voltage variation on the base caused by the change in the rate of current flow through the inductance as the unit passes through the unstable region.

¹ W. M. Webster, E. Eberhard and L. E. Barton, "Some Novel Circuits for the Three-Terminal Semiconductor Amplifier", *RCA Review*, Vol. X, No. 1, p. 5, March, 1949.

These circuits have an unusual feature in that they may be designed to be quiescent either in high or low conduction. This follows from the peaked r_m and current gain curves shown in Figures 2 and 5. The low current condition is generally preferred in practice, due to its greater inherent stability and for reasons of power economy. For triggering at a given point in the circuit, the two modes of operation offer a degree of freedom in selecting trigger pulse polarity. Generally speaking, this is not a great advantage because the oscillator may be triggered by a pulse of either polarity depending upon the point of application. In a like manner, a pulse of either polarity may be obtained from each operating condition depending upon where the output is taken. In general, output pulses of from one microsecond to several thousand microseconds in width are available from these circuits. Astable operation can readily be obtained up to frequencies of at least three megacycles.

FREQUENCY DIVIDER CIRCUITS

The relaxation oscillator circuits described above have, with some modifications, been found to be suited to frequency division of pulses. This requires that they be operated in an astable condition and synchronized with incoming pulses. Without further modifications, each of the circuits of Figure 9 may be useful for dividing by two, three, or four with some degree of stability, but for a division rate of more than four some means must be found to stabilize operation.

To this end several stabilized divider circuits have been devised. The simplest scheme is shown in Figure 10. Greater stability has been achieved here by the use of two RC networks. The circuit may be triggered by positive pulses on the emitter as shown, or by negative pulses on the base. Triggering may also be accomplished by the application of negative pulses to the collector, but this scheme is not as desirable as the other methods, since a pulse of greater amplitude is

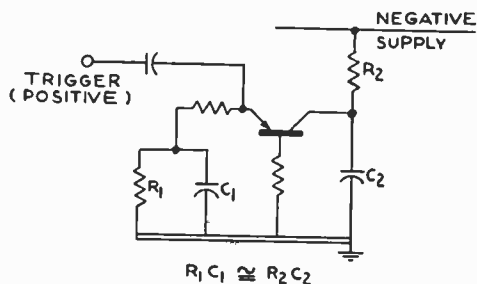


Fig. 10 — Frequency divider stage using two RC circuits.

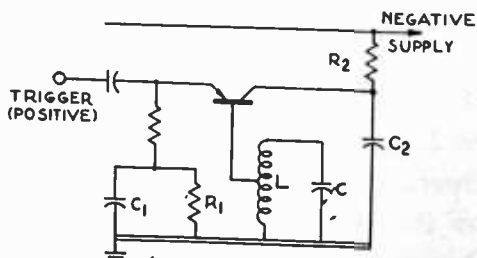


Fig. 11 — Frequency divider stage using two RC circuits and a resonant base circuit.

required. Even better stabilization may be obtained by adding an inductance as suggested by Figure 9c.

Figure 11 indicates a divider circuit exhibiting very stable properties. RC networks are employed as shown in Figure 10 and the base impedance is replaced by a parallel resonant circuit. Greatest stability is obtained if the time constant of the emitter circuit (R_1C_1) is made approximately equal to the time constant of the collector circuit (R_2C_2) and the resonant frequency of the tuned circuit is made equal to, or some multiple of, the desired output pulse repetition rate. When the circuit is triggered an oscillation is set up in the base resonant circuit, observable in Figure 17c. When this circuit is adjusted so that triggering occurs on a negative going portion of this sine wave, a considerable degree of stabilization may be obtained. This particular circuit is especially useful, since it is capable of dividing by ten with good stability and up to 40 with decreasing reliability.

The divider circuits discussed here exhibit exceptional power economy each requiring from 0.5 to 1.5 milliamperes or a power drain of 25 to 60 milliwatts. This includes power dissipated in load resistors. Positive triggering action can usually be obtained with half-volt pulses applied to either emitter or base. These circuits have one disadvantage in that the high transistor noise tends to introduce a variation in the time delay of the output pulse. This variation accumulates and may amount to a few tenths of a microsecond after the pulse has been passed through several divider stages.

DEMONSTRATION CIRCUITS

Two experimental counters employing the circuits suggested above have been built to indicate possible fields to which the transistor may be applied. One of these is a decade counter and the other a frequency divider. The first to be discussed will be the decade counter.

A photograph of the counter is shown in Figure 12. It consists of a series of four bistable and two monostable multivibrators. They are arranged as indicated in the block diagram of Figure 13. Voltage wave forms which are present at various points in the circuit are shown in Figure 14.

The input to the first stage of the counter may be either positive or negative pulses. Successive stages are triggered by positive pulses obtained by differentiating the collector square wave. Crystal diodes are used between stages to eliminate undesired parts of this differentiated wave. The first two stages are double transistor units of the type shown in Figure 3 while the last two are single transistor units of the type shown in Figure 8.

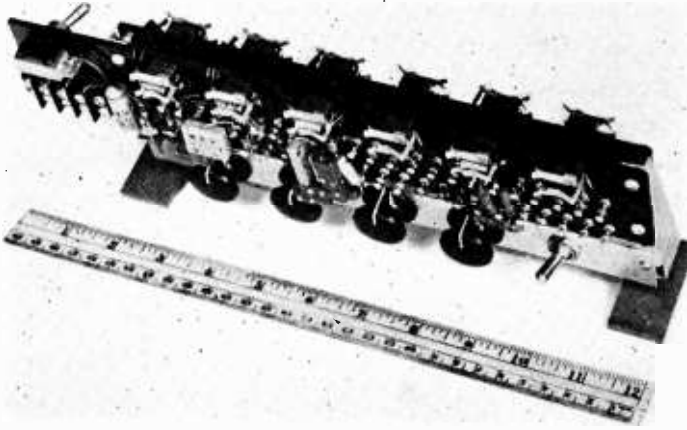


Fig. 12—An experimental decade counter using only transistors and crystal diodes. (Four unused sockets are shown.)

A cascade of four bistable multivibrators will give one output pulse for every 16 input pulses. As is common practice in this art, in order to change this count to one in ten, two feedback circuits are added as indicated in the block diagram. Switches are provided to switch the feedback in and out. Monostable oscillators, as indicated in Figure 9a, are included in these feedback circuits in order to isolate the stages from each other and to obtain a pulse of sufficient amplitude to retrigger a preceding stage. Both of these monostable circuits are triggered with negative pulses obtained by differentiation of the bistable collector wave shape. Those acquainted with this method of feedback in decade counters will recall that there is a possibility of returning a pulse through the first feedback circuit at the moment that the second feedback circuit is stepping the counter back. To avoid this difficulty, a blanking pulse is coupled from the second monostable oscillator to the first in such a manner as to stop the first from triggering at the undesired moment.

Because of changes in the direct-current characteristics of the transistor with both time and temperature, it was found desirable to incorporate several variable elements into the counter. These controls, which may be observed along the base of the stand in Figure 12, are used to vary the bias on individual units. Generally speaking, some of

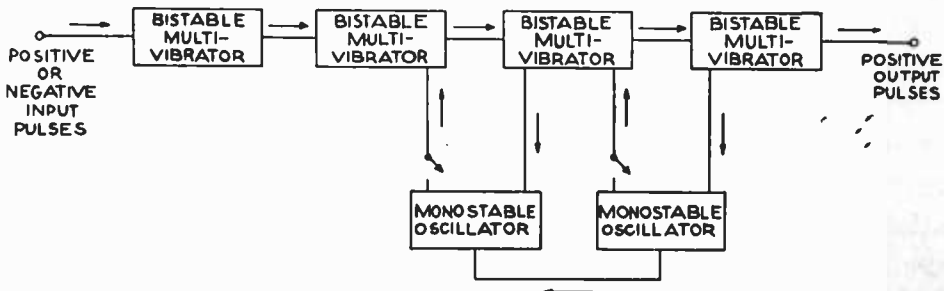
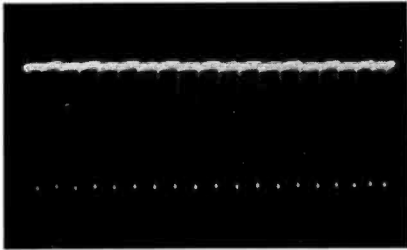


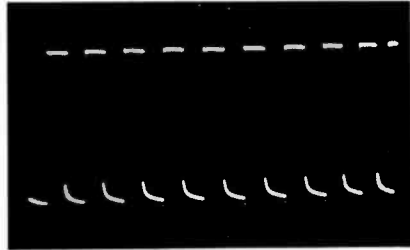
Fig. 13—Block diagram of experimental decade counter.

the controls may have to be adjusted each time the counter is started. Once started, several further adjustments may be necessary until the transistors reach a stable condition. Once this point is reached, little further adjustment is needed except when there is a large change in the ambient temperature.

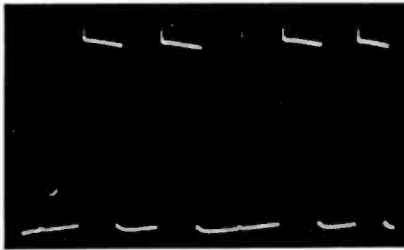
The counter of Figure 13 would operate only in the frequency range of 500 cycles to about 10 kilocycles. However, these limits were set



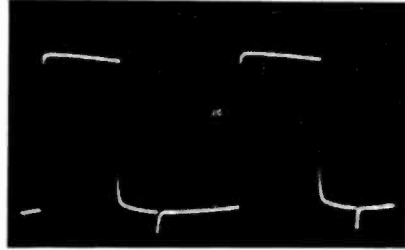
(a) Input pulses to counter (one kilocycle).



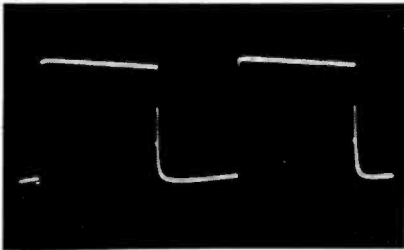
(b) Voltage wave on the collector of the second transistor of the first stage.



(c) Voltage wave on the collector of the second transistor of the second stage. Note the sharp pulse when this unit is stepped back.



(d) Voltage wave on the collector of the third stage. Note the sharp pulse when this unit is stepped back.



(e) Voltage wave on the collector of the fourth unit.

Fig. 14—Wave forms taken at several points in the experimental decade counter.

by circuit constants rather than by limitations of the transistors. The entire circuit operates from a 45-volt supply and requires about 850 milliwatts of power. This by no means represents the minimum power consumption possible. Operation at a lower supply voltage and the use of only single unit multivibrators would both tend to reduce the power drain.

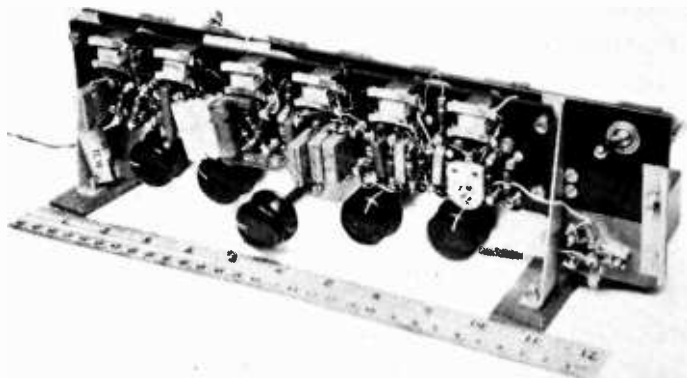


Fig. 15—An experimental frequency divider using only transistors. (The base of the 100-kilo-cycle crystal may be observed mounted at the lower right.)

The second experimental counter constructed is the frequency divider pictured in Figure 15. The block diagram of Figure 16 indicates the arrangement of the nine transistors used in this circuit. The photographs of voltage wave forms present at various points in the circuit are shown in Figure 17.

The first stage of this circuit is a crystal-controlled oscillator operating at 100 kilocycles. The sine wave output is employed to drive a pulse generator whose circuit is similar to that of Figure 9c. This stage produces positive pulses at the frequency of the oscillator. As indicated in Figure 17b the output from this stage consists of sharp pulses having a rise time of less than $\frac{1}{4}$ microsecond. The frequency of these pulses is next reduced by a factor of ten in a divider circuit as shown in Figure 11.

The following two stages are similar to the circuit of Figure 10 and each divides the frequency by five. At this point, the variation in delay, introduced by the noise of the preceding stages, has become appreciable. Accordingly, in order to preserve the inherent stability of the crystal oscillator, the principle of selecting one of the original sharp pulses with a gate pulse is employed. This is accomplished in two stages, the first of which is a monostable oscillator, and the second

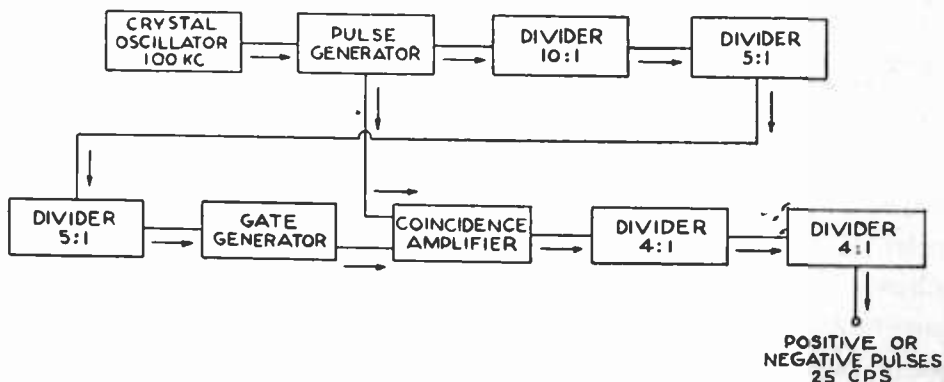
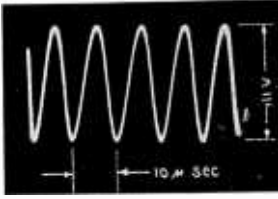
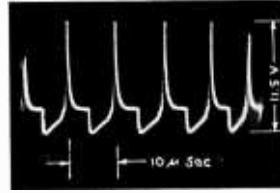


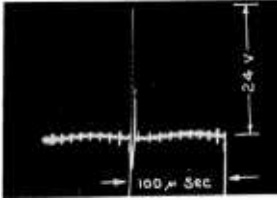
Fig. 16—Block diagram of experimental frequency divider.



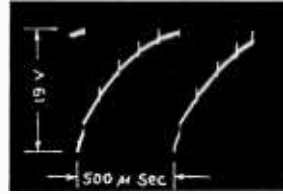
(a) Sine wave on the emitter of the crystal oscillator.



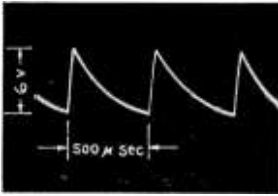
(b) Output pulses of the pulse generator after differentiation.



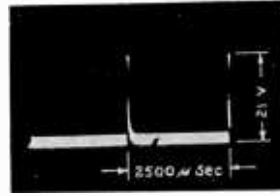
(c) Voltage wave on the base of the first divider. Note the sine wave of the base resonant circuit.



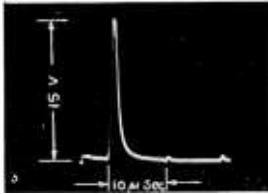
(d) Voltage wave on the emitter of the second divider.



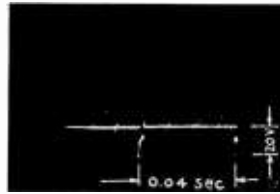
(e) Voltage wave on the collector of the second divider.



(f) Gating pulse at the collector of the gate generator.



(g) Output pulse at the collector of the coincidence amplifier. Note residual pulses not in coincidence with gating pulse.



(h) Voltage wave at the base of the last divider. A strong positive pulse, too rapid to show here, is present at the trailing edge of the negative pulse.

Fig. 17—Wave forms taken at several points in the experimental frequency divider.

a coincidence amplifier. The gate pulse (about 12 microseconds wide) and pulses from the pulse generator are mixed at the emitter of the coincidence amplifier. Note the resemblance between the voltage wave forms in Figures 17b and g. The frequency of the gated pulse is 400 cycles per second. The following two units each divide this frequency by four, giving output pulses at 25 per second.

For the same reason as in the decade counter, it was found desirable to include several variable elements. In Figure 15, these controls may be observed along the lower portion of the chassis. Usually some minor adjustment has to be made to one or more of these controls each time the divider is started. In general, once operating, no further adjustment is necessary. It appears that these circuits are not as critical to temperature changes as the bistable circuits of the first experimental counter.

The entire circuit, operating from a 45-volt source, draws about 675 milliwatts. of power. As before, it is reasonable to suppose that the divider could be designed to operate at a much lower power consumption.

CONCLUSIONS

This investigation shows that transistors can be used in several basic types of relaxation oscillators. In fact, some of their unique characteristics make possible the design of circuits having greater flexibility than an analogous vacuum-tube circuit. These characteristics allow the circuits to be stable in either high or low conduction and to be triggered by either positive or negative pulses at the same input point. The experiments demonstrated that the power capabilities are adequate for operating one stage into the next and that the average frequency response is good enough to allow counter operation to at least one megacycle. The high internal noise of the transistor may produce a variation in the circuit delay but this is not an unsurmountable problem. However, present transistors have two faults that prohibit their application to practical counters. One of these is their instability with respect to time and temperature and the other is the very wide variation in characteristics between different units. When these difficulties are overcome, the transistor should find widespread application in this field.

ARTIFICIAL LINES FOR VIDEO DISTRIBUTION AND DELAY*

BY

A. H. TURNER

Engineering Products Department, RCA Victor Division,
Camden, N. J.

Summary—The multisection artificial lines discussed in this paper have essentially lumped constants. Each section provides a low impedance feed point of full line voltage and a delay depending upon its position relative to the input end of the line. The branch lines from these feed points must behave as lumped capacitors and therefore must be unterminated and short compared to the signal wavelength.

Artificial lines composed of "T" sections, bridged-"T" sections, and especially combinations of these are capable of quite faithful distribution and delay of video signals. One combination of these is recommended because it has extremely small delay distortion to 0.85 of its cut-off frequency.

The quality of picture signals transmitted through several experimental lines of twenty sections each confirmed this theory.

The specifications of several other investigators of this subject are given but have not been tested by this writer.

The paper begins with a short history and ends with a bibliography of important closely related works.

HISTORY

WHILE working on telephone problems, G. W. Pierce^{4, †} discovered that inductive coupling of negative polarity provided useful correction of delay distortion in *T* networks. G. A. Campbell⁵ suggested the use of the lattice for delay correction and better impedance match. Very little use was made of these suggestions until about 1925 when improved lines were needed for picture and radio program transmission. The lattice⁸ became popular at this time for delay correction but not until a little later did the *B-T* (bridged-*T*) get much attention. It may have been used first on a radio program circuit between New York and Washington.

DISTORTION IN ARTIFICIAL LINES

The quality most needed in artificial lines is constant transmission time or delay of all significant components of the picture signal. This means that these components of different frequencies must arrive at

* Decimal Classification: R583.14.

† Reference numbers refer to bibliography on pages 488-489.

the far end or at any tapping points at exactly the same instant to retain accurately the form of the transmitted signal. The other two causes of waveform change, (1) amplitude and (2) "phase-intercept" distortion, are not apt to degrade the picture quality as much as delay distortion.

Constant delay of all significant frequencies in the picture means that the phase rotation through the network is exactly proportional to frequency, inasmuch as the slope of this phase-angle versus frequency curve is the transmission time delay. It can be stated here that the "phase-intercept" distortion is zero when this phase-angle curve intercepts the zero-frequency ordinate at angles of zero or any whole number of π radians. Amplitude distortion is present in small amounts in all of the filter sections to be described. The transmission losses can be minimized by winding the coils with large sizes of wire, but this does not decrease the amplitude distortion.

The problem of delay distortion is capable of at least ten partial solutions as indicated in the concluding bibliography and summary. The single characteristic common to all ten of the artificial line prescriptions is that the delay correction in the low frequency region is obtained by various coefficients of mutual inductive coupling, k , between adjacent half-sections of T 's or whole sections of π 's. And, in general, it requires twice the percentage k between half sections as between whole sections for the same delay correction.

The use of inductive coupling between filter sections requires modification of the component values to maintain the same characteristic impedance and cut-off frequency as belong to their "constant- k " (constant impedance) prototypes without coupling. The modification is handled by a factor m from which the term " m -derived" is taken.

ANALYSES OF T AND $B-T$

The constants of the important m -derived low-pass T will be given first in Figure 1.

In this ladder the design cut-off or resonant frequency, in cycles, is

$$f_c = \frac{1}{\pi\sqrt{LC}},$$

the design series inductance, in henrys, of one whole line section is

$$L = \frac{R_o}{\pi f_c},$$

the design shunt capacitance, in farads, of one whole line section is

$$C = \frac{1}{\pi f_c R_o}$$

the design characteristic or surge impedance, in ohms, is

$$R_o = \sqrt{L/C}$$

and the mutual inductance, in henrys, of two half-sections is

$$M = \left(\frac{1 - m^2}{4m} \right) L.$$

m is the factor used in the design of m -derived filters.

M has a negative sign when the coils are wound continuously in the same direction ($m > 1$) and has a positive sign when the coils are wound oppositely or when a physical coupling inductance is inserted in the center leg ($m < 1$). In Figure 1

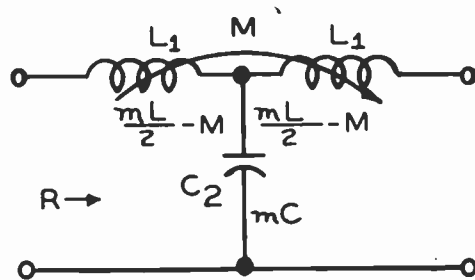


Fig. 1—Constants of the T .

$$L_1 = \frac{mL}{2} - M = \frac{2Lm^2 - Lm^2 + L}{4m} = \left(\frac{m^2 + 1}{4m} \right) L.$$

Coefficient of coupling is

$$k = \frac{M}{L_1} = \frac{m^2 - 1}{m^2 + 1} \text{ when } m > 1, \text{ from which } m^2 = \frac{1 + k}{1 - k}.$$

The angle of phase shift through one T section is

$$B = 2 \sin^{-1} \frac{m \frac{\omega}{\omega_c}}{\sqrt{1 - \left(\frac{\omega}{\omega_c} \right)^2 (1 - m^2)}} = T\omega \text{ radians,} \quad (1)$$

and the slope at each point of the curve of this angle versus the frequency ratio ω/ω_c is the time delay T_{ω_c} seconds per section between $f = 0$ and $f = f_c$ given by

$$\frac{dB}{d\frac{\omega}{\omega_c}} = \frac{2m}{\sqrt{1 - \left(\frac{\omega}{\omega_c}\right)^2} \left[1 - \left(\frac{\omega}{\omega_c}\right)^2 (1 - m^2) \right]} = T_{\omega_c} \text{ seconds.} \quad (2)$$

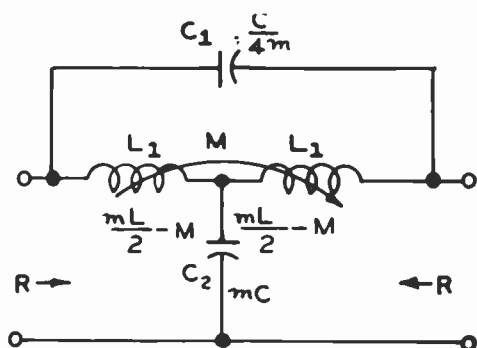


Fig. 2—Constants of the Bridged-T.

Before presenting plots of these delay curves, the constants of the other important delay network, the conventional *B-T* of Figure 2 will be given. All of the component values are exactly the same as given immediately above for the *T*, and an additional capacitor,

$$C_1 = \frac{C}{4m},$$

bridges $2L_1$. R is the same as for the *T* at zero frequency, but does not fall to zero at f_c , as does the R of the *T*. In other words, the all-pass *B-T* is much more constant in impedance than the low-pass *T*. The phase shift of one section of *B-T* is given by

$$B = 2 \tan^{-1} \frac{m \frac{\omega}{\omega_c}}{1 - \left(\frac{\omega}{\omega_c}\right)^2} = T_{\omega} \text{ radians,} \quad (3)$$

and again the first derivative is the delay

$$\frac{dB}{d\frac{\omega}{\omega_c}} = \frac{2m \left[1 + \left(\frac{\omega}{\omega_c}\right)^2 \right]}{\left[1 - \left(\frac{\omega}{\omega_c}\right)^2 \right]^2 + m^2 \left(\frac{\omega}{\omega_c}\right)^2} = T_{\omega_c} \text{ seconds.} \quad (4)$$

Several plottings of Equations (2) and (4) for the more interesting values of m are given in Figure 3. If ω is zero, the T and $B-T$ both have the same delay of $2m$. It is quite apparent that the curves for the

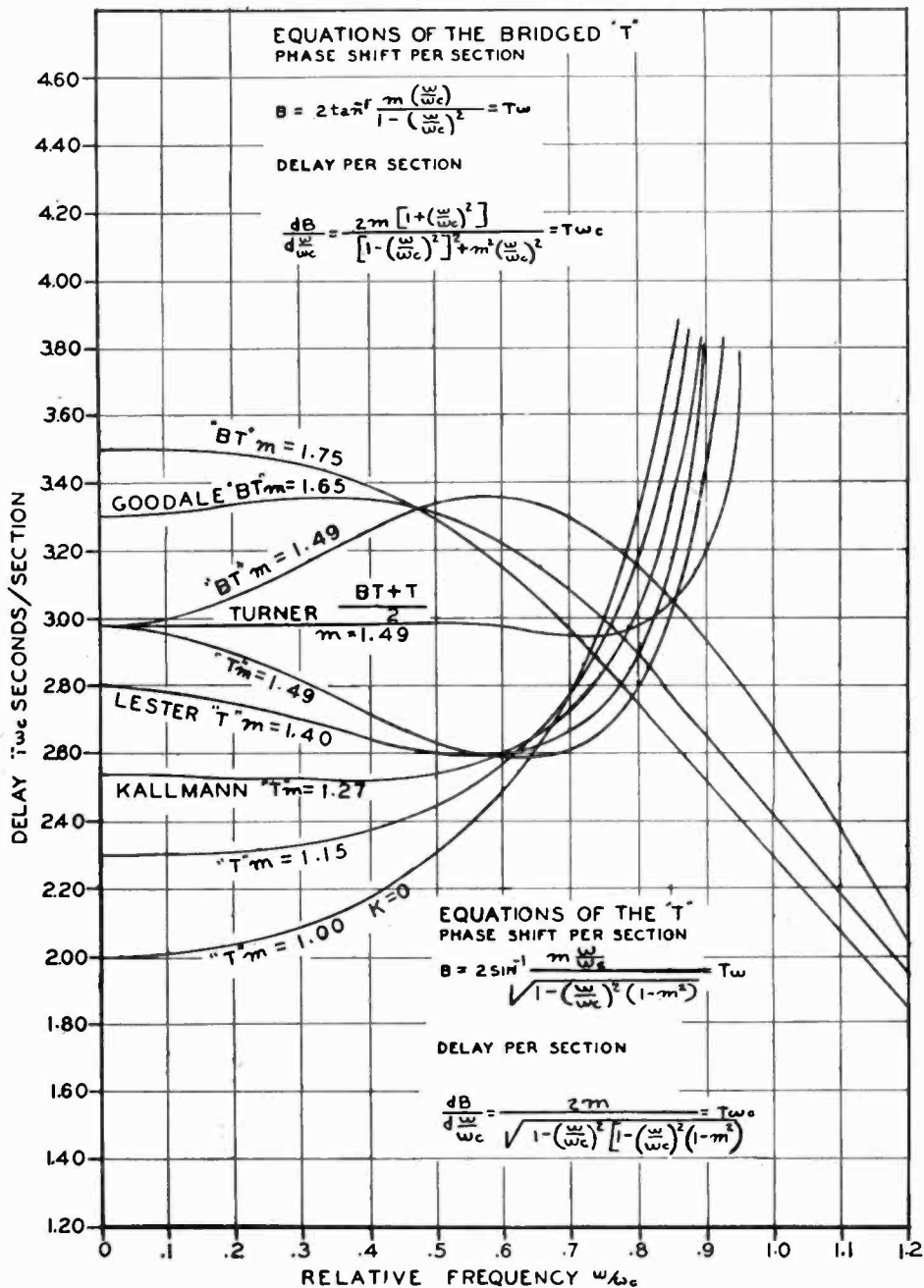


Fig. 3—Delay curves of interesting T 's and bridged- T 's, and one combination of these.

T sections pivot closely about a point $T\omega_c = 2.6$, $\omega/\omega_c = 0.6$, and the $B-T$ curves tend to pivot about $T\omega_c = 3.3$, $\omega/\omega_c = 0.47$. Furthermore, curves symmetrically located relative to these pivot points are quite compli-

mentary such that the delay distortion of a T can be compensated approximately by an equal and opposite distortion of a $B-T$ having the proper m . The most desirable combination of T and $B-T$ occurs with both having an m of 1.49 because this permits all coils to be alike. This combination also appears to maintain the compensation nearest to f_c , in this case to $0.9 f_c$.

An m of 1.75 for the $B-T$ and 1.15 for the T gives fair compensation to $0.75 f_c$ by combining curves that have no reverse curvature if this has any merit. Other single curves shown are the recommendations of Goodale (NBC) ($B-T$, $m = 1.65$), Kallmann¹³ (T , $m = 1.27$), Lester¹² (T , $m = 1.4$). Johnson⁶ recommended all T 's with an m of 1.225 or combinations of lattices and T 's which are probably quite effective but involve a mixture of balanced and unbalanced circuits. The combination of T and $B-T$ did not appear to have occurred to him, possibly because the equivalence to the lattice did not become generally realized until later.

To illustrate the use of the delay Equations (2) and (4), a delay line example will be given. Suppose a 10 microsecond delay for frequencies up to 5 megacycles is required. Using the preferred line of equal numbers of $B-T$ and T with an m of 1.49, the delay will remain very close to $2.98 T\omega_c$ seconds per section up to $.85f_c$. The resonant frequency f_c of this line of conservative design should be 5 megacycles divided by $.85$ or 5.9 megacycles.

The delay per section then becomes

$$T = \frac{2.98}{2\pi 5.9} = .0806 \text{ microseconds.}$$

The number of sections required is then

$$N = \frac{10}{.0806} = 124 \text{ sections}$$

and from this it obviously becomes necessary to keep the delay distortion per section at a minimum by choosing a preferred line assembly and by not operating the line too close to f_c .

EXPERIMENTS

Before describing some of the less conventional delay corrected artificial lines, experimental verification will be given of the foregoing analyses of the T , $B-T$, and combinations of these. Several artificial

lines of twenty sections each were assembled to test these theories. Picture quality on a 16-inch kinescope laboratory monitor was used to check the delay error. For those who wish to measure the delay error Kallmann¹² describes a convenient technique.

In general, there was a very marked difference in the character of the pictures transmitted through 20 sections of $B-T$ as through 20 sections of T . A white background test pattern came out of the $B-T$'s with white edges leading and following the black bars and ringing when the m was too low. From a similar line of T 's the pictures were "softer" and without the white edges and ringing. The effective resolutions were about the same even though the high frequency transmission was greater through the $B-T$'s. These fault differences were exaggerated by having the line resonant frequencies within the range of the transmitted picture components.

The superiority of the T over the $B-T$ was not easy to explain at first, especially since the $B-T$ was known to have much less amplitude distortion and impedance mismatch. The T and $B-T$ delay distortions were shown in Figure 3 to be roughly equal and opposite. The probable explanation of the poor behavior of the $B-T$ is that only slight attenuation occurs at f_c where the delay distortion is large. In contrast, the attenuation through the T is large at f_c , removing the faulty high frequency components.

To test the theory of combining the T 's and $B-T$'s, a 20 section line was assembled half and half. The actual m of 1.51 was close to the chosen value of 1.49. The quality of the test pattern transmitted through this combination line was the best of any of the tests with the low f_c of 5 megacycles. This result was checked several times by adding bridging capacitors one at a time while watching the output monitor. The picture slowly improved in resolution until leading and following transients appeared when more than twelve of the twenty sections were bridged.

The significance of the difference in faulty behavior of the lines near their cut-off frequencies may appear to be unimportant when a safer design is to be had by moving the filter resonances farther from the highest picture frequencies. This is safer from the delay and amplitude distortion standpoint, but still requires approximately the same total series inductance and shunt capacitance for a given time delay. However, for video distribution where vacuum tubes or short unterminated lines may replace the shunt capacitors of the line taps, lower values of f_c may be necessary to provide larger tap capacitances.

The subjects of input impedance and amplitude variation were studied in another series of tests with the T 's and $B-T$'s. A video

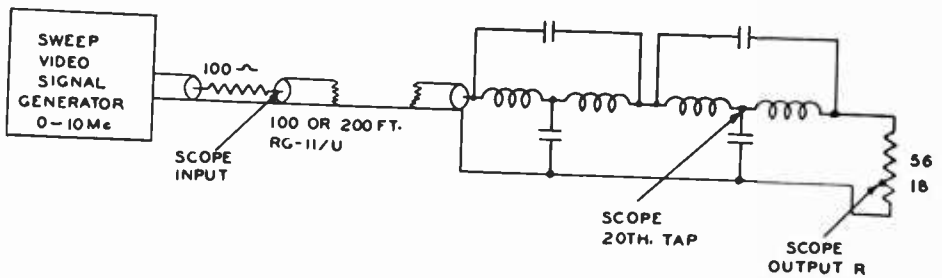


Fig. 4—Test setup to study the impedance match and attenuation of T 's and bridged- T 's.

sweep signal generator was connected to 100 or 200 feet of 75-ohm RG-11/U coaxial cable and the artificial lines under test provided the termination for this cable. The envelope outlines were observed and traced on an RCA Type 715 wideband oscilloscope. A rectifier and narrowband "scope" could have been used if certain of the linearity. Impedance mismatch was studied with the scope connected at the input of the 75-ohm reflection line. A 100-ohm resistor was used to accentuate the standing waves seen at this point. The test setup was essentially as shown in Figure 4. Typical half-envelope curves sketched from this equipment were as shown in Figure 5. This line was the only one assembled with separated coils. The curves of Figure 6 are of the same line with coils pushed together on each form.

The larger mutual coupling gives less disturbance through the f_c region and less high frequency voltage at the taps. Showing the result of still larger mutual coupling, a third coil group of twenty sections is presented as all B - T 's, all T 's, and half and half in Figures 7, 8, and 9.

It is evident from these three sets of curves that the amplitude and impedance variations of the combination of B - T 's and T 's are not as small as those of all B - T 's nor as large as those of all T 's. But more

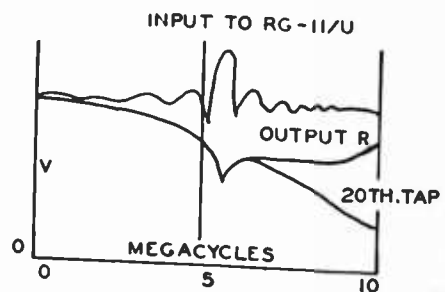
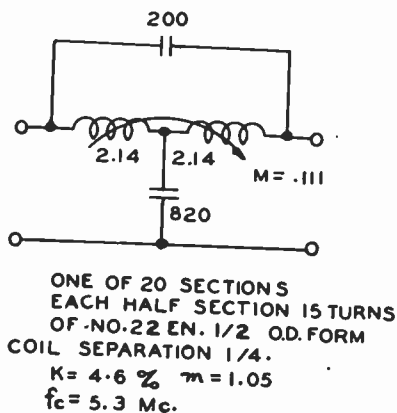


Fig. 5—Input standing wave and output voltage curves of 20 sections of bridged- T having the half-section coils separated to reduce the mutual coupling.

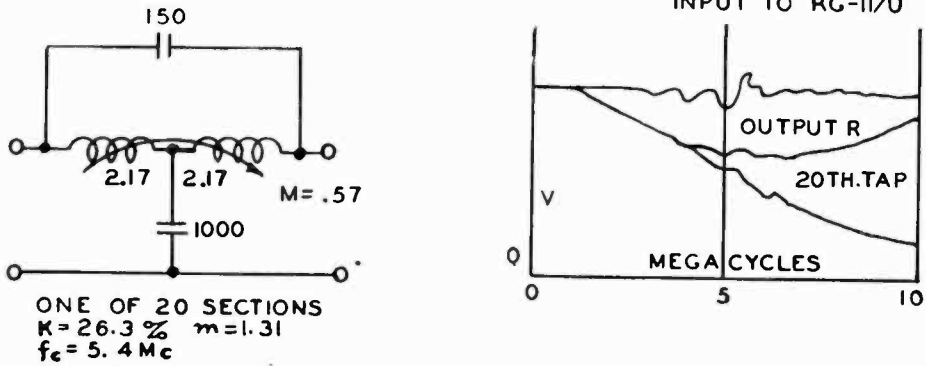


Fig. 6—Same as in Figure 5 except the half-section coils pushed together.

important is the earlier conclusion that the combination is much superior to either type alone in regard to delay variation.

The approximate relation between coil form factor, l/d , and k and m is as follows:

m	k	l/d
1.00	0	Spaced $> 2d$
1.15	0.138	2.0
1.27	0.236	1.45
1.40	0.324	0.95
1.49	0.379	0.72
1.65	0.462	0.45
1.75	0.507	0.35

$l/d =$ length of whole coil (close wound)/diameter.

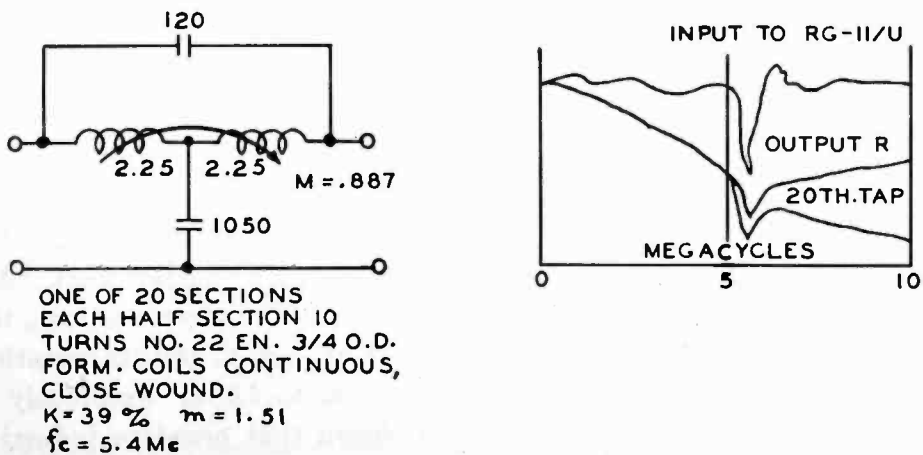


Fig. 7—Another group of coils of larger diameter to provide greater mutual coupling. Connected all bridged-T.

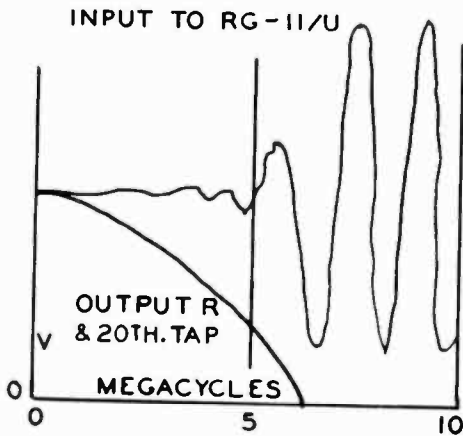


Fig. 8—Same coils as in Figure 7 except bridging capacitors removed making 20 sections of *T*.

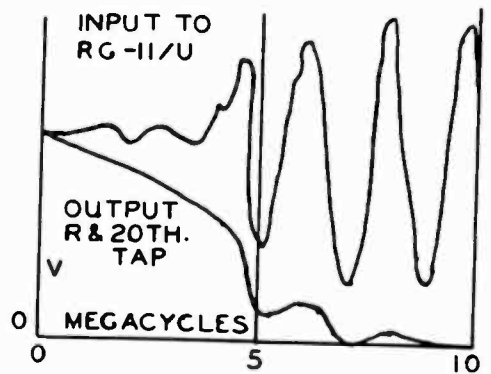


Fig. 9—Same coils as in Figures 7 and 8, but half of the 20 sections bridged, making 10 sections of bridged-*T* and 10 sections of *T*.

BRIEF DESCRIPTION OF OTHER DELAY CORRECTED ARTIFICIAL LINES

Less conventional approaches to the delay distortion problem have been made by several other investigators. Complete analyses of their works have not been made nor models of their lines tested by this writer. Some of their results appear reasonable and others do not.

Inasmuch as these lines differ largely in the treatment of the bridging reactance, a universal line is drawn in Figure 10 to show what determines the values of the bridging capacitors for a "single-frequency" network. In these continuous lines

$$f_c = \frac{1}{\pi\sqrt{LC}}$$

but in the usual isolated resonant circuit

$$f = \frac{1}{2\pi\sqrt{LC}}$$

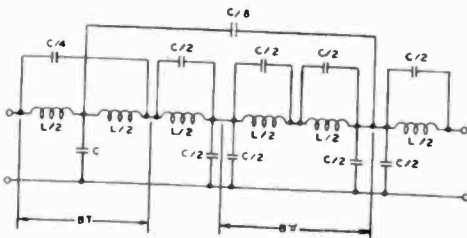
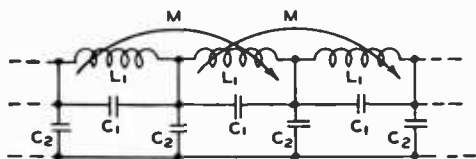


Fig. 10—Different ways of distributing *C* for "single-frequency" ladder lines.

Thus, the usual constant *LC* becomes *LC/4* for ladder lines. Accordingly, in the above sections, the product of each *C* and its shunting *L* is equal to *LC/4*. Previously it was shown that negative inductive coupling modifies these capacitor values, the bridging capacitor be-



$$K = \frac{M}{L_1} = 13.5\%$$

$$f_c = \frac{3}{2\pi T} \quad \text{WHERE } T = \text{DELAY PER SECTION}$$

$$Z_o = R = \sqrt{\frac{L_1 + 2M}{C_2}} \quad C_2 = \frac{T}{Z_o}$$

$$T = \frac{1}{\omega_c} = \sqrt{(L_1 + 2M)C_2} \quad L_1 + 2M = Z_o T$$

$$\frac{C_1}{C_2} = .022$$

$$L_1 = 787 Z_o T$$

$$M = .1063 Z_o T$$

Fig. 11 — Batchelder's line from Reference 10.

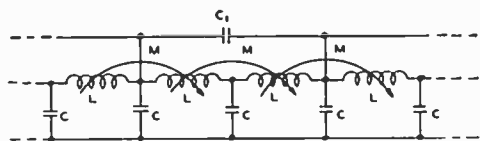


Fig. 12—Golay's line from Reference 11.

coming smaller, and shunt capacitor larger, by the factor m . With these relations in mind, we are ready to consider two more line prescriptions in Figures 11 and 12.

Whatever the basis of Batchelder's computation,¹⁰ in Figure 11, bridging capacitors having the value of $.022 C_2$ are too small to

resonate L_1 to f_c , but may be large enough to appreciably straighten the delay curve.

In Golay's work¹¹ of Figure 12, the coupling coefficient $k = 0.18$ and $C_1 = 0.08 C$. The bridging C_1 is across $2L$ as was the $C/8$ in one of the examples of Figure 10. Modifying C_1 for an m of 1.46 corresponding to this value of k would give a value of C_1 equal to $0.06 C$ instead of $0.08 C$. But the phase relations and the operation of this network with the wide bridge are not clear to this writer.

When two sections, having complex values of m , are combined into a single section, the result is as shown in Figure 13. Ghosh (RCA) found by deriving this bridged- T from its equivalent lattice, that delay is most constant when

$$m = 1.3 + j0.86,$$

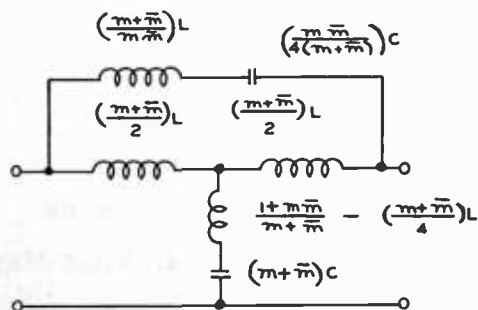


Fig. 13—The resultant network of a combination of two sections having complex values of m as calculated by S. P. Ghosh (RCA).

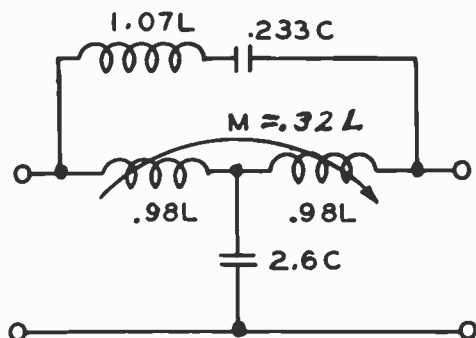


Fig. 14—In terms of the conventional L and C , Figure 13 reduces to these values.

and

$$\bar{m} = 1.3 - j0.86.$$

Thus

$$m + \bar{m} = 2.6,$$

and

$$m \bar{m} = 2.425.$$

The resulting values in terms of the conventional L and C of the ladder are as shown in Figure 14 and are: $M = .32 L$; $k = 32.7$ per cent. This uniform section solution has more elements than the $BT-T$ combination recommended by this writer, but it may correct the delay just as accurately.

Summary of Delay Corrected Artificial Line Prescriptions

Writer	Type	m	Inductive Coupling Percent		Bridging C_1 in terms of C_2	Claimed Corrected To:
			$k = \frac{M}{L_1}$	$k = \frac{M}{2L_1}$		
Pierce ⁴	π			10	0	
Johnson ⁶	T	1.225	20		0	
Batchelder ¹⁰	π			12.5	0	.7 f _c
Batchelder ¹⁰	$B\pi$			13.5	0.022 C_2	.955 f _c (?)
Goodale (NBC)	BT	1.65	46.2		0.0917 C_2	.6 f _c
Ghosh (RCA)	T	1.4	33		0	.85 f _c (?)
Ghosh (RCA)	Sp. BT	$1.3 + j.86$ $1.3 - j.86$	32.7		0.09 C_2 in series with L	.95 f _c (?)
Golay ¹³	$B\pi$			18	0.08 C_2 alt. taps	
Lester ¹⁴	T	1.4	33		0	.95 f _c (?)
Kallmann ¹⁵	T	1.27	23.7		0	.6 f _c
Turner	BT-T	1.49	37.9		0.1125 C_2 and 0	.9 f _c

SELECTED REFERENCE BIBLIOGRAPHY IN CHRONOLOGICAL ORDER

1. G. A. Campbell, U. S. Patents 1,227,113 and 1,227,114. Filed May 22nd, 1917.
2. J. R. Carson, U. S. Patent 1,315,539. Filed July 3, 1918. Recognized the problem of phase shift (delay) correction.
3. K. S. Johnson, U. S. Patent 1,613,952. Filed December 31, 1920. Shows T's with mutual coupling, but in this case positive.

4. G. W. Pierce, U. S. Patent 1,576,459. Filed December 24, 1921. Use of negative mutual inductive coupling (10 per cent).
5. G. A. Campbell, "Physical Theory of Electric Wave Filter", *Bell Sys. Tech. Jour.*, Vol. II, p. 1, November, 1922. Suggests the use of the lattice for phase shift correction.
6. K. S. Johnson, U. S. Patent 1,781,396. Filed January 15, 1925.
7. O. J. Zobel, U. S. Patent 1,538,964. Filed May 26, 1925.
8. S. P. Mead, "Phase Distortion and Phase Distortion Correction", *Bell Sys. Tech. Jour.*, Vol. VII, p. 195, April, 1928.
9. O. J. Zobel, U. S. Patent 1,850,146. Filed March 22, 1932.
10. L. Batchelder, U. S. Patent 2,250,461. Filed May 28, 1938. A bridged- π artificial line.
11. M. J. E. Golay, "The Ideal Low-Pass Filter in the Form of Dispersionless Lag Line", *Proc. I.R.E.*, Vol. 34, p. 138, March, 1946. Bridged- π artificial line.
12. J. M. Lester, "Transient Delay Line", *Electronics*, Vol. 10, No. 4, p. 14, April, 1946. A conventional line of T 's with m of 1.4.
13. H. E. Kallmann, "Equalized Delay Lines", *Proc. I.R.E.*, Vol. 34, p. 646, September, 1946. Discusses lines with distributed and lumped constants.
14. A. T. Starr, **ELECTRIC CIRCUIT AND WAVE FILTERS**, Pitman Publishing Corp., New York, N. Y. This text, written in England, is one of the better reference books for the average engineer who is looking for design information.

DUO-CONE LOUD SPEAKER*#

By

HARRY F. OLSON†, JOHN PRESTON† AND D. H. CUNNINGHAM‡

Summary—A simplified version of the duo-cone loud speaker has been developed consisting of two coaxial, congruent and separately driven cones. A large cone and voice coil are used to reproduce the low frequency range and a small cone and voice coil are used to reproduce the high frequency range. A bridge type magnetic structure makes it possible to supply two air gaps with magnetic flux from one magnet. The response of the loud speaker covers the frequency range from 40 to 12,000 cycles. The directivity pattern covers an angle of 60 degrees without appreciable frequency discrimination.

INTRODUCTION

THE almost universal use of the direct radiator loud speaker is due to its simplicity of construction and the relatively uniform response frequency characteristic. Uniform response over a moderate frequency band may be obtained with any simple direct radiator loud speaker. However, reproduction over a wide frequency range is restricted by practical limitations. The portion of the speech frequency range required for intelligibility falls in the mid-audio frequency band. The range of the fundamental frequencies of most horn, reed and string musical instruments also falls within this band. This is rather fortunate, because it is a simple task to build a direct radiator dynamic loud speaker to cover this mid-frequency band. The two extreme ends of the audio frequency band are the most difficult to reproduce with efficiency comparable to the mid-frequency range. Inefficiency at the low frequencies is primarily due to small radiation resistance. Inefficiency at the high frequencies is primarily due to large mass reactance.

The volume range is another factor. An increase in the volume and frequency ranges of a loud speaker multiplies the problems connected with obtaining low nonlinear distortion and broad directivity patterns. When the high frequency range is increased, the directivity pattern becomes quite narrow, and some means must be devised for obtaining

* Decimal Classification: R365.21.

RCA-Type 515S1.

† Research Department, RCA Laboratories Division, Princeton, N. J.

‡ Parts Product Engineering Department, RCA Victor Division, Camden, N. J.

a broad directivity pattern. The problem of nonlinear distortion is multiplied when the frequency range is increased. From the foregoing it is quite evident that there are many problems to be considered in the development and production of a high quality, wide range loud speaker.

Wide frequency range, low distortion loud speakers are required for monitoring in radio and television broadcasting, phonograph and motion picture recording, high quality sound systems and for custom sound reproducing systems. The demand for a reasonably priced high quality loud speaker by connoisseurs of high quality reproduction is rapidly increasing. The direct radiator loud speaker is particularly suited for these applications because the acoustical power required is relatively low and the space requirements comparatively small.

Some time ago a duo-cone loud speaker was developed and manufactured and sold as the RCA-Type LC1A. It has now been in the field for almost two years. The principles embodied in this device have been found to be fundamentally sound and highly desirable. The LC1A duo-cone loud speaker^{1, 2} still remains the de luxe item and particular pains are taken in manufacture to maintain the high performance characteristics with no compromise in quality. The problem of incorporating the desirable features of the LC1A loud speaker into a simplified and lower cost mechanism with certain compromises was considered, and, as a result, a simplified version (RCA-Type 515S1) has been developed, designed and commercialized. It is the purpose of this paper to describe this loud speaker mechanism.

MAGNETIC STRUCTURE

In the duo-cone 515S1 loud speaker, it was decided to use two separate cones driven by separate voice coils. Furthermore, the coaxial and congruent arrangement of the cones would be maintained essentially the same as in the duo-cone LC1A. This type of vibrating system required two separate air gaps. It is the purpose of this section to describe a single magnet, two air gap magnetic structure.

A fundamental study of two air gap magnetic structures was carried out and, as a result, a magnetic bridge system with two air gaps supplied by a single magnet was developed. A schematic view and the magnetic network of the magnetic system are shown in Figure 1.

¹ H. F. Olson and J. Preston, "Wide Range Loud Speaker Developments", *RCA Review*, Vol. VII, No. 2, p. 155, June, 1946.

² H. F. Olson, *ELEMENTS OF ACOUSTICAL ENGINEERING*, 2nd Edition, D. Van Nostrand Company, New York, N. Y., 1947.

The flux densities in the air gaps can be obtained from a consideration of the magnetic network.

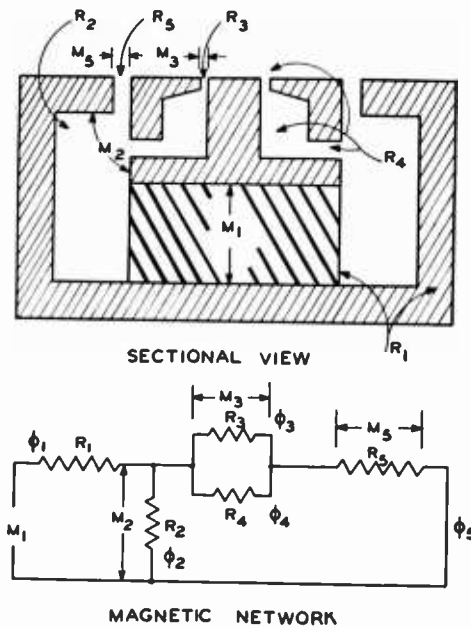


Fig. 1—Schematic sectional view and the magnetic network of the magnetic structure. M_1 , the magnetomotive force developed by the permanent magnet. M_2 , the magnetomotive force drop across the two air gaps. M_3 , the magnetomotive force drop across the large air gap. M_5 , the magnetomotive force drop across the small air gap. R_1 , the reluctance of the leakage gap. R_2 , the reluctance of the added gap and leakage. R_3 , the reluctance of the small air gap. R_4 , the reluctance of the added gap and leakage. R_5 , the reluctance of the large air gap. ϕ_1 , the total flux. ϕ_2 , the leakage flux. ϕ_3 , the flux in the small gap. ϕ_4 , the leakage flux and the flux through the added gap. ϕ_5 , the flux in the large gap.

The total flux, ϕ_5 , in maxwells, in the large air gap is given by

$$\phi_5 = \frac{M_1 R_2}{R_1 R_2 + \left(R_5 + \frac{R_3 R_4}{R_3 + R_4} \right) (R_1 + R_2)} \quad (1)$$

where

- R_1 = reluctance of the iron path,
- R_2 = reluctance of the leakage air gap,
- R_3 = reluctance of the small air gap,
- R_4 = reluctance of the added air gap,
- R_5 = reluctance of the large air gap, and
- M_1 = magnetomotive force of the magnet, in gilberts.

The total flux, ϕ_3 , in maxwells, of the small air gap is given by

$$\phi_3 = \phi_5 \left(\frac{R_4}{R_3 + R_4} \right) \quad (2)$$

From Equations (1) and (2), it will be seen that the magnitude of the flux in the two air gaps is governed by the magnetomotive force developed by the magnet. The relative flux in the two air gaps can be adjusted by varying the value of R_4 .

The flux density, B_5 , in gaussess, in the large air gap is given by

$$B_5 = \frac{\phi'_5}{A_5} \quad (3)$$

where A_5 = area of the large air gap, in square centimeters, and
 ϕ'_5 = total flux through the area A_5 , in maxwells.

The flux density, B_3 , in gaussess, in the small air gap is given by

$$B_3 = \frac{\phi'_3}{A_3} \quad (4)$$

where A_3 = area of the small air gap, in square centimeters, and

ϕ'_3 = total flux through the area A_3 , in maxwells.

The flux densities in the two air gaps as a function of the reluctance of the air gap R_4 are shown in Figure 2.

From the preceding considerations of the magnetic network, it will be seen that practically any ratio of flux densities in the two air gaps may be obtained by suitable selection of parameters. The magnitude of the flux density in the air gaps is governed by the magneto-

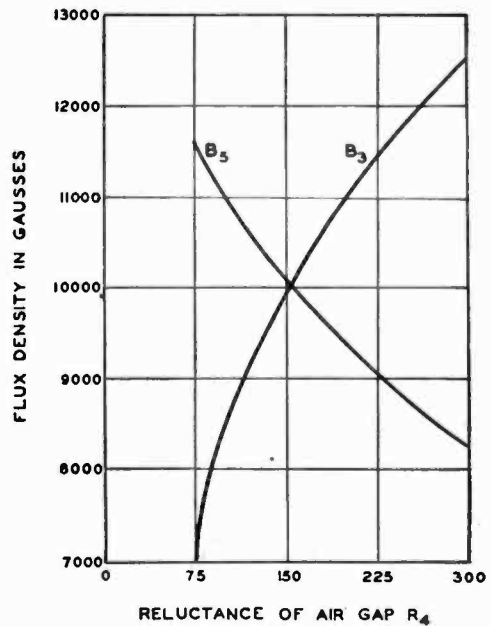


Fig. 2—The flux densities in the large air gap, B_5 , and the small air gap B_3 as function of the reluctance of the air gap R_4 .

motive force developed by the permanent magnet. The magnetic efficiency of this combination structure is higher than that of two separate magnetic structures in spite of the fact that the flux in the gap R_4 is lost. This is due to the smaller percentage of leakage in this structure as compared to that of two separate magnetic structures.

VIBRATING SYSTEM

A sectional view and the mechanical network of the vibrating system of the duo-cone Type 515S1 loud speaker is shown in Figure 3.

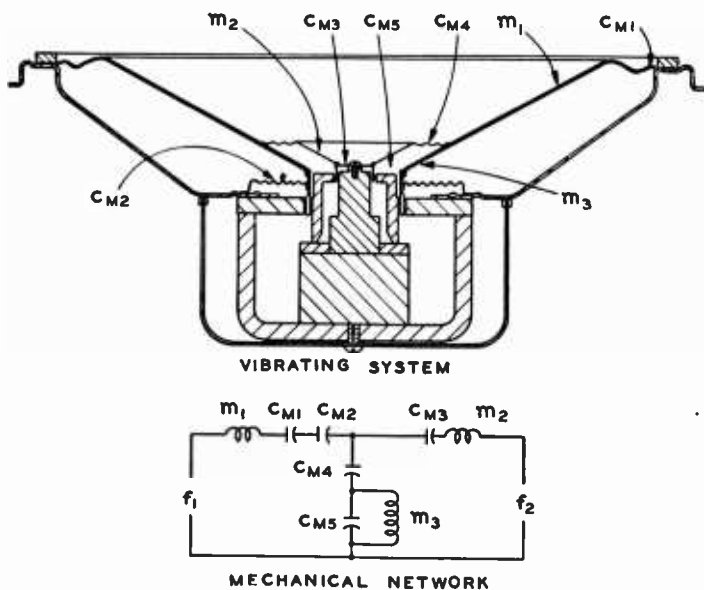


Fig. 3—Sectional view and mechanical network of the duo-cone loud speaker. In the mechanical network: f_1 , the driving force in the low frequency voice coil. m_1 , the mass of the low frequency cone and coil. C_{M1} , the compliance of the outer suspension system of the low frequency cone. C_{M2} , the compliance of the centering suspension of the low frequency cone. f_2 , the driving force in the high frequency voice coil. m_2 , the mass of the high frequency cone and coil. C_{M3} , the compliance of the centering suspension of the high frequency cone. C_{M4} , the compliance of the outer suspension of the high frequency cone. C_{M5} , the compliance of the cavity between the low and high frequency cones. m_3 , the mass of air in the vent holes in the low frequency cone.

Front and rear view photographs of the new duo-cone loud speaker mechanism are shown in Figures 4 and 5. The vibrating system consists of a large cone driven by a large voice coil for the reproduction of the low frequency range and a small cone driven by a small voice coil for the reproduction of the high frequency range. It will be seen that the outside suspension of the small cone is fastened to the large cone. This construction eliminates a dishpan or other outside support for the small cone. It also makes it possible to place the small

cone very close to the large cone so that as far as acoustical radiation phenomena are concerned the two cones are congruent. In this construction, certain precautions must be taken to keep the vibrations of the large cone from being transmitted to the small cone. How this may be accomplished can be obtained by a consideration of the mechanical network of Figure 3.



Fig. 4—Photograph of the front of the duo-cone loud speaker mechanism, Type 515S1.



Fig. 5—Photograph of the back of the duo-cone loud speaker mechanism Type 515S1.

From the mechanical network of Figure 3, the velocity, \dot{x}_1 , in centimeters per second, of the large cone is given by

$$\dot{x}_1 = \frac{f_1(z_2 + z_3) + f_2 z_2}{z_1 z_2 + z_1 z_3 + z_2 z_3} \quad (5)$$

where
$$z_1 = j\omega m_1 + \frac{1}{j\omega C_{M1}} + \frac{1}{j\omega C_{M2}},$$

$$z_2 = \frac{1}{j\omega C_4} + \frac{j\omega m_3}{1 - \omega^2 m_3 C_{M5}},$$

$$z_3 = j\omega m_3 + \frac{1}{j\omega C_{M3}},$$

m_1 = mass of the large cone, in grams,

C_{M1} = compliance of the outer suspension of the large cone, in centimeters per dyne,

C_{M2} = compliance of the center suspension of the large cone, in centimeters per dyne,

m_2 = mass of the small cone, in grams,

C_{M3} = compliance of the center suspension of the small cone, in centimeters per dyne,

m_3 = mass of the air in the vent hole, in grams,

C_{M4} = compliance of the outer suspension of the small cone, in centimeters per dyne,

C_{M5} = compliance of the air chamber behind the small and large cones, in centimeters per dyne,

f_1 = driving force in the voice coil of the large cone, in dynes,

f_2 = driving force in the voice coil of the small cone, in dynes,

$f_1 = B_5 l_1 i_1$,

B_5 = flux density in the large air gap, in gaussses,

l_1 = length of the conductor, in the large voice coil, in centimeters,

i_1 = current, in the large voice coil, in abamperes,

$f_2 = B_3 l_2 i_2$,

B_3 = flux density in the small air gap, in gaussses,

l_2 = length of the conductor in the small voice coil, in centimeters, and,

i_2 = current, in the small voice coil, in abamperes.

The velocity, \dot{x}_2 , in centimeters per second, of the small cone is given by

$$\dot{x}_2 = \frac{f_1 z_2 + f_2 (z_2 + z_1)}{z_1 z_2 + z_1 z_3 + z_2 z_3} \quad (6)$$

From Equations (5) and (6), it will be seen that vibrations of the large cone will not be transmitted to the small cone if the compliance, C_{M3} , of the small cone is very small compared to the compliance, C_{M4} , of the center suspension of the small cone. In order to prevent coupling between the two cones through the compliance C_{M5} , it is necessary to vent the space behind the small cone. Under these conditions, the compliance, C_{M5} , of the cavity will be ineffective because the effective mass, m_3 , of the air in the vent holes shunts the compliance of the air cavity. If the cavity were not vented, the compliance C_{M5} , would serve as a coupling means between the cones. By these expedients the motion transmitted to the small cone by the vibration of the large

cone is negligible. The vibrating system of Figure 3 retains the advantages of two separately driven, coaxial congruent cones.

Referring to Equations (5) and (6), it will be seen that it is desirable to make the driving force f_2 as small as possible in the low frequency range so that the vibrations will be confined to the large voice coil and cone in this frequency region. In the same way, it is desirable to make the driving force f_1 as small as possible in the high frequency range so that the vibrations will be confined to the small coil and cone in this frequency region. These conditions can be obtained by means of a suitable electrical network which allocates the currents of different frequencies to the appropriate voice coil.

MECHANICAL DESIGN AND MANUFACTURING ASSEMBLY

In any dynamic loud speaker, in order to assure good operation for a long life period under all conditions of humidity and temperature changes, it is very important to have a good mechanical assembly of the moving parts relative to the stationary parts. The slightest interference to the movement of the voice coil and cone creates a noise disturbance too severe to be acceptable to the listener. This problem is greater in the duo-cone speaker because two sets of voice coils, cones, and air gaps must be properly aligned in their assembly. The solution to this problem was provided by properly designing the parts so as to give them full lateral freedom during their assembly. This principle of assembly allows the parts to be accurately assembled in a coaxial arrangement and without producing stresses resulting in off-center parts following the removal of assembly fixtures. The steel pole piece members and the magnet are firmly bonded to one another and to the yoke with solder over their entire contacting areas. This type of junction is capable of resisting any movement with shock or other disturbing forces. The magnet is made of Alnico V and weighs two pounds.

Ample clearances of voice coils to the pole piece members are provided to prevent any interference to the movement of the voice coils.

The cones, voice coils, and suspensions are all anchored to one another and to the metal speaker frame with cement. This cement is of a thermal setting type especially developed for having good adhesion to paper, metal, and cloth, and is resistant to loosening or deteriorating with temperature, humidity, and aging effects.

ELECTRICAL NETWORK

The cross-over network is an important consideration in a two unit direct radiator loud speaker. In the design of two-unit loud speakers

in which there is a considerable path length between the two units, a cross-over network with relatively sharp cutoffs is required in order to prevent interference in the cross-over frequency range. In the design of the duo-cone loud speaker, since the large cone is effectively a continuation of the small cone, the cross-over between the low and high frequency cones need not be confined to a narrow frequency band

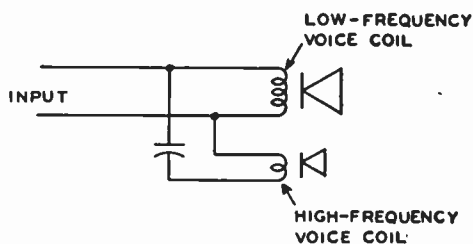


Fig. 6—The electrical cross-over network of the duo-cone loud speaker.

because the two cones vibrate as a single cone in this region. This arrangement makes it possible to use a very simple cross-over network.

The cross-over electrical network is shown in Figure 6. The total electrical impedance, z_{ET} , in ohms, at the input to the loud speaker is given by

$$z_{ET} = \frac{z_{E1}z_{E2}}{z_{E1} + z_{E2}} \quad (7)$$

where $z_{E1} = r_{E1} + j\omega L_1$,

$$z_{E2} = r_{E2} + j\omega L_2 + \frac{1}{j\omega C_E},$$

r_{E1} = electrical resistance of the large voice coil, in ohms,

L_1 = inductance of the large voice coil, in henries,

r_{E2} = electrical resistance of the small voice coil, in ohms,

L_2 = inductance of the small voice coil, in henries, and

C_E = electrical capacitance of the capacitance in series with the small voice coil, in farads.

The current, i_1 , in amperes, in the low frequency coil for an applied voltage, e , in volts, at the input terminals is given by

$$i_1 = \frac{e}{r_{E1} + j\omega L_1} \quad (8)$$

The current, i_2 , in amperes, in the high frequency coil is given by

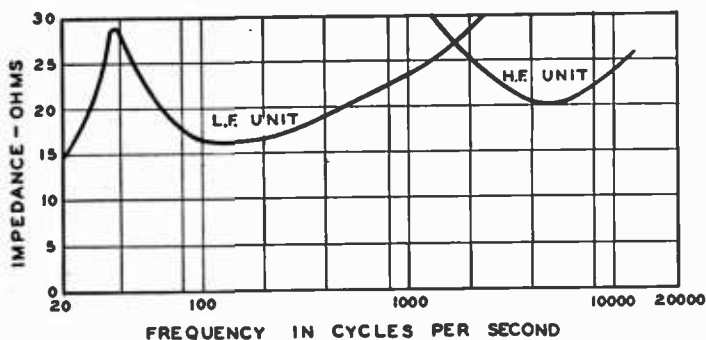


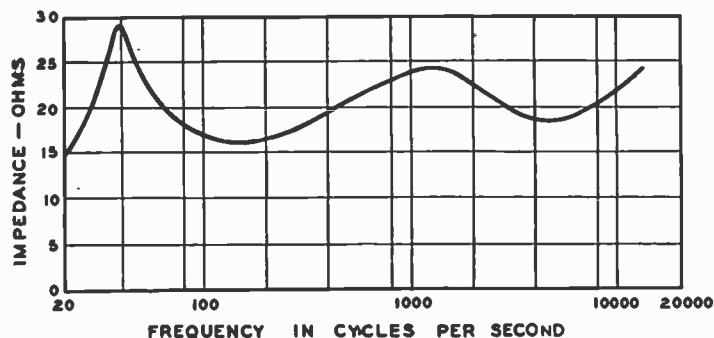
Fig. 7—The electrical impedance frequency characteristics of the low and high frequency units of the duo-cone loud speaker.

$$i_2 = \frac{e}{r_{B2} + j\omega L_2 + \frac{1}{j\omega C_E}} \quad (9)$$

The electrical impedance frequency characteristics of the low and high frequency units are shown in Figure 7. From Equations (8) and (9), it will be seen that the current in the large coil decreases rapidly with frequency when the inductance becomes the predominant electrical impedance. From Figure 7, this occurs above 1500 cycles in this loud speaker. The current in the high frequency coil decreases rapidly below the frequency at which the electrical capacitance becomes the predominant electrical impedance. From Figure 7 this occurs at 1500 cycles.

From the foregoing, it will be seen that it is not necessary to use an inductance in series with the low frequency coil to reduce the current in this coil in the high frequency region. The only external element required for the cross-over network is a capacitor in series with the high frequency unit which limits the current through the high frequency unit at the low frequencies. The electrical impedance frequency characteristic with the cross-over network and normal operation of the mechanism is shown in Figure 8. The cross-over frequency in this system extends well over an octave. However, this

Fig. 8—The overall electrical impedance characteristic of the duo-cone loud speaker using the cross-over network of Figure 6.



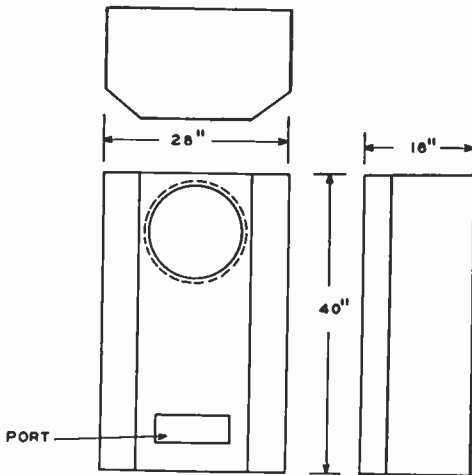


Fig. 9—One type of cabinet which may be used with the duo-cone loud speaker. Wood $\frac{3}{4}$ " thick used.

absorbs standing wave systems and reduces the amplitude of the fundamental resonance. The cabinet is equipped with a port which may be used to accentuate the low frequency response if this type of response frequency characteristic is desired. The cabinet dimensions for the duo-cone mechanism are not critical. Satisfactory operation can be obtained with any well designed cabinet having a cubical content of approximately 5 to 7 cubic feet. The mechanism may also be used in a flat baffle.

is not objectionable because in the overlap region the two cones vibrate as a single unit.

CABINETS

For most applications the direct radiator loud speaker is housed in some type of cabinet. One design of cabinet which has been found to be suitable for this loud speaker is shown in Figure 9. The loud speaker mechanism is designed to be flush mounted on the front face of the cabinet. The cabinet is completely lined with 1-inch Ozite. This

RESPONSE FREQUENCY CHARACTERISTIC

The measured response frequency characteristics of the duo-cone loud speaker mechanism mounted in the cabinet of Figure 9 are shown in Figures 10 and 11. These characteristics show the effect of the port opening in the cabinet upon the low frequency response. The response with the port closed is relatively uniform from 50 to 11,000 cycles. These characteristics also show that the response is uniform in the overlap frequency range of the low and high frequency units.

Fig. 10 — Response frequency characteristics of the high and low frequency units of the duo-cone loud speaker operating in the cabinet of Figure 9 with the port closed.

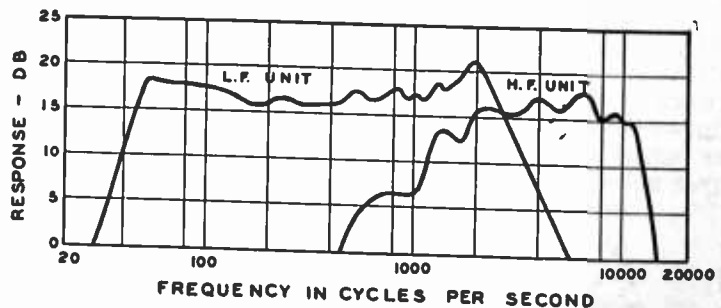
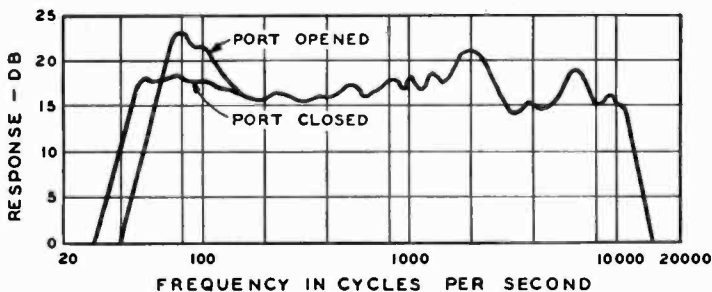


Fig. 11—The overall response frequency characteristics of the duo-cone loud speaker mechanism operating the cabinet of Figure 9 with the port open and closed.



The response frequency characteristic of the duo-cone loud speaker mechanism mounted in a flat baffle is shown in Figure 12.

DIRECTIONAL CHARACTERISTICS

The directional patterns of a high quality loud speaker should be substantially independent of the frequency over a broad angle. The directional characteristics of a cone loud speaker are a function of the frequency. At the low frequencies where the dimensions are small compared to the wavelength the system is nondirectional. When the dimensions of the cone become comparable to the wavelength the system becomes directional. Above this frequency the directional pattern becomes progressively sharper with increase in frequency. A uniform directional pattern may be obtained by decreasing the size of the radiator with frequency. This is approximated in this loud speaker by the use of two cones—a large cone for the low frequency range and a small cone for the high frequency range. The directional pattern of a cone is also a function of the cone angle. This is due to the finite velocity transmission of sound in the cone. By increasing the angle of the cone, the directional patterns become broader at the higher frequencies. Relatively wide angle cones were used in the duo-cone loud speaker in order to obtain broad directional patterns in the high frequency range.

The directional characteristics of the duo-cone loud speaker for the frequencies 500, 1000, 2000, 3000, 5000, 7000 and 10,000 cycles are shown in Figures 13, 14, 15, 16, 17, 18 and 19. A consideration of

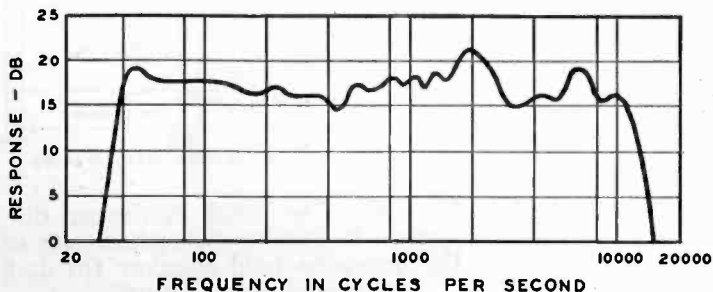


Fig. 12—The overall response frequency characteristic of the duo-cone loud speaker mechanism operating in a flat baffle about 5 feet across.

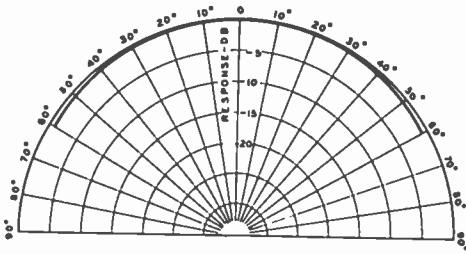


Fig. 13—Directional characteristic of the duo-cone loud speaker at 500 cycles.

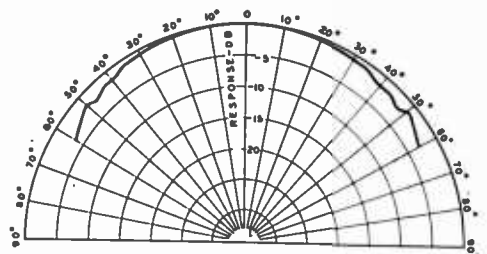


Fig. 14—Directional characteristic of the duo-cone loud speaker at 1000 cycles.

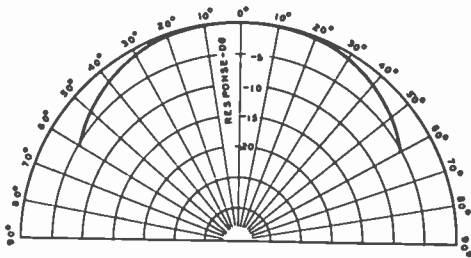


Fig. 15—Directional characteristic of the duo-cone loud speaker at 2000 cycles.

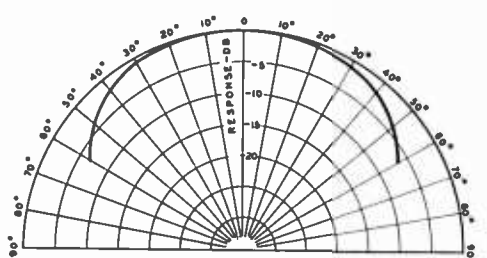


Fig. 16—Directional characteristic of the duo-cone loud speaker at 3000 cycles.

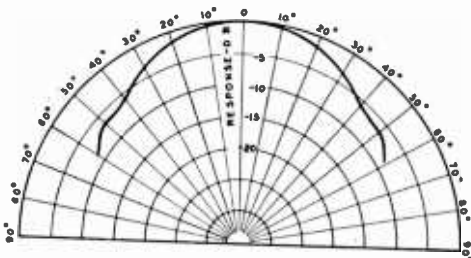


Fig. 17—Directional characteristic of the duo-cone loud speaker at 5000 cycles.

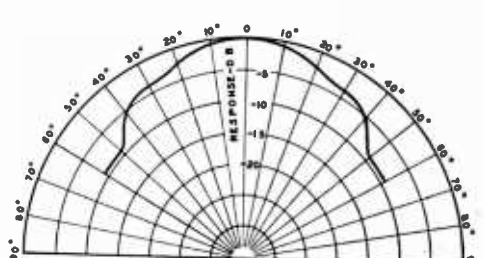


Fig. 18—Directional characteristic of the duo-cone loud speaker at 7000 cycles.

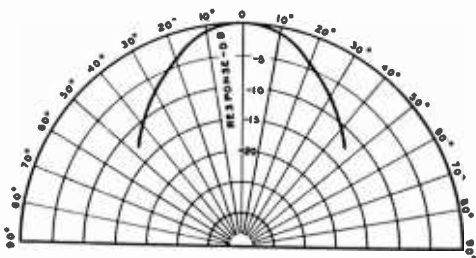


Fig. 19—Directional characteristic of the duo-cone loud speaker at 10,000 cycles.

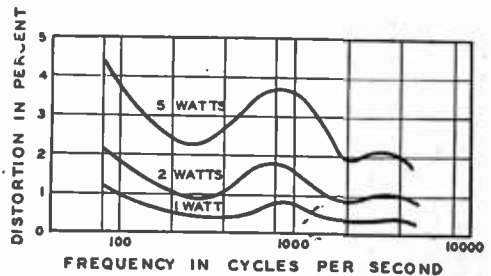


Fig. 20—The total nonlinear distortion frequency characteristics of the duo-cone loud speaker for 1, 2 and 5 watts input.

these characteristics shows that a broad directivity pattern is maintained over the entire response range.

NONLINEAR DISTORTION

The nonlinear distortion frequency characteristic depicts the spurious harmonics which are generated by a loud speaker.

There are many possible sources of distortion in a direct radiator dynamic loud speaker. A few of the most common sources of distortion are as follows: The suspension system; in the cone due to lack of rigidity; inhomogeneity of the air gap flux; inadequate flux density in the air gap. The expedients for reducing or eliminating these distortions have been considered at length in the literature and will not be repeated here. Every effort was made to develop a system in which these distortions would be as low as possible without adding unduly to the complexity of construction, the sensitivity or the cost. The total r-m-s distortion frequency characteristics of the duo-cone loud speaker for 1, 2 and 5 watts input are shown in Figure 20. The average input to this loud speaker for a level of 80 decibels in the average living room is less than .1 watt. The distortion under these conditions is negligible. Even at an input of 5 watts the distortion is quite low.

A SIX-MEGACYCLE COMPATIBLE HIGH-DEFINITION COLOR TELEVISION SYSTEM*

A Report

BY

RCA LABORATORIES DIVISION, PRINCETON, N. J.

Editor's Note: This report comprises Exhibit No. 209 submitted by Radio Corporation of America at the Hearing before the Federal Communications Commission in Docket Nos. 8736, 8975, 9175 and 8976, September 26, 1949 et seq.

Previous reports on the new color system are contained in Exhibit Nos. 206 and 207 submitted to the Federal Communications Commission on August 25 and September 6, 1949.

Additional information on various aspects of the system is under preparation. It is planned to publish this information as it becomes available.

INTRODUCTION

THE color system described herein has its roots in the simultaneous method first disclosed on October 30, 1946 and subsequently described in detail at a Hearing before the Federal Communications Commission in Docket No. 7896 and in various published technical papers.^{1,2}

The new system, as in the case of the wide-band simultaneous system, is completely compatible with the current black-and-white television system.

In addition, the new system includes later developments which, in essence, compress the simultaneous system into a 4-megacycle band suitable for a total channel assignment of 6 megacycles. Not only is the system so compressed, but no detail is lost in the process. This in turn insures a high-definition color picture, while at the same time preserving the normal definition of the black-and-white picture.

The compression of the simultaneous system is accomplished by a combination of two processes:

- (a) use of the mixed-highs principle; and
- (b) color-picture sampling and time-multiplex transmission.

These band-saving techniques are described in the following pages.

* Decimal Classification: R583.

¹ RCA Laboratories Division, "Simultaneous All-Electronic Color Television," *RCA Review*, Vol. VII, No. 4, p. 459, December, 1946.

² R. D. Kell, G. C. Sziklai, R. C. Ballard, A. C. Schroeder, K. R. Wendt and G. L. Fredendall, "An Experimental Simultaneous Color Television System," *Proc. I.R.E.*, Vol. 35, No. 9, p. 861, September, 1947.

STUDIO AND RELATED EQUIPMENT CHARACTERISTICS

A block diagram of the color television broadcasting station is shown in Figure 1.

Studio Apparatus

The color camera (live, film, or slide), its related equipment, and the synchronizing generator are the same components used in the wide-band simultaneous system. These were described in Dockets No. 7896 and No. 8976 and in References (1) and (2).

This studio apparatus provides three signals, one for each of the primary colors (green, red and blue). Each of these signals may contain frequency components out to a maximum of four megacycles, and in addition an average or dc component.

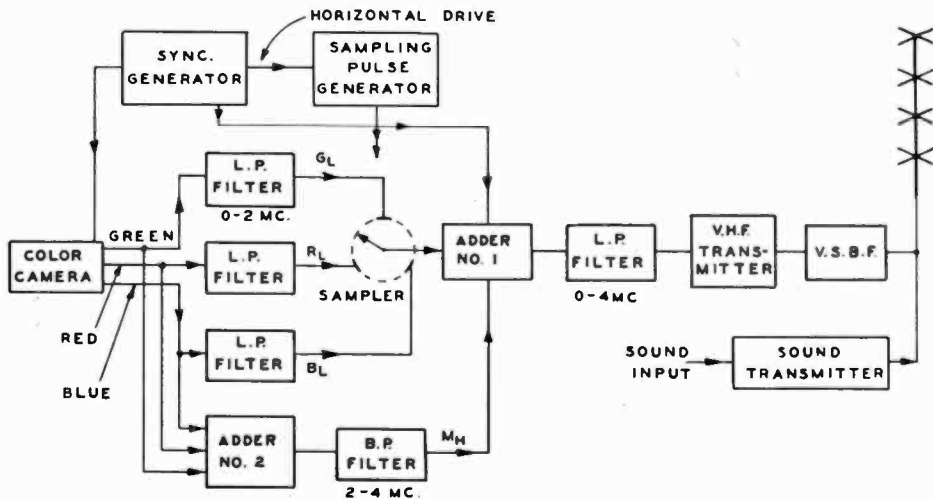


Fig. 1—Block diagram of the color television transmitter.

Signal Routing

For one signal routing of Figure 1, each color signal passes through a low-pass filter which eliminates frequency components above two megacycles. The green-channel signal coming out of its particular low-pass filter is designated as G_L on Figure 1, indicating that at this point the signal contains the dc component and ac components with frequencies of two megacycles or less. The three low-frequency signals, G_L , R_L and B_L are then sent into an electronic commutator or sampler (discussed below).

For the second signal routing of Figure 1, the three-color signals from the camera are combined in electronic Adder No. 2 and then are passed through a band-pass filter. The output of this filter contains

frequencies from two to four megacycles, with contributions from each of the three color channels. The signal at the output of the band-pass filter is designated as M_H , the mixed-high signal. The mixed-high frequencies are fed to Adder No. 1 which, as will be seen, is also receiving the signal from the sampler and from the synchronizing generator.

Mixed-Highs

The principle of mixed-highs, referred to above, was described in Docket Nos. 7896 and 8976. It has been demonstrated that the mixed-highs procedure is successful and satisfactory in a wide-band simultaneous system.

In the new system, at the transmitting end, the sampling process (discussed below) is capable by itself, of providing high-frequency components of each color signal. Since the sampling frequency determines the highest frequency which will be passed, when the high-frequency components of each color signal are combined the resulting band-width does not exceed four megacycles.

However, photocells used with flying-spot devices in film and slide scanners inherently have poor high-frequency response, particularly in the red. It is often necessary, therefore, to peak the higher-frequency response of such devices. This peaking, of course, raises the level of the high-frequency noise components. When the entire frequency band of zero to four megacycles is sampled, the 3.8-megacycle sampling frequency beats the high-frequency noise to low frequency and vice versa. Because, in the case of pickup devices of the type referred to above, the high-frequency noise has been peaked, an even interchange of noise components does not occur, as it would if the noise spectrum were uniform. Consequently, after the sampling process has taken place, the low-frequency noise components will have been accentuated. This causes a coarse-grain structure in the picture which may be objectional to the eye.

Experience has shown, therefore, that there is a definite advantage gained in sampling only the lower half of the video band (up to two megacycles) and using the principle of mixed-highs for the upper half of the video band (from two to four megacycles), and this procedure is used at the transmitting end.

In pick-up equipment with uniform noise characteristics, no such effects as above described exist. This means that either the dual procedure given in the above paragraph or sampling only may be used. This also applies to receiving equipment.

Sampling and Combining Process

The sampling pulse generator, which embodies time-multiplexing techniques, is an integral part of the electronic commutator and makes use of the trailing edge of the horizontal synchronizing pulse to time the sampling of each of the color signals.

In the sampler, each color signal is sampled for a very short time, at a rate of 3.8 million times per second for each color. The samples for each scanning line are timed with respect to the horizontal synchronizing pulse for that line. However, for alternate line scans the timing of the sampling pulse is such that samples of any one color

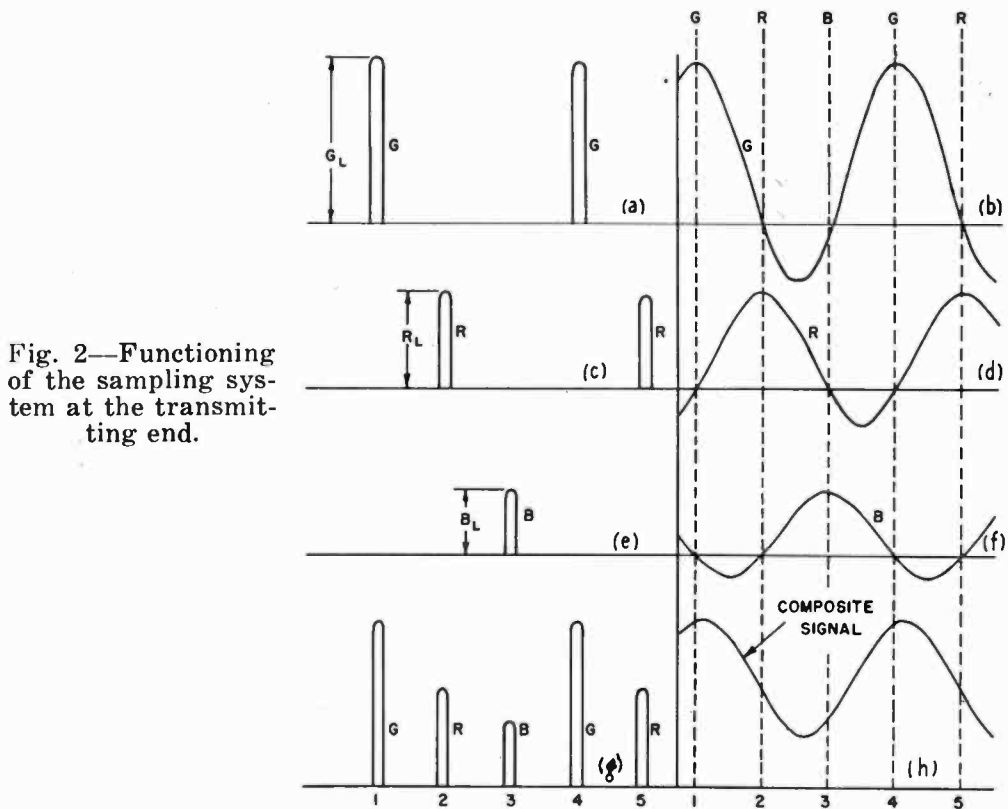


Fig. 2—Functioning of the sampling system at the transmitting end.

are taken at a point midway between samples of the same color in the line above. Alternate scans of the same line are displaced in this same way. Thus, the second samples are taken midway between the first samples, resulting in dot interlacing (to be discussed in more detail in Part IV).

Figure 2 illustrates the functioning, at the transmitting end, of the sampling system in the pickup of large uniform polychromatic areas, with the three primary colors represented by three different signal strengths. Figure 2(a) shows the output of the sampler due to the green signal only. The green channel signal is sampled every

0.263 microsecond ($0.263 = 1/3.8$). At a time 0.0877 microsecond after a green sample, a sample is taken of the red signal. This time delay is one-third of the time between successive green samples. The red samples continue to be taken 0.263 microsecond apart as shown in Figure 2(c). The blue samples are taken at the same rate and follow the red samples by a time of 0.0877 microsecond, as indicated in Figure 2(e). The composite output of the sampler consists of a superposition of the green, red, and blue trains of pulses or samples. Figure 2(g) shows the signal in the circuit at the output of the sampler.

From the sampler the signals pass to an electronic combining device called Adder No. 1 in Figure 1. Standard synchronizing signals from the synchronizing generator are also applied at this point.

This signal and the synchronizing pulses from Adder No. 1 feed into the low-pass filter. In the case of large area color only, the mixed-highs signal is not present.

The narrow green pulses of Figure 2(a), occurring at a rate of 3.8 million pulses per second, are smoothed by the low-pass filter to give the result shown in Figure 2(b). This wave consists of a dc component, which is the average of the pulse sample, plus a sine wave which has a frequency of 3.8 megacycles (the filter having removed the higher order harmonics). The 3.8-megacycle sine wave and the dc component change together, as the green signal changes in strength, in such a way that the signal of Figure 2(b) always passes through zero at the same interval of time after the peak regardless of the strength of the green signal. The smoothed sample of the green signal may be expressed as: $\frac{1}{3} G(t) [1 + 2\cos(2\pi ft)]$ where $G(t)$ is the green signal as a function of time, and f is the sampling frequency, namely 3.8 megacycles. A study of this expression reveals that the smoothed green sample goes through zero 120 and 240 electrical degrees after the signal has reached its maximum value.

The above equation is an excellent approximation of the conditions existing in the circuit when the duty cycle of the samples for a given color is 15 per cent or less. Accordingly, the duty cycle of the system is maintained within these limits.

The red samples of Figure 2(c) are smoothed by the filter to yield the result shown in Figure 2(d). This again is made up of a dc component and a sine wave with a frequency of 3.8 megacycles.

Smoothing of the blue sampling pulses results in the contribution shown in Figure 2(f). It should be noted in Figures 2(b), 2(d), and 2(f) that when any one color signal reaches its maximum value, the other two responses are crossing the zero axis.

While the curves of Figures 2(b), 2(d), and 2(f) have been shown separately for illustrative purposes, it should be remembered that the pulse train of Figure 2(g) goes into the low-pass filter. Thus the composite signal of Figure 2(h) comes out of this filter. In this figure, the dc component is the sum of the dc components of the green, red, and blue signals, while the 3.8 megacycle sine wave is the sum of three sine waves of the same frequency. This results in a composite 3.8-megacycle sine wave with a new amplitude and phase position superimposed on the composite dc component.

The action of the system in the pick-up of varying color areas is illustrated by means of Figure 3. In Figure 3(a), the three color signals are shown as they enter the sampler, with the appropriate sampling pulses as they come out of the sampler indicated by vertical lines. These same pulses are shown in Figure 3(b), with the envelope indicating the result of smoothing in the filter. It will be appreciated that Figure 3 is not quantitative and is used purely for illustrative purposes. Fine detail of the color picture, carried by the higher frequency components, is, of course, now supplied by the mixed-highs signal, but this cannot be easily shown in the diagram.

TRANSMITTER

The output (time-multiplexed color signal, mixed-high color signal, and synchronizing signals) of the low-pass filter (zero to four megacycles) in the right center of Figure 1 is applied to the modulator of a conventional VHF or UHF television transmitter.

From this point on, including the transmitter itself, together with the vestigial sideband filter, diplexer, sound channel and antenna, the system is that of a normal black-and-white television station, with no changes necessary.

The signal transmitted is consistent with the "Standards of Good Engineering Practice Concerning Television Broadcast Stations."

RECEIVING EQUIPMENT CHARACTERISTICS

Figure 4 is a block diagram of one type of color television receiver. The radio-frequency circuits, the picture intermediate-frequency amplifiers, the second detector, the sync separator, the sound intermediate-frequency amplifiers, the discriminator, and the audio circuits are identical with those of a conventional black-and-white receiver.

The composite video and synchronizing signals from the second detector enter the sync separator, which removes the video signal and

sends the synchronizing pulses to the deflection circuits and to the sampling pulse generator.

Sampling and Smoothing Process

The sampling pulse generator utilizes the trailing edge of the horizontal synchronizing pulse to actuate the receiver sampler in identical fashion and in synchronism with the transmitter sampler.

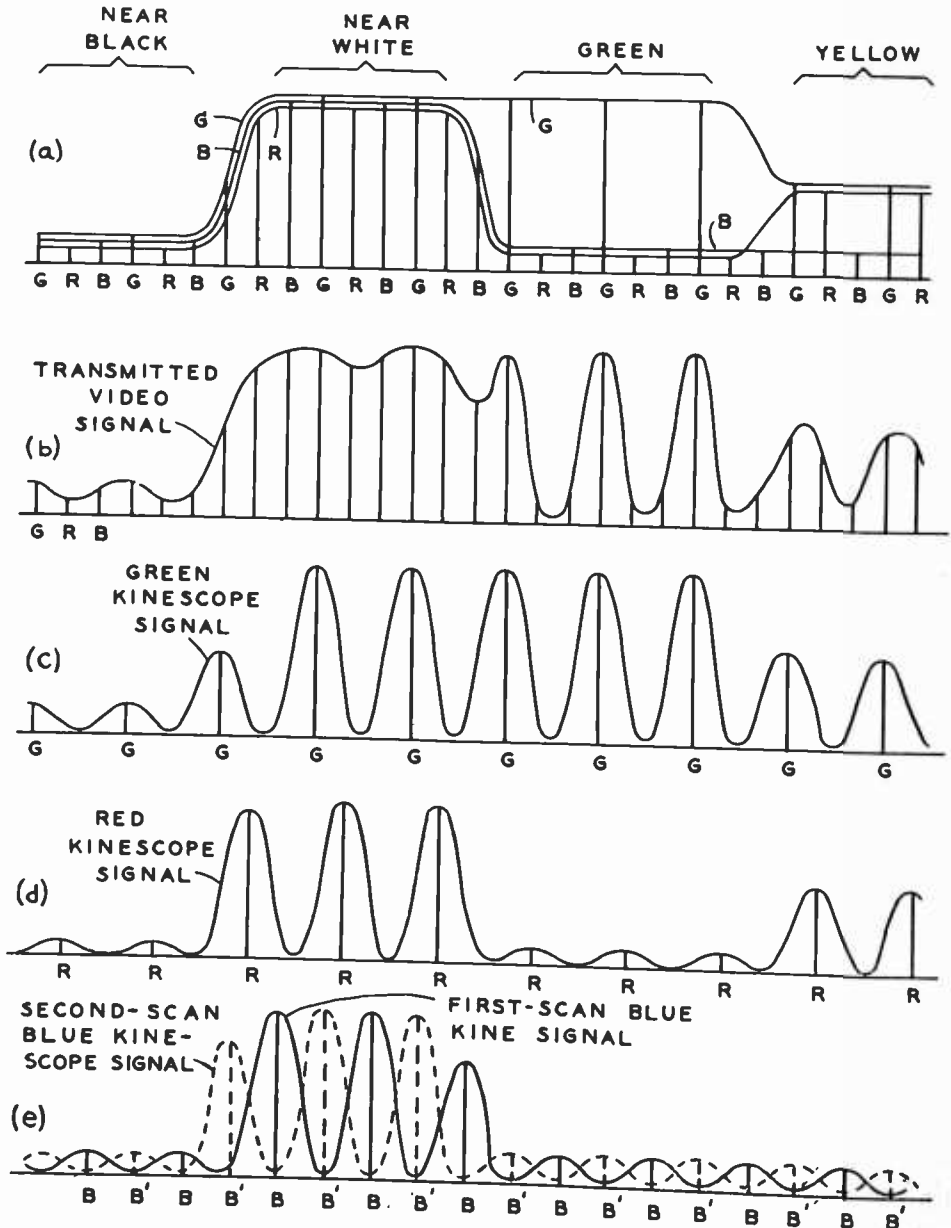


Fig. 3—Action of the system in the presence of varying color areas.

The signal from the second detector also enters the sampler. It has the same form as the composite signal of Figure 2(h), or as the solid

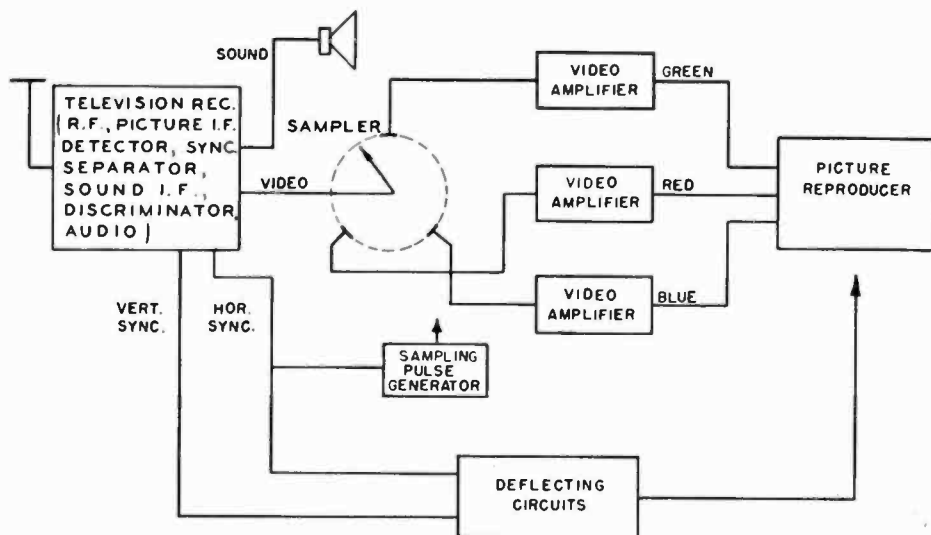


Fig. 4—Block diagram of one type of color television receiving equipment.

envelope of Figure 3(b). For ease of reference, Figure 2(h) has been reproduced as Figure 5(a). Again, the case of large uniform polychromatic areas is used for illustrative purposes.

The electronic commutator samples the composite signal every 0.0877 microsecond, producing the short pulses shown in Figure 5(a). The amplitude of each of these pulses is determined by the amplitude of the composite wave at that particular instant.

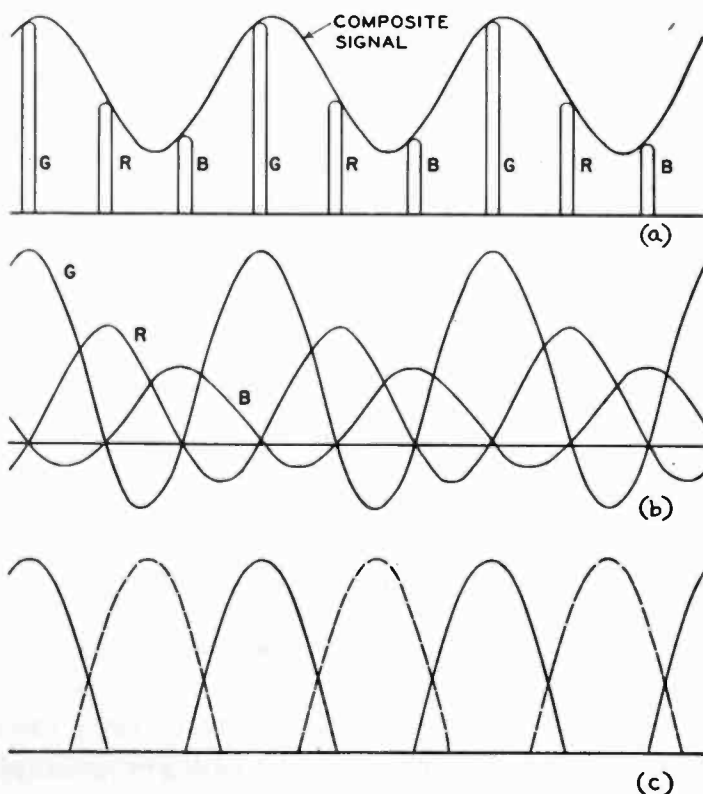


Fig. 5—Functioning of the sampling system at the receiving end.

The commutator feeds these pulses into three separate video amplifiers which in turn control the picture-reproducing apparatus which may consist of three cathode-ray tubes or kinescopes having appropriate color-producing phosphors. This method for portraying the single color picture with three kinescopes is similar to that demonstrated to the Commission during the Hearing on Docket No. 7896 and in References (1) and (2).

The video amplifiers have a flat frequency response to four megacycles, and must cut off completely at 7.6 megacycles. (Reference here is to the frequency response of the video amplifiers only and not to channel requirements.)

The sampler sends the pulses to each of the video amplifiers and its attendant kinescope in succession. For instance, in Figure 5(a), the first pulse shown in green goes to the green kinescope, the next pulse goes to the red, while the third pulse is sent to the blue. The green receives the fourth, seventh, tenth, and so on. Thus, while the individual pulses coming out of the sampler are 0.0877 microsecond apart, the green pulses going to the video amplifier for the green picture repeat every 0.263 microsecond. The green channel pulses of Figure 5(a), in passing through the video amplifier, lose all frequency components except the fundamental frequency of 3.8 megacycles and the dc component. The resultant smoothed signals are shown in Figure 5(b). The green, red, and blue signals are shown in superposition on this figure for illustration. It should be remembered that at this point the green signal shown is that fed to the green kinescope, while the red and blue signals are applied to their individual kinescopes.

Examination of Figures 2(b), 2(d), 2(f), and 2(h), has already revealed that, when the green signal is maximum, the red and blue signals are passing through zero. Hence, since the composite signal is sampled for green by a narrow pulse at the receiver at this exact instant, the receiver sampling pulse is a true measure of the green signal and includes no dilution from the red or blue signals. Likewise, the red and blue samples are each taken at points on the composite signal where no crosstalk is contributed from the other two color signals.

The above statement concerning absence of crosstalk holds good for all frequency components up to one-half the sampling frequency. For frequency components approaching the sampling frequency in order of magnitude, from a purely circuit aspect, crosstalk is present. However, the physiological characteristics of the eye which make possible the application of the mixed-highs principle apply equally well

to the crosstalk of the higher-frequency components. Consequently, crosstalk in the fine detail is of no consequence.

Assuming that the kinescope actually cuts off with negative applied signal, and neglecting the nonlinearity of the input control-voltage versus light-output characteristic of the kinescope, the solid lines of Figure 5(c) may be regarded as the effective light intensity along one line scan in green. Figures 3(c), 3(d), and 3(e) show the effective signals for the green, red, and blue kinescopes, again for a single line scan.

Picture Dot Interlacing and Scanning Sequence

Returning now to Figure 5(c), it may be seen that a single line scan on the green channel lays down a series of green dots on the screen as shown by the solid lines. As was indicated above, these dots occur at a rate of 3.8 million times per second. If fine detail were involved to such an extent that two adjacent pulses in the green channel in a single line scan were of different amplitude, it is basic that the highest frequency component of use in establishing picture detail would be a sine wave which went from a crest to a trough in the time between the two adjacent green pulses. This sine wave would then have a frequency of 1.9 megacycles.

The fact that each pulse has a rise equivalent to twice this frequency allows the use of picture-dot interlacing to secure full detail up to a frequency band 3.8 megacycles wide. This is accomplished by shifting the sampling pulses the next time that the same line is scanned so that the dots are then laid down between the dots that were laid down in the first scan. This second series of green dots is shown by the broken curves in Figure 5(c). In this figure, the dots shown by broken curves are the same amplitude as the dots shown by the solid curves. For resolution of very fine detail, the dots laid down in the first scan would differ in amplitude from the dots laid down in the second scan of this same line.

Inspection of Figure 5(d) reveals that while a single line scan lays down a series of green dots on the screen with space between dots, this space is filled at the same time by red and blue dots, with great overlapping of the dots. The effect of the successive scans of a single line, Figure 5(e), shows even more clearly the complete covering of the line area with picture dots of three colors.

The scanning and interlace pattern used in the new color television system is illustrated in Figure 6. Each letter represents the center of a color dot area on the screen. The actual areas, of course, overlap to a great extent as discussed above.

During the first scanning field, illustrated in the upper diagram in Figure 6, the odd numbered lines are scanned in order. Colored dots are laid down in order along line 1 as shown. Next, line 3 is scanned with a displacement for each color dot shown, in the same fashion as described for the sampling at the transmitting end. The remaining odd lines are scanned in order. This scanning of the first field takes place in one-sixtieth of a second.

During the second field, the even lines are scanned, first line 2 with the colors laid down as shown, then line 4, and so on. The dot pattern laid down during the third field is shown by the lower diagram, where the odd lines are scanned in succession. During the fourth field, the even lines are again scanned in succession with the color dot pattern shown.

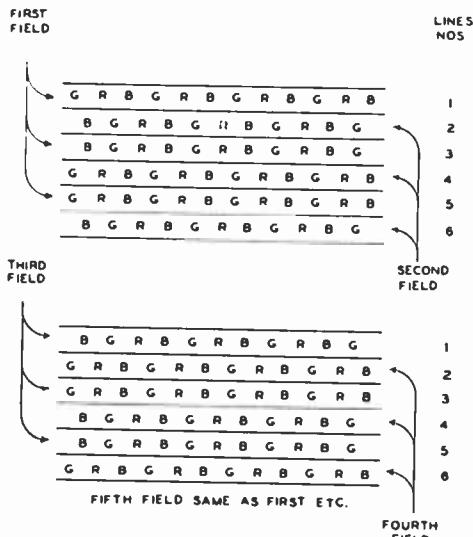


Fig. 6—Scanning and interlace pattern.

with say, green dots. Simultaneously, the area is being covered with red dots and with blue dots. Since there are 60 fields per second, it may be said that there are 15 complete color pictures per second.

It should be remembered that the effective rate for large-area flicker is 60 fields per second, the same as for current black-and-white receivers. At viewing distances such that the picture line structure is not resolved, the effect of small-area flicker due to line interlace and picture-dot interlace is not visible.

Receiving Systems

In the receiver shown in Figure 4, the total signal consisting of the sampled signal plus the mixed highs has been inserted in the

Thus, the odd lines are scanned during the first field, but dots of the same primary color are separated by spaces. The even lines are scanned during the second field, again with spaces between like color dots. During the third field, the odd lines are again scanned but the color dots displaced so that the spaces are filled. The even lines are scanned during the fourth field, with the color dots displaced to fill in the spaces left during the second field scanning. Four scanning fields are required to completely cover the picture area, with all spaces filled,

receiver sampler and picture-dot interlacing has been used to achieve high definition as discussed in detail above.

Another receiver arrangement is possible. In such a receiver, shown in Figure 7, the entire signal is fed into the sampler as before, but, in this case, low-pass filters with cut-off frequencies of approximately two megacycles are inserted between the sampler and the kinescopes. The low-frequency filters smooth out the pulses of Figure 5(c), so that the adjacent dots of a single color in one line scan now almost completely overlap. Because the pulses have been broadened by the two-megacycle filters in this receiver, horizontal resolution will not be increased by picture-dot interlacing at the receiver. Full resolution, however, is restored by obtaining mixed highs from the signal ahead of the receiver sampler and by-passing the mixed highs through a band-pass filter to the green, red, and blue kinescopes.

The color television receiver of Figure 4 and the alternate receiver of Figure 7 are examples of the flexibility afforded by this color system.

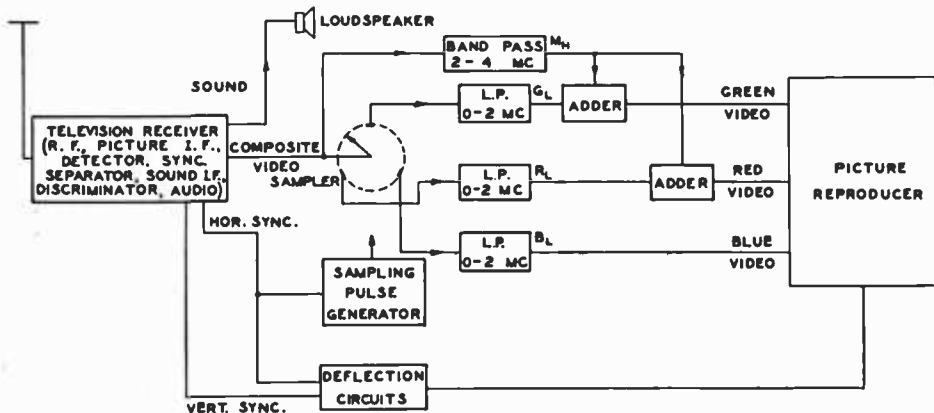


Fig. 7—Block diagram of color television receiver using by-passed highs.

Reception in Black-and-White

When the color television signal is received on a current black-and-white receiver, the output of the second detector is represented by Figure 2(h), or, when the picture is of varying color, by the envelope of Figure 3(b). With mixed highs also transmitted as shown in Figure 1, the black-and-white receiver then develops on its kinescope a black-and-white picture with full resolution. The 3.8-megacycle sine wave superimposed on the picture signal produces a dot pattern on the kinescope in high chroma areas, but the dots are not visible at normal viewing distance. Examination of Figure 2 shows that in white areas, where the dot pattern would be objectionable if present, the three color signals are of the same amplitude and the composite signal consists of the dc components only. Hence, there is no dot pattern.

For color transmissions received in monochrome on a current black-and-white receiver, no band saving is involved, but because the transmitted signal contains all the resolution which a black-and-white signal of the same scene would have, the resulting monochrome picture will have the full resolution of the current standards.

Using the standard wedge pattern to test horizontal resolution, the same resolution figure has been obtained when reproducing the color transmission on an unchanged current model black-and-white receiver as may be obtained with the same receiver on a well-designed, well-adjusted black-and-white system using present broadcast standards. The vertical resolution is also consistent with current black-and-white standards.

When a color receiver is tuned to a television broadcasting station transmitting a black-and-white signal, the picture will appear in black-and white with full resolution on the color receiver picture reproducer. The successive pulses delivered to the three kinescopes will all be of equal magnitude, and, hence, will produce varying intensities of white—or a normal black-and-white picture.

RECEIVERS AND COLOR CONVERTERS*

Picture Reproducing Systems

One method for portraying a single color picture makes use of three kinescopes, reflective optics, and dichroic mirrors in a projection system. This has been previously demonstrated and described during the Hearing in Docket No. 7896 and in References (1) and (2).

Another method also makes use of three kinescopes in a projection system but uses refractive optics and dichroics instead of reflective optics. This system appears to lend itself more readily to compact design.

A third method uses three kinescopes with a pair of dichroic mirrors so arranged to permit essentially direct viewing. This system appears to lend itself more readily to a lower cost design.

A fourth method uses two kinescopes with a single dichroic mirror. This system appears particularly attractive for use in inexpensive receivers and color converters.

Because color receivers will probably be simplified by a color picture

* The various receivers and color converters illustrated and described in this section are research models designed to test and demonstrate the basic principles of the system. While indicative of possible approaches to the design of suitable receiving equipment, they are not intended to represent receivers and color converters of commercial design.

reproducer of the single-tube type, intensive research efforts on the problem are being continued.

Direct-View Receiver

Figure 8 represents a direct-view picture-reproducing system utilizing three kinescopes which are standard in every respect except that the phosphors are green, red and blue, respectively. The green, red and blue signals are impressed on the grids of their respective tubes. The deflecting yokes of the three tubes are connected in parallel, so that the rasters produced on the three screens are identical.

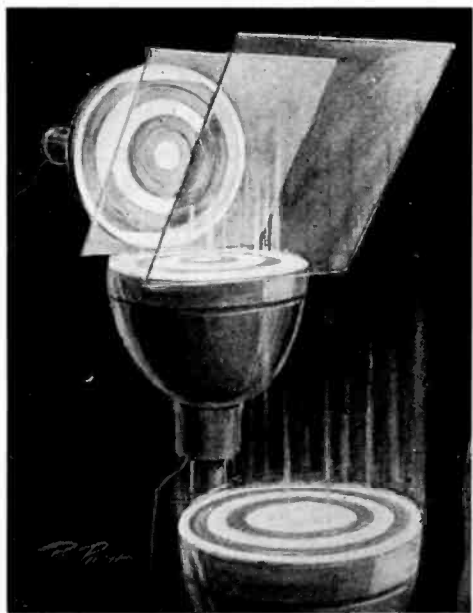


Fig. 8—Direct-view picture-reproducing system using three kinescopes and a pair of dichroic mirrors.

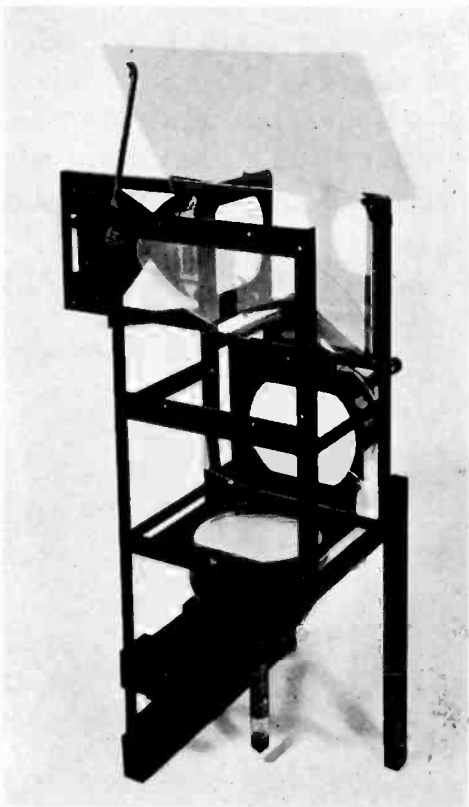


Fig. 9—Positioning of ten-inch kinescopes for direct-view picture-reproducing system.

The tubes are viewed through dichroic mirrors. The red dichroic mirror reflects the red image from the red tube, the blue dichroic mirror reflects the blue image from the blue tube, and both mirrors are transparent to green light, so that the green tube is viewed directly through both dichroic mirrors. The red dichroic mirror is also transparent to blue light, so it does not interfere with the blue image. The mirrors and tubes are properly arranged so that to the eye the three pictures appear superimposed and are viewed as one picture.

Figure 9 shows three standard-size ten-inch kinescopes and the two dichroic mirrors mounted in a framework for proper viewing from

the top, through a fully silvered mirror. A receiver using the above arrangement could be housed in a cabinet of the type shown in Figure 10. It is possible in this arrangement that, if the kinescopes are short-ended, the cabinet size can be materially reduced.

Projection Receiver

Another type of picture reproducing system is shown in Figure 11. This gives a projection picture, 15 × 20 inches. Three projection kinescopes are used which are standard except for the phosphors. Each tube control-grid is connected to the appropriate video channel, and the deflection yokes are supplied from a common source. Each tube is arranged in a reflective optical system. The light rays from each tube first strike a plane mirror, from which they are reflected to a spherical mirror of the proper focal length to produce an image on the screen. Beyond the spherical mirror the rays pass through a correcting lens and thence via a plane reflecting mirror to the projection screen.

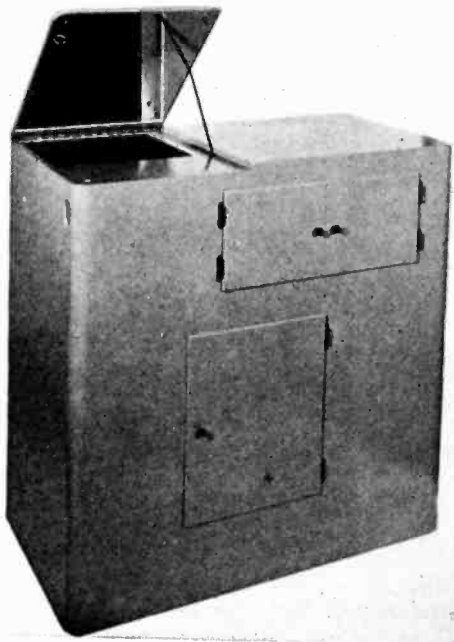


Fig. 10—One type of cabinet for direct-view receiver utilizing three kinescopes and a pair of dichroic mirrors.

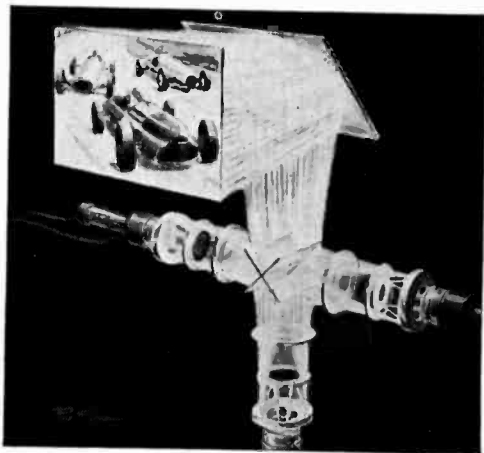


Fig. 11—Projection picture-reproducing system using three projection kinescopes, reflective optics and a pair of dichroic mirrors.

The green image passes through the red-and-blue-reflecting dichroic mirrors. The red image is reflected to the screen by the red-reflecting dichroic mirror. Similarly, the blue image is reflected to the screen by the blue-reflecting dichroic mirror. The complete optical system is so arranged that the three images are superimposed, in register and focus, on the projection screen, where they are viewed as a single color picture.

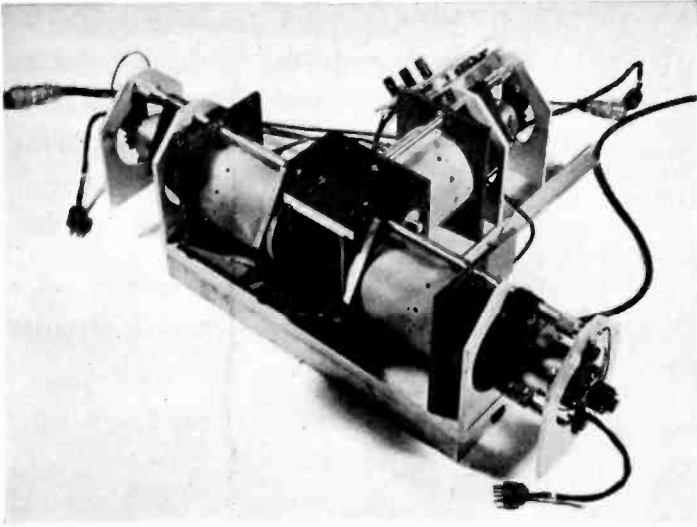


Fig. 12—Arrangement of the projection tubes and optical system used in the projection receiver.

Figure 12 is a photograph of the reflective optical system showing the mechanical arrangement of the projection tubes and the optical system. The receiver employing this system is shown in Figures 13 and 14.

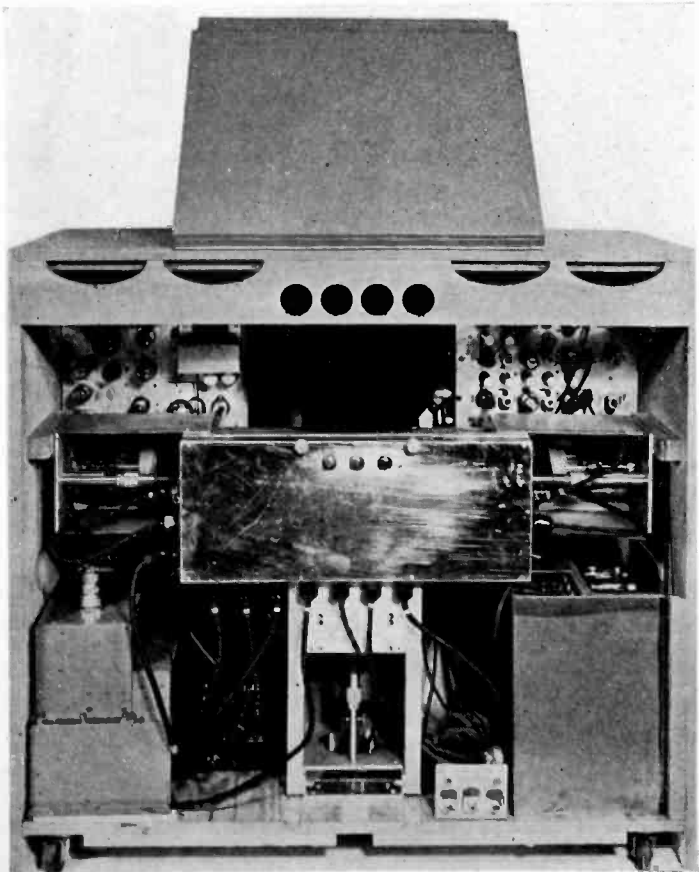


Fig. 13—Rear view of the projection receiver with 15 by 20 inch picture.

Projection Receiver with Magnifying Lens

The same type of projection picture reproducing system, referred to above, is used in the television receiver shown in Figure 15. Here the projected picture is smaller, and is viewed through a magnifying lens.

Color Converters

To convert a current black-and-white receiver to receive color transmissions in color requires the addition of color sampling circuits and a picture reproducer.

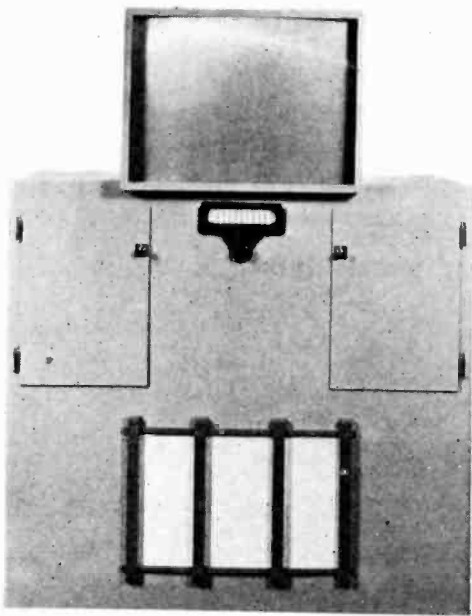


Fig. 14—Projection receiver with 15 by 20 inch picture.

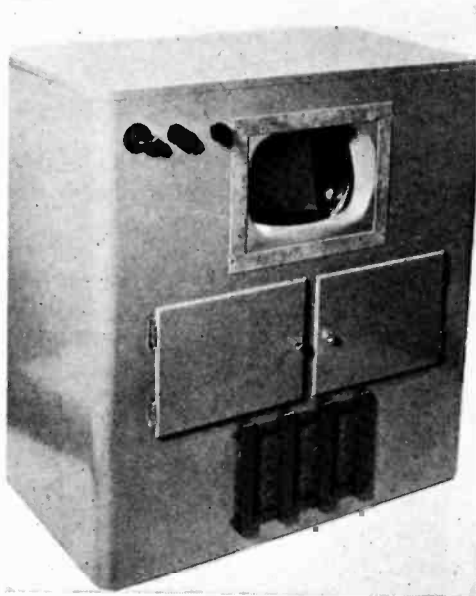


Fig. 15—Projection receiver using reflective optics and magnifying lens.

The size of the color converter for a direct-view picture or for a large projected picture is determined by the size of the kinescopes and the optical system. When the cabinet size and shape have been determined by these elements, the circuit components which need to be added to those already available in the black-and-white receiver can be fitted around the kinescopes and optical system in the cabinet without increasing its size.

A direct-view converter using three 10-inch kinescopes is shown in Figure 16. Interconnections between the standard receiver and the converter are made by a simple harness cable plugged into the tube sockets of the standard receiver. (Reduction in cabinet size through the use of shorter kinescopes, previously mentioned in connection with the direct-view color receiver, applies as well to this color converter.)

A smaller color converter can also be made which gives a projected picture. Three 1½-inch projection tubes are mounted as shown in Figure 17. The complete kinescope and optical system assembly is mounted on the back of a standard television receiver, which can be either a table model or a console. The kinescope (any size) is removed from the black-and-white receiver and the color picture is projected, through the space it occupied, to a screen mounted in the normal picture-mask opening. An additional chassis containing the sampling circuits, reflecting circuits and power supplies is mounted under or back of the television receiver.

Figure 17 shows this system as applied to a color converter, but the principles apply equally well for a color receiver.

Two-Color Systems

Color transmissions can be received on a simplified receiver which reproduces the picture in two colors only, instead of three. The two colors used are green-red and blue-green.

A block diagram of such a receiver is shown in Figure 18. This system is similar to that shown in Figure 4 except that only two video channels are required, and the method of sampling the composite signal is altered.

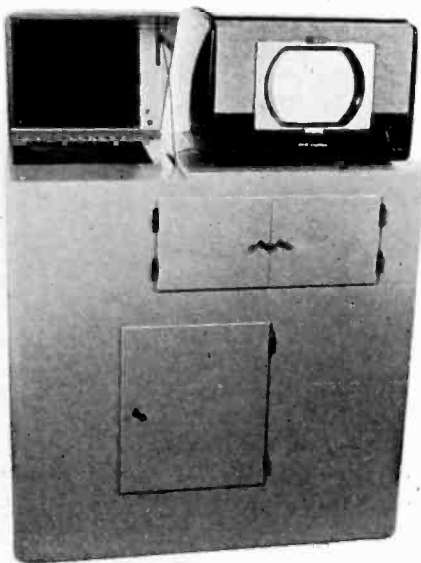


Fig. 16—Direct-view color converter.

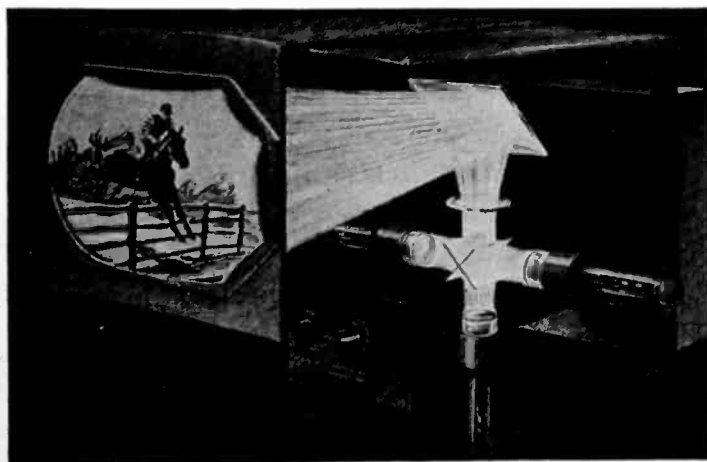
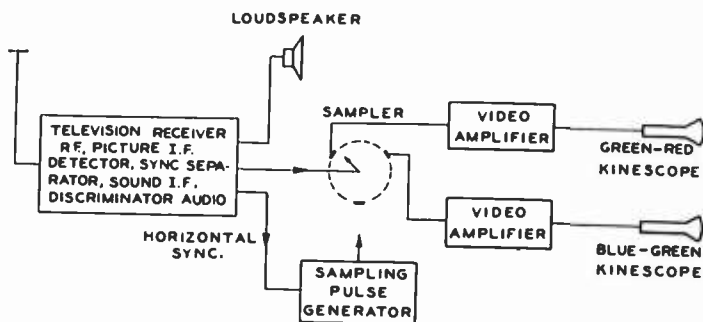


Fig. 17—Color converter using small projection kinescopes and refractive optics.

Fig. 18—Block diagram of two-color television receiver.



With reference to Figure 3, it was explained that, for the three-color system, the composite signal was sampled for green at the instant the red and blue components were passing through zero. In like manner, it was sampled for red and for blue when the other two colors in each case were zero. Figure 19 represents the same signals as Figure

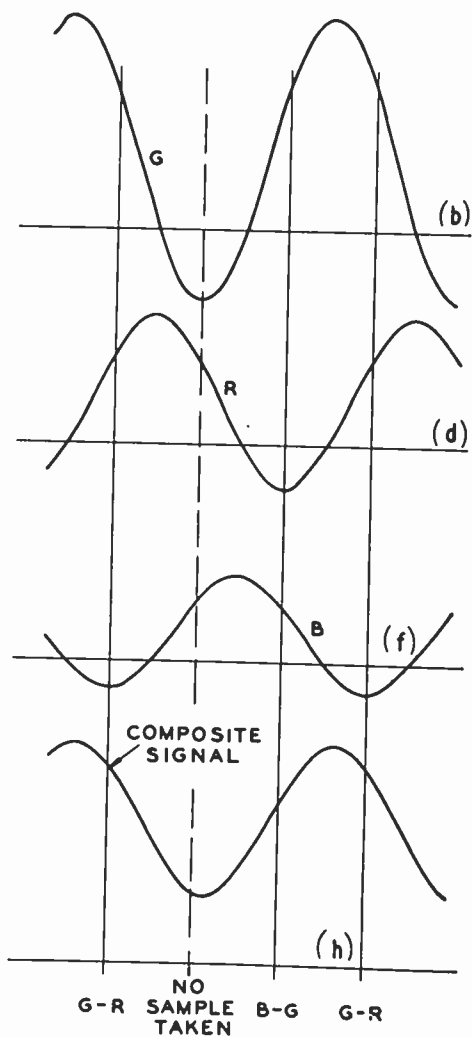


Fig. 19—Receiver sampling positions for the two-color system.

2 and shows the different positions of the sampling pulses for a two-color picture-reproducing system. The composite signal is sampled for blue-green at a time when both blue and green components are present in a positive direction. This is indicated by the line labeled *B-G*. The composite signal is sampled for green-red at a time represented by the lines marked *G-R*. As indicated in Figure 19, no sample is taken at the third point. The sampling is repeated for each of the two color combinations once each 0.263 microsecond.

After the composite signal is sampled, the two color signals are amplified in separate video amplifiers having frequency cutoff characteristics as described in connection with the three-color receiver. They are then impressed on the grids of their respective kinescopes.

In the case of a color converter for an existing black-and-white receiver, the black-and-white kinescope in the receiver is used with a

suitable color filter placed in front of it. Another kinescope is added and viewed through a dichroic mirror and suitable color filter.

The color converter employing this two-color system is shown in Figure 20. All of the components of the standard black-and-white receiver are used, including the deflecting circuits and second anode power supply. The only equipment that is added is the second kinescope and the sampling circuit. Connections between the television receiver and the color converter are few and are easily made. The foregoing points to the possibilities for a very low-cost color converter.

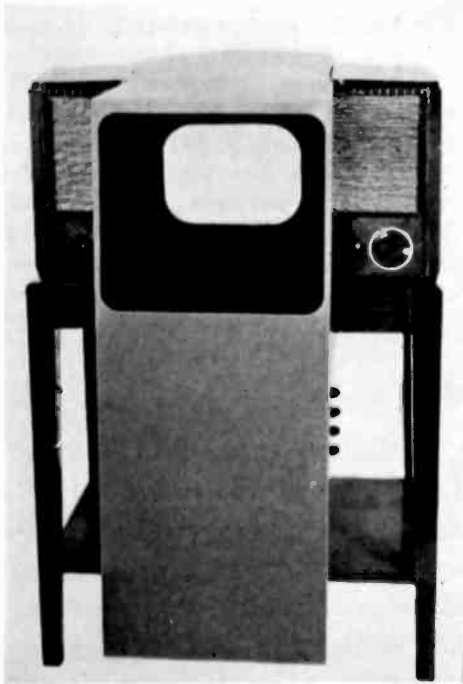


Fig. 20 — Color converter using two-color picture-reproducing system.

The principle of the two-color system is illustrated in Figure 21.

The two-color picture-reproducing system is also applicable to a simple and inexpensive color re-



Fig. 21 — Two-color picture-reproducing system.

ceiver. In this case, however, the two kinescopes will be made with the proper color phosphors and no filters are required.

SUMMARY OF SYSTEM CHARACTERISTICS

The all-electronic color television system described herein is a fully compatible system, employing the current standards of 525 lines, sixty fields per second, and line interlacing. It provides a high-definition color (and black-and-white) picture in the standard six-megacycle channel through the use of the mixed-highs principle and time-multiplexing with picture dot interlacing.

The transmitted signal is consistent with the "Standards of Good Engineering Practice Concerning Television Broadcast Stations." This is the fundamental basis for compatibility and means that a current monochrome receiver will respond in the same way as it would if a standard black-and white camera originated the picture signal.

PHOTOMULTIPLIERS FOR SCINTILLATION COUNTING*†

By

GEORGE A. MORTON

Research Department, RCA Laboratories Division,
Princeton, N. J.

Summary—The scintillation counter occupies a very important position in the nuclear field — its very short resolving time, high efficiency and energy discrimination capabilities permitting nuclear particle detection measurements which were previously impossible. The multiplier phototube is an essential element in a scintillation counter. In order to obtain maximum performance, the photomultiplier must fulfill certain requirements of photocathode geometry, electron efficiency and gain. Various commercially available multipliers are discussed in terms of these requirements. The performance of scintillation counters is analyzed in terms of the action of the photomultiplier. Photoelectric efficiency, multiplication statistics, resolving time and dark current pulse behavior are considered in some detail. An outline is given of basic multiplier power supplies and output circuits useful for scintillation counters.

INTRODUCTION

IN SPITE OF the relatively short time in which scintillation counters have been known, they have achieved a position of considerable importance as nuclear radiation detectors. As their importance increased and as more and more of them have been put into use, there has been a transition from the original qualitative pictorial understanding of their operation to a more definitely quantitative understanding.

A conventional scintillation counter is shown in Figure 1. A nuclear particle of high energy striking the phosphor crystal produces a flash of light. This light is allowed to fall on the photocathode of a secondary emission multiplier, where it produces photoelectrons. These are multiplied by the tube and give rise to a pulse at the output. The pulses at the output of the multiplier are analyzed and counted in such a way as to obtain the greatest possible amount of information about the nuclear event causing the scintillations. In addition to information on the intensity of the nuclear radiation indicated by the frequency

* Decimal Classification: (R800) 535.38.

† This work was done in part under Bureau of Ships Contract NObsr 42460. The material was written for inclusion in the Handbook of Nuclear Instruments and Techniques being prepared under the auspices of the National Research Council Committee on Nuclear Science.

of occurrence of scintillations, the flashes also can furnish information about the energy of the nuclear particles, and the time of occurrence of a nuclear event. The multiplier, as a link in the information channel between the scintillating crystal and the observer, necessarily introduces some distortion. A full understanding of the multiplier is necessary on the part of both the designer and user in order to reduce this distortion to a minimum. Furthermore, the residual distortion must be put into quantitative form so that it can be taken into account in interpreting data from a scintillation counter.

Three fundamental causes of distortion that exist in all photomultipliers are transit time effects, the statistical nature of electron multiplication and the dark current pulses. The spread in the transit time of electrons through a multiplier introduces an ambiguity as to the exact time of occurrence of a nuclear event, and limits the resolving time of the device for coincidence work and similar applications. The statistical nature of secondary emission photomultiplication means that a series of scintillations, each representing exactly the same num-

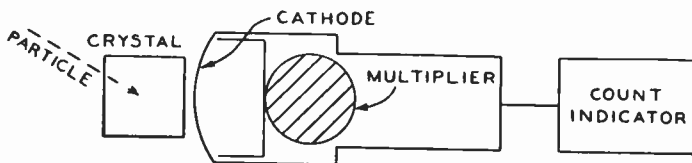


Fig. 1—Schematic of overall system.

ber of photons, will not produce a series of identical pulses at the output of the multiplier. Rather the pulse heights will be distributed statistically in a pattern characteristic of the multiplier. Finally, a multiplier in darkness generates pulses which are indistinguishable from the pulses due to scintillations under certain conditions. This can limit the ultimate sensitivity of the device for particle detection.

In addition to these fundamental effects, many practical limitations and idiosyncrasies are encountered in the secondary emission multiplier. These, as well as the basic characteristics, circumscribe the range of application of the device. In planning an experiment with a scintillation detector, all of these considerations must be taken into account.

The following discussion of photomultiplier performance, will first describe the tubes available for the work. Next, the general operating characteristics of the tubes will be considered. The fundamental effects mentioned in a preceding paragraph will be treated in some detail. Finally, some of the aspects of multiplier circuitry will be presented which may be of assistance when certain ends are to be achieved.

TYPES OF MULTIPLIER PHOTOTUBES

Of the two principal types of secondary emission multipliers, the static and the dynamic (i.e., Farnsworth Multipactor), only the former has been used to any extent for scintillation counting. Static multipliers may in turn be subdivided into several classes. Among these are the magnetically focused multipliers, the electrostatically focused multipliers and the unfocused multipliers.

The magnetic multiplier, though quite efficient, is rather critical in adjustment. Because of this it has not been widely used and is not commercially available. Since it does not play a significant role in scintillation counting, it will not be discussed further in this article. The interested reader is referred to Reference (4) for further information.

In this country the electrostatically focused multiplier is by far the most widely used tube for scintillation work. The secondary emitting plates or dynodes of this type of multiplier are so shaped that the potential distribution between two successive dynodes is such that (1) the electrons from the working surface of one strike the working surface of the next, and (2) there is a gradient at the working surface of each which draws electrons away. Other conditions which must be satisfied by the dynode shapes are that free paths between the positive collector and the photocathode or early dynodes must be avoided to prevent ion feedback, sharp points and very close spacing must be eliminated to reduce cold discharge effects, the shapes should be such that they can easily be made and assembled by mass production methods, and the general design should conform to good tube practice and the efficient utilization of space.

The unfocused multiplier has been used far more widely abroad than in this country for scintillation work. The simplest example of this form of multiplier is the Weiss type, where the dynodes are mesh screens treated to have a high secondary emission ratio. Electrons strike the wires of one screen and produce secondary electrons which are drawn through the screen to the next mesh dynode. Frequently a very transparent, fine wire screen is placed between each pair of dynodes connected to the higher potential dynode of the pair in order to improve the field conditions drawing secondary electrons away from the second screen. Another type of unfocused multiplier employs dynodes having a Venetian blind type of structure. Again screens are interposed between the dynodes to improve the field conditions. The advantage of the unfocused multiplier is that it is less affected by interference from magnetic and electric fields. It has the serious dis-

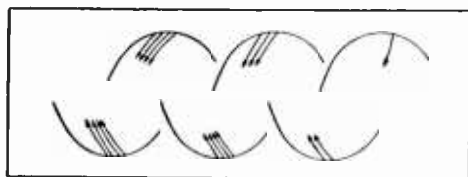


Fig. 2a—Focused multiplier.

advantage that a large fraction of electrons skip stages thereby making the pulse height distribution poorer than for a focused multiplier.

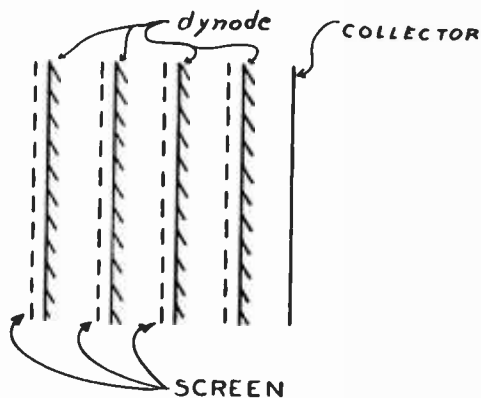


Fig. 2b—Venetian blind multiplier.

There are a number of photomultipliers suitable for scintillation work which are commercially available in this country and abroad. Some of these will be described in detail in the succeeding paragraphs.

RCA 931A—A nine stage multiplier phototube with the dynodes arranged around a center in order to economize in space. The design of this multiplier shown schematically in Figure 3. The tube has an internal photocathode on a metal electrode which is an integral part of the structure. Because of its rather small area and its distance from the glass envelope, it is rather difficult to obtain good optical coupling between the photocathode and a crystal phosphor. Other characteristics such as gain, stability, life and uniformity lend themselves well to scintillation counting. A list of the most important characteristics pertinent to scintillation counter design are given in Table I.

ECA 1P21—A multiplier identical in form and design to the 931A, but selected for gain, low dark current, stability and uniformity. (See Table I).

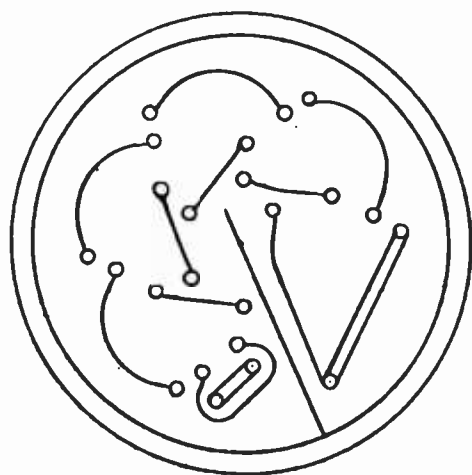


Fig. 3a—Dynode structure of 931A.

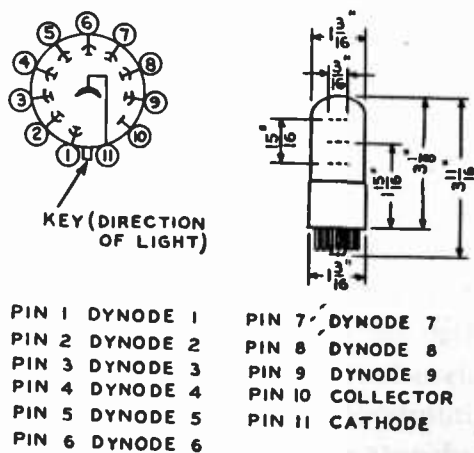


Fig. 3b—Bulb and pin arrangement of 931A.

RCA 1P28—Like the 931A in design but sealed in a Vicor envelope, which permits its use with ultraviolet radiation. (See Table I).

RCA 5819—A ten-stage head-on multiplier with a large area photocathode on the glass end of the tube. The arrangement of the cathode and dynodes is shown in Figure 4. The dynode assembly itself is the same as that of the 931A, but the electrode, which in the latter is the photocathode, is activated in such a way as to have the same secondary emission characteristics as the other dynodes and serves as first dynode. An electron optical system directs the electrons from the large photocathode to this first dynode. The size and arrangement of the photocathode makes it very suitable for optically coupling to a large phosphor crystal. It has been found to give excellent results in scintillation counting. For a listing of its most important physical and electrical characteristics, see Table I.

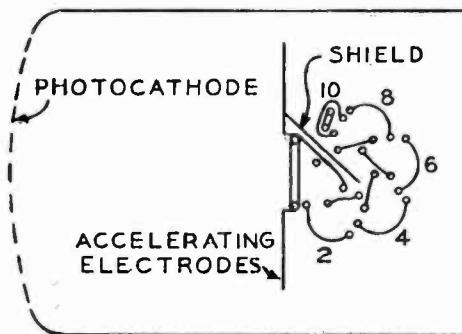


Fig. 4a—Dynode arrangement of 5819.

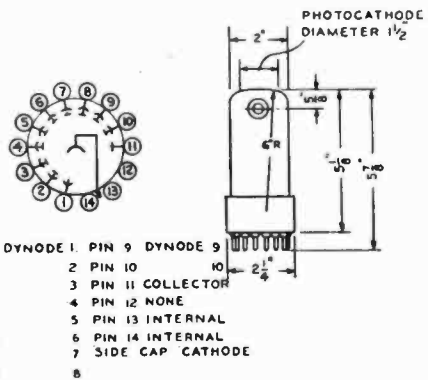


Fig. 4b—Bulb and pin arrangement of 5819.

EMI* 4588—A nine-stage Venetian blind type multiplier with a large area internal photocathode. In spite of the photocathode being an internal electrode, it is, in general, large enough to permit efficient optical coupling to a phosphor crystal. The fact that it is an unfocused multiplier means that the gain for a given overall voltage is somewhat lower than for a focused multiplier. Furthermore, the pulse height distribution is considerably broader for this type of multiplier. This will be taken up in greater detail in a later section. The general operating characteristics of this type of tube are listed in Table I.

EMI 5060—Like the EMI 4588, this multiplier employs a Venetian blind type structure. There are, however, eleven multiplying stages and the photocathode is on the glass end of the tube. The photocathode in this tube has only about 1/25 the area of that in the EMI 4588. The small area minimizes the dark current, while the on-the-glass cathode permits good optical coupling. Both of these tubes have given

* Electric and Musical Industries, Ltd., Great Britain.

Table I—Characteristics of commercial photomultipliers.

Tube Type	RCA 931A	RCA 1P21	RCA 1P22	RCA 1P28	RCA 5819	EMI 4588	EMI 5060	EMI 5311
Photo-cathode	internal 1.9 cm ² S-4 4000 A° 7000 A° 10 μa/1	internal 1.9 cm ² S-4 4000 A° 7000 A° 40 μa/1	internal 1.9 cm ² S-8 4200 A° 8000 A° 3 μa/1	internal 1.9 cm ² S-5 3400 A° 7000 A° 15 μa/1	tube end 11 cm ² S-9 4800 A° 7000 A° 40 μa/1	internal 20 cm ² like S-4 — — 40 μa/1	tube end 0.7 cm ² like S-9 — — 20 μa/1	tube end 5 cm ² like S-9 — — 20 μa/1
area	1.9 cm ²	1.9 cm ²	1.9 cm ²	1.9 cm ²	11 cm ²	20 cm ²	0.7 cm ²	5 cm ²
spectral class	S-4	S-4	S-8	S-5	S-9	like S-4	like S-9	like S-9
peak response	4000 A°	4000 A°	4200 A°	3400 A°	4800 A°	—	—	—
longwave cutoff	7000 A°	7000 A°	8000 A°	7000 A°	7000 A°	—	—	—
sensitivity	10 μa/1	40 μa/1	3 μa/1	15 μa/1	40 μa/1	40 μa/1	20 μa/1	20 μa/1
number of stages	9	9	9	9	10	9	11	11
volts per stage	100	100	100	100	90	150	160	160
average gain	10 ⁶	2 × 10 ⁶	2 × 10 ⁵	2 × 10 ⁵	6 × 10 ⁵	~10 ⁶	10 ⁷	10 ⁷
Capacity	coll. to last dynode 4 μμf	4 μμf	4 μμf	4 μμf	5 μμf	—	—	—
	coll. to total structure 6.5 μμf	6.5 μμf	6.5 μμf	6.5 μμf	8 μμf	—	8 μμf	—
Voltage	overall (maximum) 1250	1250	1250	1250	1250	1500	—	—
	coll. to last dynode 250	250	250	250	150	150	180	180
Current	coll. (maximum, average) 1.0 ma	.1 ma	1.0 ma	2.5 ma	.75 ma	1 ma	1 ma	1 ma
	dark current .25 μa	<.1 μa	.25 μa	—	.05 μa	.03 μa	.01 μa	.1 μa
Dimensions	length 3 1/16"	3 1/16"	3 1/16"	3 1/16"	5 7/8"	~10"	8 3/8"	8 3/8"
	diameter 1 5/16"	1 5/16"	1 5/16"	1 5/16"	2 1/4"	2"	2"	2"

excellent results in scintillation counting. Working data on the EMI 5060 is given in Table I.

EMI 5311—Like EMI 5060 but with large photocathode.

PHOTOCATHODE AND ELECTRON COLLECTOR SYSTEM

The photocathode and electron optical system for directing the photocurrent to the first dynode must meet the most exacting requirements of the entire multiplier. Losses here, as with those in the first stage of a high sensitivity amplifier, contribute directly to poor signal-to-noise ratio, bad statistics, etc. Therefore, the utmost care must be exercised in designing these parts. Furthermore, in using a multiplier nothing must be done which interferes with the efficient operation of these elements.

An intermetallic compound, Cs_3Sb , forms the basis of the photocathodes of the six multipliers described in the preceding section. The material is probably an internal photoemitter, by which is meant photons absorbed within the volume of the film are effective in producing external photoemission. The peak of its spectral response is in the violet and its long wavelength cut-off above 6500 angstrom units. This means that its work function is quite high and consequently its thermionic emission small. The quantum efficiency of this photocathode is the highest of any material known. The surface is prepared in two ways, namely the caesium-antimony may be deposited on a metal surface giving the S-4 (used in 931A, 1P21, EMI 4558) spectral characteristic or it may be coated on a transparent glass layer forming the semitransparent S-9 emitter (used in 5819, EMI 5060). The S-5 (used in 1P28) ultraviolet material is identical with the S-4 but is in an ultraviolet transmitting glass envelope.

The spectral response of the S-4 surface is shown in Figure 5. Its peak response is at approximately 4000 angstrom units. The quantum efficiency, γ , at this wavelength is about 0.3 per cent per microampere per lumen measured with a tungsten source at 2870 degrees Kelvin color temperature. Thus if a photosurface gives 30 microamperes per lumen its quantum efficiency will be 9 per cent. In other words, one photon of each 11 causes the release of a photoelectron. Photosensi-

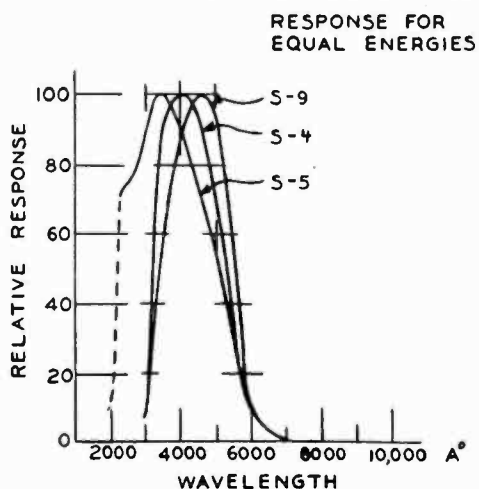


Fig. 5—Photocathode spectral response curves.

tivities as high as 100 or more microamperes per lumen have been reported for these surfaces.

The quantum efficiency for radiation of wavelengths other than that corresponding to the peak response can be determined with the aid of the spectral response curves. Since these are given on an equal energy basis, a correction must be made for the difference in wavelength. Thus the quantum efficiency, γ_λ , to be determined will be

$$\gamma_\lambda = \gamma_{\lambda_0} \cdot \frac{R_\lambda}{100} \cdot \frac{\lambda_0}{\lambda}$$

where λ = wavelength of radiation in question,
 λ_0 = wavelength of peak response,
 R_λ = response at wavelength λ ,
 γ_{λ_0} = quantum efficiency at peak response.

The room temperature thermionic emission is important in determining the dark current pulse performance of a photomultiplier. Measurements indicate that the S-4 surface emits about 10^3 electrons per square centimeter at 30 degrees centigrade. The emission approximately doubles for each 10-degree rise in temperature.

As has already been pointed out, the S-5 surface is identical with the S-4 except for the glass enclosing it. The spectral response of a tube using the S-5 combination is shown in Figure 5. The thermionic characteristics are of course exactly the same as those for the S-4 surfaces.

Although the S-9 surface is also a Cs_3Sb film, its characteristics differ somewhat from the S-4 photoresponse. This is primarily due to the filtering action of the material on radiation passing through both the emitting material and the semitransparent conducting film which backs it up. The thinness of the photoactive layer may also in part cause the difference in the response characteristic. The spectral response of a typical S-9 surface is given in Figure 5. The exact position of the response is quite variable since a variety of backing layers may be used. For the 5819 the peak response is at about 4800 angstrom units. However, for some on-the-glass caesium-antimony photocathodes it may be below 4500 angstrom units. The quantum efficiency for this response is lower than for the S-4 being about 0.2 per cent per microampere per lumen. A surface measured as 25 microamps per lumen will give a photoelectron for one photon out of every 20, that is 5 per cent quantum efficiency. There is some indication that the thermionic emission for this surface may be very slightly lower than for the S-4

surface. The difference, however, is so small as to be of little or no practical importance.

The silver-caesium oxide-caesium S-1 photosurface has been used in photomultipliers. The peak of response for such surfaces is between 8000 and 9000 angstrom units and the long wave cut-off 10000 to 14000 angstrom units. However, the quantum efficiency is much lower, and a surface having a sensitivity of 40 microamperes per lumen has a quantum efficiency of only 0.4 per cent. Furthermore, the thermionic emission from such surfaces is many orders of magnitude higher than for the caesium-antimony photoemitters (i.e., $> 10^6$ electrons per second per square centimeter). For these reasons they have not been widely used for scintillation counting.

High photosensitivity alone does not suffice to ensure that a multiplier will be entirely satisfactory for scintillation work. It is quite possible for two multipliers to have the same photocathode sensitivity and the same measured gain, and for one to exhibit excellent statistical characteristics so that it gives a narrow range of pulse heights for scintillations from mono-energetic particles, while the other shows poor statistical properties and produces a very broad band of pulse heights under the same conditions. This will occur when a large percentage of the photoelectrons are collected and multiplied in one multiplier and a large fraction lost in the other.

Primarily the efficient collection of photoelectrons is a problem of multiplier design. However, it is possible for a correctly designed multiplier to be operated in such a way that a large fraction of the photoelectrons is lost. One cause of loss is inadequate voltage between the photocathode and first dynode. Figure 6 shows the effect of this voltage on collection efficiency for different points of illumination of the photocathode in the case of the 931A. Another cause of poor photoelectron collection is the presence of magnetic field. The interfering field may be the result of external causes or due to parts of the multiplier being magnetized. If the former, it can be corrected by shielding or by compensating coils, if the latter, the multiplier must be demagnetized. This can be done by passing the tube a few times through a coil carrying alternating current.

It is not difficult to measure the photoelectron collection efficiency

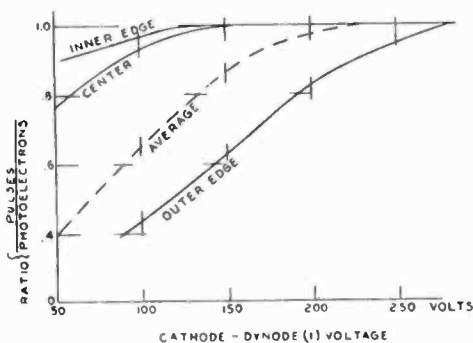


Fig. 6—Collection as function of voltage (931A).

of a multiplier, and it is advantageous to make this measurement when setting up a critical scintillation counter experiment (e.g. a scintillation spectrometer, etc.). This information, together with a knowledge of the quantum efficiency of the photocathode and the statistics of multiplication is necessary to interpret the data from measurements.

To carry out an efficiency measurement it is necessary to know the gain of the multiplier. Methods of measuring multiplier gains will be discussed in the next section. With the gain G and the output current i_o of the multiplier when a small amount of light is allowed to fall on the photocathode, the number of photoelectrons, n_p , leaving the cathode is determined from the expression

$$n_p = \frac{i_o}{eG}.$$

Next an integrated pulse height curve is determined, the multiplier being operated under the same conditions of illumination and gain. This type of curve is measured with the aid of an amplifier, a pulse height discriminator which passes all pulses above a preset and adjustable amplitude, and a scaler or register. The number of pulses per second as a function of pulse height is measured and plotted. These measurements cannot be extended to zero pulse height because of amplifier noise, however, the curve can be extrapolated to zero pulse height, giving the number of pulses per second n'_p which exceed zero pulse height. If the collection of photoelectrons were perfect, n'_p would equal n_p . In practice n'_p will be less than n_p and the ratio $= n'_p/n_p$ is the efficiency η_p of photoelectron collection. Normally this ratio ranges in value from 50 to 90 per cent depending upon the multiplier and conditions of operation.

MULTIPLIER GAIN

For practical scintillation counting, the gain of the multiplier should not be less than a few hundred thousand and preferably should be one or more orders of magnitude higher. If, for example, the multiplier gain is 3×10^5 and the total output capacity 10 micro-microfarads, one electron from the photocathode will give a pulse of 5 millivolts. A pulse appreciably smaller than this is difficult to amplify with the type of wide band amplifier required for scintillation work. On the other hand, if the multiplier gain is 10^9 the pulse will be 15 volts, and it may be possible to dispense with an amplifier ahead of the pulse height selector and counting system.

The gain of a multiplier depends upon the secondary emission ratio,

σ , of the dynodes, the efficiency, η , of transfer of electrons from one stage to the next and the number of stages, m . Thus the average gain G of a multiplier will be

$$G = (\eta\sigma)^m.$$

The secondary emission ratio depends upon the material and processing of the dynode and upon the bombarding voltage of the primary electrons. The secondary emission ratios of a number of surfaces commonly employed as dynodes are shown in Figure 7. For antimony-caesium used in most of the multipliers described above, the ratio is about 4 at 100 volts bombarding voltage and almost 6 at 150 volts.

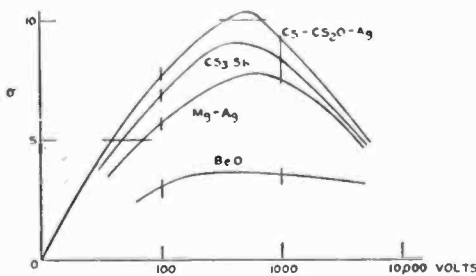


Fig. 7—Secondary emission ratios.

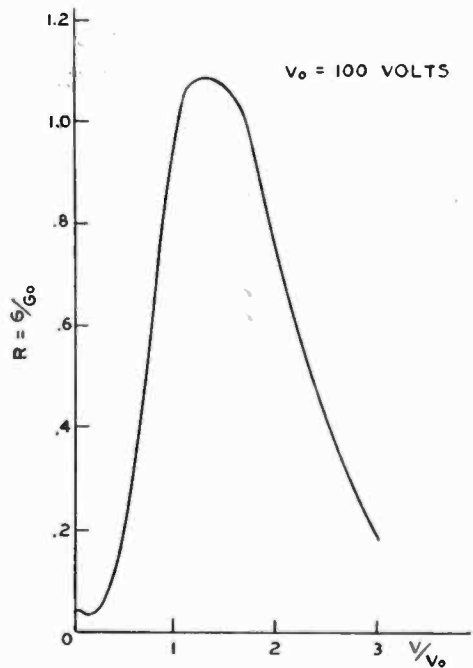


Fig. 8—Focusing curve (931A).

In a focused multiplier the transfer efficiency, η , is close to unity when the tube is operated with the correct voltage ratios. An unfocused multiplier in general will have a much lower transfer efficiency (i.e. around 60 per cent). If the voltage ratios between stages in a focused multiplier are not correct the transfer efficiency falls very rapidly. The curve given in Figure 8 illustrates the effect on efficiency when the voltage on one dynode is changed for a multiplier of the type 931A. For most purposes this critical focus is disadvantageous in that it places rather stringent requirements on the resistive voltage divider generally used to supply the dynodes. However, this property can be advantageously used to stabilize the gain against overall voltage changes, as will be described in the section discussing multiplier circuitry.

If the secondary emission ratio were proportional to the primary voltage, so that

$$\sigma = kV,$$

the total gain of a multiplier would be expressed as follows:

$$G = \sigma^m = k^m \left(\frac{V_o}{m + 1} \right)^m$$

where V_o is the overall voltage.

This relation holds for low voltage but it will be seen from Figure 7 that the secondary emission ratio, σ , begins to increase less rapidly than indicated by this expression at bombarding energies considerably below 100 volts. Over the range where this relation is applicable the fractional change, in terms of a change in voltage, will be

$$\frac{\Delta G}{G} = m \frac{\Delta V}{V}.$$

Thus for a nine stage multiplier a 1 per cent change in voltage would produce a 9 per cent change in gain. At the normal operating voltage of 100 volts per stage a 1 per cent change in voltage causes about a 7 per cent change in gain because of the rounding off of the secondary emission curve.

Since the percentage change in gain is 7 times as great as the percentage change in overall voltage, the power supply used with the multiplier must have very good regulation, where the experiment demands high multiplier stability. Suitable power supplies will be discussed in a later section.

It is frequently useful to be able to measure the gain of a multiplier. In general, the measurement cannot be made simply by putting current meters in the input and output leads, because even when the output current is the maximum permitted for the multiplier, the input current will be too small to be conveniently measured. One method of making the determination is as follows:

First the multiplier is operated with a low overall voltage (e.g. 300 to 500 volts) so that the gain is in the neighborhood of 1000. At this low gain the input and output current can be measured with no great difficulty. For example, a given amount of light may produce 100 microamperes at the output with an input current of 0.1 microampere. The light is then reduced until the output current is 0.1 microampere. The input current will then be 10^{-10} ampere since the (low) gain remains unchanged. Next, leaving the illumination the same, the voltage on the multiplier is increased until it is operating

under normal conditions, and the output current again measured. In the example cited above, the output current might be found to be 90 microamperes. The average gain G is therefore $90 \times 10^{-6}/10^{-10} = 0.9 \times 10^6$. In other words, the average gain is the measured output current divided by the calculated input current.

Other methods of making gain measurements will occur to the reader. For example, the gain of the first $m/2$ stages may be measured as one operation and then that of the remaining stages as a second separate operation. The total gain will of course be the product of the two partial gains.

In making gain measurements, care must be taken to correct for dark current and electrical leakage. This can usually be done by taking the difference in current in the lead being measured when the photocathode is illuminated and when it is in darkness. Excessive dark current can almost always be reduced by cooling the tube.

It should be pointed out that a different type of gain may be defined for a multiplier. This is the gross gain G' or gain experienced by the electrons actually entering the multiplier. The gross gain is determined from n'_p , the number of electrons actually entering the multiplier and the output current i_o by the following relation:

$$G' = \frac{i_o}{en'_p}$$

Clearly the gross gain is related to the average gain G as follows:

$$G/G' = n'_p/n_p = \eta_p$$

The concept of a gross gain is useful when considering the electron statistics of a multiplier, discussed in the next section.

STATISTICAL CONSIDERATIONS

The secondary emission ratio, σ , and the gain, G , have, in the preceding paragraphs, been referred to as definite values. Actually the secondary emission ratio and consequently the gain are statistical quantities. A primary electron striking a dynode has a certain probability $P(Z)$ of producing Z electrons, the expectation for this distribution being the secondary emission ratio, σ . There is reason to believe that the distribution may be close to a Poisson distribution. However, experimental data is not yet available which establishes with certainty the distribution law followed by secondary emission.

Assuming a Poisson distribution law to be applicable, the probability that a primary electron will produce exactly Z secondary electrons when the secondary emission ratio is σ is

$$P(Z) = \frac{e^{-\sigma} \sigma^Z}{Z!}.$$

For such a distribution the root mean square deviation is $\sqrt{\sigma}$.

The properties of the distribution obtained by cascading stages each having a Poisson distribution can be found by setting up a suitable generating function and solving it for the various statistical moments. If the number of electrons entering a multiplier is δ with a root mean square deviation of $\sqrt{\delta}$ and the dynodes have a secondary emission ratio σ , the fractional mean square deviation of the output will be

$$\frac{\overline{\Delta Z^2}}{Z^2} = \frac{1}{\delta} \frac{\sigma^{m+1} - 1}{\sigma^m (\sigma - 1)} \approx \frac{1}{\delta} \frac{\sigma}{\sigma - 1}.$$

It will be noticed that the fractional square deviation is simply the mean square deviation of the entering electrons $\frac{1}{\delta}$ increased by the amount $\frac{\sigma}{\sigma - 1}$ due to the effect of the multiplier.

Where the secondary emitting surfaces are dynodes of a multiplier with effective secondary emission ratio σ , the root mean square deviation may be $\sqrt{\epsilon \sigma}$ instead of $\sqrt{\sigma}$ (due either to focusing losses in the multiplier or to the distribution being other than that assumed above). Under these circumstances the fractional square deviation becomes:

$$\frac{\overline{\Delta Z^2}}{Z^2} = \frac{1 - \epsilon}{\delta} + \frac{\epsilon}{\delta} \frac{\sigma}{\sigma - 1} = \frac{1}{\delta} \left(1 + \frac{\epsilon}{\sigma - 1} \right).$$

The coefficient ϵ can be evaluated from an integrated pulse height distribution curve for photoelectrons, such as mentioned in a preceding section. If the standard deviation for secondary emission is $\sqrt{\sigma}$ the fractional square deviation of this curve will be:

$$\frac{\overline{\Delta Z^2}}{Z^2} = \frac{1}{\sigma} \frac{\sigma}{\sigma - 1} = \frac{1}{\sigma - 1}.$$

On the other hand, if the standard deviation is instead $\sqrt{\epsilon\sigma}$, the fractional square deviation becomes

$$\frac{\overline{\Delta Z^2}}{Z^2} = \frac{\epsilon}{\sigma - 1}$$

By measuring the deviation of the photoelectron pulse height distribution and comparing it with $\frac{1}{\sigma - 1}$, the coefficient ϵ can be determined.

PHOTOELECTRON PULSE HEIGHT DISTRIBUTION CURVE

The integrated pulse height distribution curve is sufficiently valuable in giving information about the performance of a multiplier in a scintillation counter chain to warrant further discussion. It has already been pointed out that the number of electrons n'_p actually

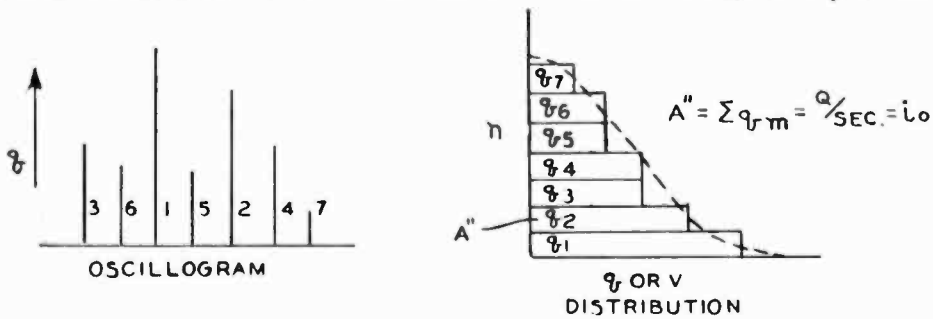


Fig. 9—Construction of distribution curve.

entering the multiplier can be determined by extrapolating this type of distribution curve to zero pulse heights. The integrated distribution can also be used to calibrate the amplifier and count indicator in terms of electrons entering the multiplier as well as to determine the multiplier distribution characteristics.

Consider for the moment the significance of the distribution curve in terms of the way in which it is made. Suppose the method of measurement consisted of observing the pulse heights on an oscilloscope. The series of pulses in a particular unit of time (e.g. one second) might have the appearance shown in Figure 9. An integrated distribution curve for these pulses would be constructed as shown in the figure and really amounts to an ordering of the individual pulses in terms of their height. Normally, these pulses would be measured in terms of volts at the pulse height selector, and they each represent a certain charge, q_k , coming out of the multiplier. The relation between the pulse height in volts, V_k , and q_k is

$$q_k = \frac{C}{A} V_k,$$

where

C = effective input capacity,
 A = amplifier gain.

If the pulse height distribution curve is given in terms of the number of units of charge in the pulse rather than the voltage of the pulse, it is evident that the area under the curve represents the total charge output from the multiplier per unit time, or, in other words, the area is equal to i_o , the output current. While in actuality, each pulse, irrespective of the charge at the output, is the result of a single electron entering the multiplier and being multiplied by a gain which varies from electron to electron due to its statistical nature, the output pulses can equally well be thought of as being the result of electrons of different sizes entering the multiplier and being multiplied by a constant gain. The distribution curve could therefore be plotted in terms of the effective fraction ρ_k of an electron entering the multiplier and being multiplied by a gain G' which gives the observed charge q_k at the output. Since ρ on the average must be one, it is clear that the area under the curve plotted in this way must be equal to n'_p . The following sets of relations will help to clarify this point:

$$\rho_k = q_k / eG', \quad A'' = \sum q_k = i_o,$$

$$A' = \sum \rho_k = \frac{\sum q_k}{eG'} = \frac{i_o}{eG'} = n'_p,$$

where

A'' is area under distribution curve in terms of output charge,

A' is area under distribution curve in terms of electrons ρ .

If now the integrated pulse height distribution curve is taken in the normal way and plotted in terms of pulse height in volts, the number of volts corresponding to one electron from the photocathode is found simply by taking the area under the distribution curve in volts counts per second and dividing it by n'_p .

There is considerable advantage to be gained in plotting scintillation pulse heights distribution curves in terms of electron heights, ρ . This makes the results independent of the amplifier and multiplier gain and also of the coupling circuit between the collector and amplifier input. Also, as is evident from arguments given above, this way of

plotting data permits an immediate evaluation of δ needed for the determination of the multiplier electron statistics.

A typical photoelectron distribution curve for a 5819 is given in Figure 10. Here n'_p is 5540 counts per second, and the area under the curve is 149000 volts counts per second. Therefore, the pulse height produced on the average by a single electron entering the multiplier is 27 volts. The curve can now be plotted in terms of electron heights as abscissas. This scale has been marked on the figure.

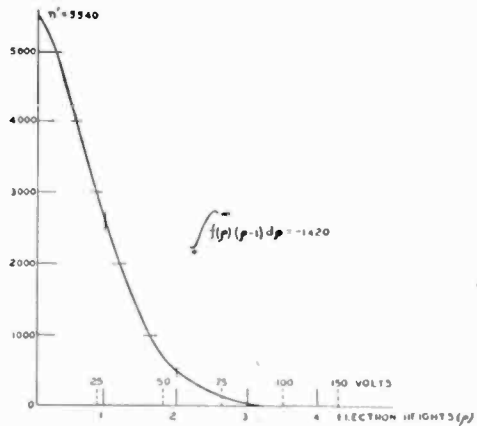


Fig. 10 — Photo-electron pulse height distribution.

To evaluate ϵ for the statistical correction factor $\left(1 + \frac{\epsilon}{\sigma - 1}\right)$

it is merely necessary to find the mean square deviation of the normalized derivative curve corresponding to the integrated curve of the type shown in Figure 14. In other words, if the figure represents $n = f(\rho)$ then

$$\frac{\overline{\Delta Z^2}}{Z^2} = \frac{\epsilon}{\sigma - 1} = \frac{1}{n'_p} \int_0^\infty -f'(\rho) (\rho - 1)^2 d\rho.$$

It is not necessary to actually perform this operation. Instead the following shortcut may be employed:

Integrating by parts

$$\int_0^\infty u dv = uv \Big|_0^\infty - \int_0^\infty v du,$$

where

$$\begin{aligned} u &= (\rho - 1)^2 & du &= 2(\rho - 1) d\rho \\ dv &= -f'(\rho) d\rho & v &= -f(\rho). \end{aligned}$$

Hence

$$\frac{1}{n'_p} \int_0^\infty -f'(\rho) (\rho - 1)^2 d\rho = - \frac{(\rho - 1)^2}{n'_p} f(\rho) \Big|_0^\infty +$$

$$\frac{2}{n'_p} \int_0^\infty f(\rho) (\rho - 1) d\rho = 1 + \frac{2}{n'_p} \int_0^\infty f(\rho) (\rho - 1) d\rho.$$

The integral $\int_0^\infty f(\rho) (\rho - 1) d\rho$ can readily be evaluated from Figure 14 by picking off appropriate values of $f(\rho)$ at equal increments $\Delta\rho$ and multiplying by the various values of $(\rho - 1)$ and summing.

Carrying out the evaluation for a Type 5819 multiplier operating at a gain of 10^6 , the value for ϵ is found to be 1.54.

To illustrate the application of the methods outlined in the preceding sections to the general problem of scintillation measurements consider again the system illustrated in Figure 1. Here the crystal is being bombarded with 0.600-megavolt β -rays. The crystal produces one photon for each 50 electron volts of energy. Thus 12000 photons are produced. Approximately $\frac{1}{3}$ of these reach the photocathode. If the latter has a photosensitivity of 30 microamperes per lumen, its quantum efficiency is 6 per cent and 240 electrons will be released. The ratio n'_p/n_p in the multiplier may be taken as 0.5. This means that 120 photoelectrons will enter the multiplier. The fractional

deviation of this number is $\frac{1}{\sqrt{120}} = 9$ per cent. The deviation is increased by the factor $\left(1 + \frac{\epsilon}{\sigma - 1}\right)^{\frac{1}{2}}$. If the multiplier has 10 stages

and a gain $G = 10^6$ the secondary emission ratio is $\sigma = 4$. The coefficient ϵ has been determined for a 5819 and found to have a value 1.54. This means that the deviation will be increased by about 25 per cent. In other words the output pulse distribution will have a root mean square deviation of 11.2 per cent. Therefore, the pulse height distribution curve obtained from the monochromatic 0.600-megavolt β -rays would be a peak with a root mean square deviation of 11 per cent.

Another example is in the case of determining a figure of merit for phosphor screens used in α particle detection. A distribution curve is obtained for a particular monochromatic source which has a maximum corresponding to 150 electrons and a half height width of 50 electron heights. This means that the root-mean-square deviation is about 25 electron heights out of 150 or 17 per cent. The standard deviation of the 150 electrons entering the multiplier is 8.2 per cent and the enhancement factor 1.25 making the total width 10.1 per cent. The standard deviation of the screen alone is therefore $\sqrt{17^2 - 10^2} \sim 14$ per cent. A 14 per cent root-mean-square deviation means that the

phosphor screen is quite good and entirely suitable for most applications.

So far the analysis has been confined to distributions which are of the form of single peaks. To round out the discussion, the problem of analyzing a general distribution will be considered very briefly.

Assume that a general distribution has been measured with a scintillation counter giving a derivative distribution curve of pulse heights $n = F(\rho)$. The multiplier distribution curve of number of pulses of height ρ when p electrons enter the multiplier is measured to be: $f(p, p - \rho)$. Further, let it be assumed that the true function giving the photon distribution is $n = G(p)$, which is to be determined. Then, the relationship between the quantities is given by the following

integral equation: $F(\rho) = \int_0^\infty G(p) f(p, p - \rho) dp$. Both $F(\rho)$ and $f(p, p - \rho)$ are empirical quantities which have been determined during the course of the measurements. It would be necessary, therefore, to evaluate the above integral equation by graphical or numerical methods which is a very difficult and frequently impossible problem.

It is possible to make certain approximations and simplifications which lead to a much less cumbersome equation relating the above quantities, yet capable of giving quite good results. The function $f(p, p - \rho)$ can, in general, be fairly closely approximated by a Gaussian

$$f(p, p - \rho) = \frac{1}{\sqrt{2\pi k\rho}} e^{-\frac{(p - \rho)^2}{2k\rho}}$$

where $1/k$ is the enhancement factor $\left(1 + \frac{\epsilon}{\gamma - 1}\right)$. This assumes that p and ρ are large compared with unity. Hence:

$$F(\rho) = \int_0^\infty \frac{G(p)}{\sqrt{2\pi k\rho}} e^{-\frac{(p - \rho)^2}{2k\rho}} dp.$$

If now the variables are transformed by $x = p - \rho$ and it is assumed that the integrand is zero except for x small (which is obviously the case if the multiplier statistics are good), the following approximation is valid:

$$F(\rho) \cong \int \frac{G(\rho + x)}{\sqrt{2\pi k\rho}} e^{-\frac{x^2}{2k\rho}} dx.$$

Next, G is expanded in powers of x and integrated, giving

$$F(\rho) \cong \frac{1}{\sqrt{2\pi k\rho}} \sum_{n=0}^{\infty} G^{2n}(\rho) \frac{(k\rho)^n}{(2n)! 2^n n!}$$

Finding the successive derivatives of $F(\rho)$ with respect to ρ and simplifying leads to:

$$F(\rho) = G(\rho) + \frac{k\rho}{4} G''(\rho) + \frac{(k\rho)^2}{192} G^{IV}(\rho) + \dots$$

$$F'(\rho) = G'(\rho) + \frac{k}{4} G''(\rho) + \frac{k\rho}{4} G^{III}(\rho) + \frac{k^2\rho}{96} G^{IV}(\rho) + \dots$$

$$F''(\rho) = G''(\rho) + \frac{k}{2} G^{III}(\rho) + \left(\frac{k\rho}{4} + \frac{k^2}{96} \right) G^{IV}(\rho) + \frac{k^2\rho}{48} G^V(\rho) + \dots$$

$$F^{III}(\rho) = G^{III}(\rho) + \frac{3k}{4} G^{IV}(\rho) + \dots$$

Solving these simultaneous equations, the following first approximation can be readily obtained:

$$G(\rho) = F(\rho) - \frac{k\rho}{4} F''(\rho)$$

$$G'(\rho) = F'(\rho) - k/4 F''(\rho)$$

$$G''(\rho) = F''(\rho) - k/2 F^{III}(\rho)$$

$$G^{III}(\rho) = F^{III}(\rho) - 3/4 F^{IV}(\rho).$$

Higher approximations can be found if the particular circumstances make it advisable. Usually, however, the two terms of the above approximation give all the accuracy that most data will warrant.

NOISE PULSE DISTRIBUTION

For certain applications the dark current pulses generated by a multiplier will set a definite limit to what can be done with a scintillation counter. This occurs for example when the wanted pulses are very infrequent, when the energy of the particles producing the scintillations is small, or when a very large or remote crystal is being used.

Within limits, the dark current itself does not interfere with scintillation counting. Rather, it is the fluctuations in this current which are harmful. The dark current is the sum of several contributing causes. The first and most basic source is thermionic emission from the photocathode. The thermionic electrons are multiplied by the succeeding dynodes exactly as are photoelectrons. Second, any small amount of residual gas left in the tube may become ionized and give rise to dark current. Third, sharp points or edges at any of the electrodes may lead to field emission due to high gradients. Finally, electrical leakages, either ohmic or nonohmic, over insulating surfaces which support the multiplier parts will contribute to the dark current.

Thermionic electrons from the photocathode give rise to a pulse height distribution which is exactly the same as the photoelectron distribution discussed in preceding sections. The dynodes may also be thermionic emitters and these electrons will also be multiplied, but, depending upon which dynode is the source, they are amplified by less than the full gain of the multiplier and thus give rise to small pulses. Field emission can also give rise to pulses, but in general, these pulses will be small (unless there is actual sparking in the tube) since the emitted electrons are not multiplied by the full gain of the tube. Ions, on the other hand, may give rise to pulses which are considerably larger than those due to thermionic emission. This occurs when positive ions are accelerated back to the photocathode and cause the emission of several electrons at once. Ohmic leakage in general contributes almost nothing to the pulse output.

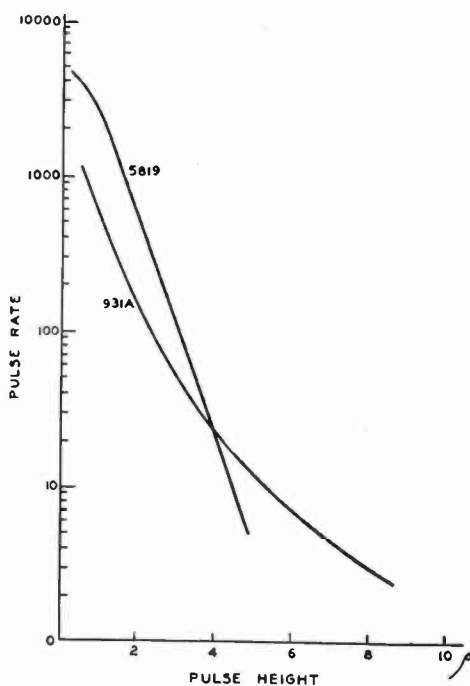


Fig. 11—Noise pulse distribution.

The dark pulse output of the RCA 931A type, and the 5819, are shown in Figure 11. It will be noticed that some of these curves are different from the photoelectron distribution curves. This is not surprising since they may include a large number of small pulses due to electrons originating from later stages of the multiplier, as well as large pulses due to ions and other effects. The curves shown are plotted in terms of electron heights entering the multiplier. In this

form the distributions are essentially independent of voltage as long as the sources of the pulses remain unchanged. Experimentally, this has been shown to be true over a considerable voltage range (i.e. from ~ 70 to 130 volts per stage). At higher voltage, effects of field emission and ion feedback become increasingly serious and the dark pulse rate tends to become higher.

The temperature at which the tube is operated has a very pronounced effect upon the dark pulse output. At temperatures in the neighborhood of dry ice the dark pulse rate drops to a very low value and is even lower when the tube is cooled to liquid air temperature. In the neighborhood of room temperature, the dark pulse rate doubles for each 10-degree-centigrade rise in temperature.

The pulse performance of certain multipliers can be greatly affected by the voltages of external shields which are in contact with the glass envelope. This is particularly so when the glass used is somewhat conducting, and hence the shield potential can affect the fields in the vicinity of the photocathode. It is most frequently found that the pulse rate becomes a minimum when the shield potential is brought close to that of the photocathode. It should be noted that this expedient can be used to reduce the dark pulses from a particularly noisy multiplier but it will not significantly improve the performance of a good multiplier.

MULTIPLIER RESOLVING TIME

One reason for the importance of the scintillation counter is its high speed. It is faster by one or more orders of magnitude than any of the gas discharge types of particle detectors. The points of limit of the resolving time of the system are the crystal phosphor, the multiplier and circuitry following the multiplier. The flash duration of certain crystals is extremely short, being of the order of 10^{-8} second. The circuitry which follows the multiplier can in general be arranged in such a way that it does not limit the speed of the system. For example, the crystal diode coincidence circuits discussed in the next section can be designed so as not to constitute a limit. The resolving time of the multiplier itself is the subject of this section.

When an electron starts from the photocathode of the multiplier and proceeds to produce generations of secondary electrons which eventually reach the collector, a certain amount of time is required. This transit time in itself does not limit the resolving time of the multiplier, but rather simply acts as a delay.

However, the electrons produced by one or more photoelectrons initiating simultaneously from the photocathode do not reach the

collector at exactly the same time. This spread in transit time sets the ultimate limit of the resolving time of the multiplier.

A number of possible causes must be examined in determining the nature and magnitude of the transit time spread. These are

1. Emission time of secondary electrons.
2. Effect of initial velocities.
3. Difference in electron path lengths.
4. Space-charge effects.

Considering these factors in order, the secondary emission time is one or two orders of magnitude shorter than some of the other delay effects. The exact emission time has not yet been determined, but frequency measurements on certain devices where secondary emission is involved show that this time is less than 10^{-10} second. Indeed, it was shown by Greenblatt and Miller that a certain fraction at least of secondary electrons must be emitted in less than 10^{-12} second.

The spread in initial velocities of secondary electrons is important in its effect on transit time spread. A good secondary emitter will emit most (85 per cent) of its electrons with initial velocities in the range of 0 to 3 volts. The fractional decrease in transit time for electrons between parallel plates with a potential difference V between them if an electron is emitted with a velocity ΔV volts is

$$\frac{\Delta t}{t} = \sqrt{\frac{\Delta V}{V}}.$$

This approximation is sufficiently good for the present estimate of transit time effects. At 100 volts per stage an electron leaving with 3 volts initial velocity will require 17 per cent less time to reach the next dynode than one leaving with zero velocity.

The difference in path lengths of electrons leaving from different points on a dynode is the largest factor involved in transit time spread. A single stage of one form of linear electrostatic multiplier is shown in Figure 12 giving electron trajectories and equipotential surfaces. Computing the transit time difference between the longest and shortest paths, it is found to be about 1.7×10^{-9} second. If the effect of initial velocity is included the difference becomes 1.9×10^{-9} . Where several stages are involved the spread does not increase linearly with the number of stages, but rather, more nearly with the square root of the number of stages. Therefore, the spread in transit time for a 9 stage multiplier would be something less than 6×10^{-9} second. This

is in fair agreement with frequency response measurements made on multipliers.

Space charge was mentioned as a factor in determining transit time effects. It can be shown that the transit time for electrons from a space-charge-limited emitter is increased by about 50 per cent. Space-charge effects can only occur in the final stages of a multiplier where very large gains are employed. If the gain is taken as 10^6 and the transit time spread as 10^{-9} second, one electron produces an instantaneous current of 10^{-4} ampere at the collector. This is well below the current which will produce any serious space-charge effect. However, if the gain of the multiplier is 10^{10} then the current is the order of an ampere and space charge may well increase the transit time spread.

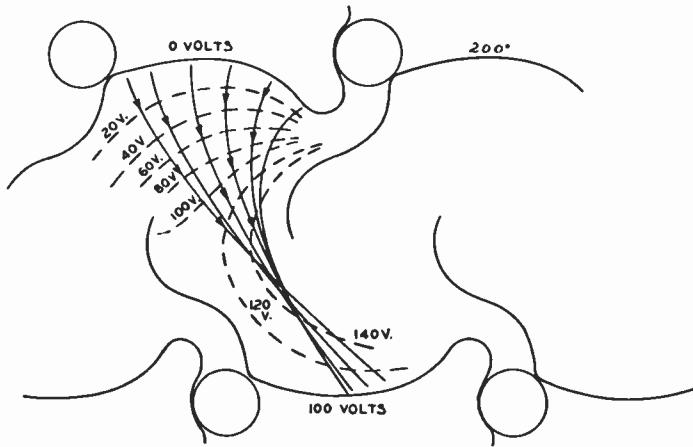


Fig. 12 — Electron trajectories and potential distribution between two successive dynodes of a typical multiplier.

MULTIPLIER CIRCUITRY

Most of the circuitry used with a scintillation detector is unique to the particular experiment being carried out, and therefore its design must be predicated on general circuit theory rather than on data from an article on photomultipliers. However, a few elements of the circuitry are characteristic of the multiplier and consequently fall within the scope of this discussion.

The multiplier requires for its operation an overall voltage of one to two thousand volts divided into steps of 100 to 150 volts each. With an unfocused multiplier the steps do not need to be uniform, and can frequently be larger (150 to 200 volts) than for a focused multiplier. Because of having to satisfy conditions of electrostatic focus, the voltage steps for a focused multiplier (i.e. 931A, 5819 etc.) must be uniform or nearly uniform. Normally, with these multipliers, uniform steps (70 to 120 volts) are used. Sometimes, however, it is advantageous to use a somewhat non-uniform arrangement of steps such as:

Stage	Potential Difference (Volts)	Stage	Potential Difference (Volts)
p-1	120	5-6	140
1-2	100	6-7	140
2-3	100	7-8	140
3-4	100	8-9	140
4-5	120	9-c	150

for a 931A or 1P21. Here a slightly higher voltage is used with the photocathode to ensure good collection, and higher voltages are used on the later stages to obtain higher gain without increasing the dark pulse rate. It might be pointed out that with a 5819 the photocathode to first dynode voltage does not affect the multiplier focus. Consequently, it is advantageous to make this voltage as high as possible without introducing additional dark pulses.

It is evident from the discussion of multiplier gain that the voltage source must be well regulated for any precise experiment. A given percentage variation in overall voltage produces nearly ten times as large a variation in gain. While the need for a large number of voltage steps complicates the power supply and regulation problem, the very small current required by the multiplier is a simplifying factor.

It has been found most practical to obtain the voltage steps required for a multiplier from a resistance voltage divider. This divider can be made up of small resistors soldered directly to the multiplier socket, to avoid complicated wiring. When this is done, the overall resistance should not be less than a megohm, otherwise the power dissipated by the divider may raise the temperature of the multiplier unduly. On the other hand, difficulties may be encountered with stability, etc. of resistors, if the resistance value is above one or two hundred megohms. Where the divider is separate from the multiplier and wired to the various socket connections, the lower limit of resistors used is only determined by practical power supply considerations and cooling requirements.

It is frequently necessary to use small condensers to by-pass the resistors supplying the last few stages of the multiplier. This is particularly so when the multiplier gain is high and a high resistance divider is employed. In general, the average current at the output of a scintillation counter never exceeds a few microamperes; however, the instantaneous current may be quite high.

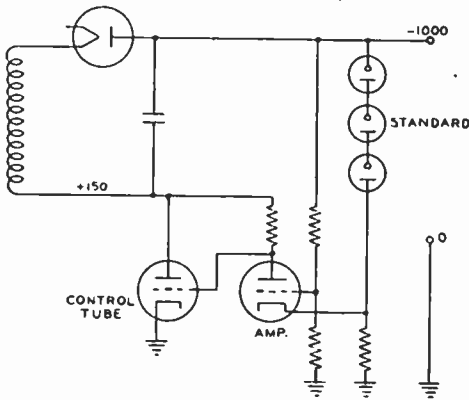


Fig. 13—Regulated power supply.

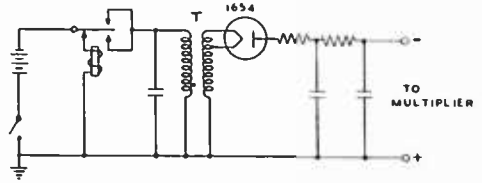


Fig. 14—Vibrator power supply.

Any one of a large number of fairly conventional 60-cycle power supplies may be used as the voltage source. Figure 13 illustrates an electron-tube-regulated supply which is entirely suitable. It is also practical to use magnetic regulation, the only added condition being that the filter between the rectifier and the multiplier must have a long enough time constant to match the relatively slow speed of this type of regulator. With a high impedance divider, the filter problem, using a number of resistor-condenser stages, is very simple. In order to simplify the circuits following the multiplier, the positive side of the supply should be grounded.

Radio-frequency power supplies are also very practical for multiplier work. When this form of supply is employed, care must be exercised in shielding to prevent electric and magnetic pickup.

For portable scintillation counters it is necessary to power the multiplier with batteries. For this purpose three or four 300 volt batteries, or a battery-powered impulse high voltage generator may be used. Two types of impulse supplies are common. One employs a vibrator and transformer, and may be operated from three- or six-volt batteries. The second uses a relaxation oscillator (e.g. a gas discharge tube-condenser-resistor combination) and a transformer. In general 90 or more volts are required to power this form of supply. Schematic diagrams for these two forms of supplies are shown in Figures 14 and 15.

Neither vacuum tube nor magnetic regulators lend themselves particularly well to the last mentioned group of power supplies. Practical regulators for them can be made using a large number of neon discharge tubes (NE51). However, this type of regulator requires hand selecting of neon tubes, and tends to change with time and use. Recently corona discharge regulator tubes have become available which are fairly practical. It is also pos-

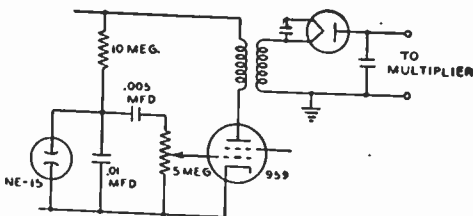


Fig. 15—Gas tube oscillator power supply.

sible to use the focusing properties of a multiplier to obtain constant gain even when there are quite large variations in overall voltage. Figure 16 illustrates a regulator of this type, together with its gain-voltage characteristic. The principle here is that an overall increase in gain, due to a rise in voltage, is balanced by the focusing loss at dynode 6 where the voltage between dynodes 5 and 6 is held constant by a zero-current 90-volt battery. The battery may of course be replaced by a constant voltage gas discharge tube.

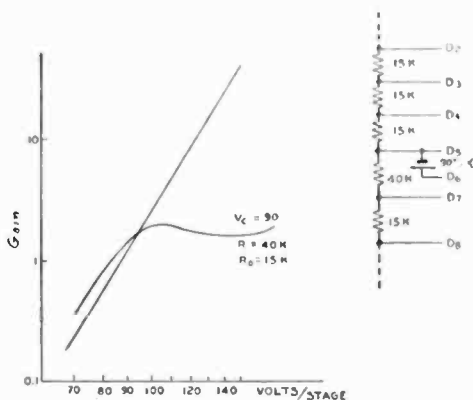


Fig. 16—Gain regulation by focus compensation.

The output circuit of the multiplier should follow general good pulse-circuit practice. Where a multiplier of the 931A or 5819 type is resistance coupled to the grid of an amplifier tube, the coupling resistor must be of low value (i.e. < 1000 ohms) if the pulse is to be limited by the multiplier transit time spread. In all cases lead lengths should be short and capacitances to ground etc. minimized.

The very short resolving time of a multiplier makes it very useful for coincidence work. In order to take advantage of this speed, it is necessary to use very wide band amplifiers where conventional coincidence circuits are used. By using multipliers at voltages somewhat higher than their rated voltage (this cannot be done with all multipliers) sufficient output signal can be obtained to operate coincidence circuits based on rectifying crystals (e.g. 1N34) without amplification between the crystal and multipliers. This greatly decreases circuit complexities. Two examples of this are shown in Figures 17 and 18.

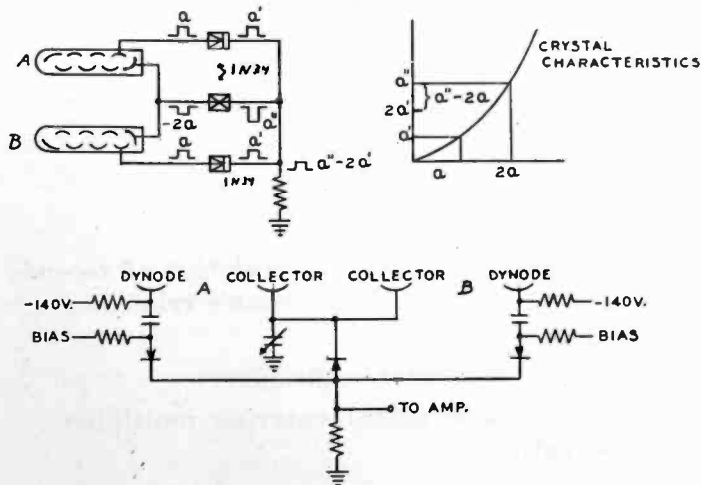


Fig. 17—Three-crystal coincidence circuit.

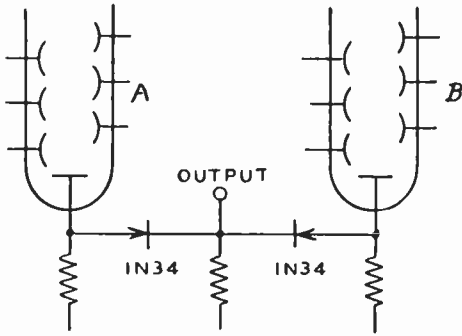


Fig. 18 — Two-crystal coincidence circuit.

The three crystal circuit has greater sensitivity and better discrimination ratios than the two crystal system, but is much harder to adjust.

These examples are given simply to illustrate two of the many ways in which circuit "tricks" can simplify making use of the valuable time characteristics of the multiplier. Many similar simplifications can be found which help in the solu-

tion of problems connected with the various experimental applications of this tube in scintillation detection.

LIST OF SYMBOLS

- A Amplifier gain.
- A' Area under integrated pulse height curve (input electrons).
- A'' Area under integrated pulse height curve (charge output).
- C Effective coupling capacity between multiplier and amplifier.
- $f(\rho)$ Integrated pulse height distribution (pulse rate versus number of electron-equivalents input).
- G Average gain.
- G' Gross gain.
- i_p Photo current.
- i_o Output current.
- m Number of stages.
- n Pulse counting rate.
- n_p Number of electrons from photocathode per second.
- n'_p Number of electrons entering multiplier per second.
- p Number of photons per second.
- q_k Charge in k^{th} output pulse.
- V Voltage per stage, voltage.
- V_o Overall multiplier voltage.
- Z Arbitrary number of electrons.
- γ Quantum efficiency (of photocathode).
- δ Number of electrons entering multiplier.
- ϵ Coefficient of departure of mean square deviation of secondary electrons from that given by Poisson's relations.
- η Transfer efficiency.
- η_p Photoelectron collection (transfer) efficiency.
- ρ_k, ρ Effective charge (in electron units) entering multiplier.
- σ Secondary emission ratio.

1. H. Bruining, "Secondary Emission of Metals with a Low Work Function," *Physica*, Vol. 4, p. 473, June, 1937.
2. R. Kollath, "Secondary Electron Emission from Solids," *Phys. Zeit.*, Vol. 38, p. 202, April, 1937.
3. D. E. Wooldridge, "Theory of Secondary Emission," *Phys. Rev.*, Vol. 56, p. 562, September 15, 1939.
4. V. K. Zworykin, G. A. Morton and L. Malter, "The Secondary Emission Multiplier—A New Electronic Device," *Proc. I.R.E.*, Vol. 24, p. 351, March, 1936.
5. W. Shockley and J. R. Pierce, "A Theory of Noise for Electron Multipliers," *Proc. I.R.E.*, Vol. 26, p. 321, March, 1936.
6. Z. Bay, "Electron Multiplier as an Electron Counting Device," *Nature*, Vol. 141, p. 284, February, 1938.
7. V. K. Zworykin and J. A. Rajchman, "The Electrostatic Electron Multiplier," *Proc. I.R.E.*, Vol. 27, p. 558, September, 1939.
8. J. A. Rajchman and R. L. Snyder, "An Electrostatically Focused Multiplier Phototube," *Electronics*, Vol. 13, p. 20, December, 1940.
9. R. B. Janes and A. M. Glover, "Recent Developments in Phototubes," *RCA Review*, Vol. 6, p. 43, July, 1941.
10. M. Blau and B. Dreyfus, "The Multiplier Photo-tube in Radioactive Measurements," *Rev. Sci. Inst.*, Vol. 16, p. 245, September, 1945.
11. R. W. Engstrom, "Multiplier Phototube Characteristics: Application to Low Light Levels," *Jour. Opt. Soc. Amer.*, Vol. 37, p. 420, June, 1947.
12. H. Kallmann, *Natur und Technik*, July, 1947.
13. J. W. Coltman and F. H. Marshall, "Photo-Multiplier Radiation Detector," *Phys. Rev.*, Vol. 72, No. 6, p. 528, September 15, 1947.
14. G. A. Morton and J. A. Mitchell, "Performance of 931-A Type Multiplier in a Scintillation Counter," *RCA Review*, Vol. 9, p. 632, December, 1948.

DIRECT-READING ELECTRONIC TIMER*†

By

R. R. FREAS

Engineering Products Department, RCA Victor Division,
Camden, N. J.

Summary—The application of resistance-coupled multivibrators to binary and decade counter chains is described, with suggestions for improved stability. Several independent counts may be selected and registered on counter dials from one continuously operating electronic counter with the coincidence indicator circuits shown. The electronic counter may be automatically reset to zero or any advance count with the reset circuit presented.

BINARY COUNTER CIRCUIT

A RESISTANCE-coupled multivibrator may be used as a binary counter or divider.¹ See Figure 1. This type of multivibrator, in which one side is conducting and the other cut off, requires a driving pulse to change from one of its two stable positions to the other. If this pulse is applied at the common plate resistor, a second identical pulse will cause the multivibrator to return to its original condition. Thus the circuit completes one cycle in response to two driving pulses, and may be used as a binary divider.

If driving pulses are equally spaced, one plate waveform will be a symmetrical square wave and the waveform at the other plate will be identical except for opposite polarity. A differentiating circuit at either plate would produce an output pulse similar to the driving pulse but of half the frequency. This may be used to drive another stage, and so on.

The change from one stable condition of the multivibrator to the other is accomplished as follows:

- (a) A negative pulse is applied at the common plate resistor.
- (b) This negative pulse appears, attenuated, at the grid of the conducting section.

* Decimal Classification: R355.913.5.

† The work described in this paper was performed for the Engineering Division of the Air Material Command on Contract W-33-038-AC-17427.

¹ I. E. Grosdoff, "Electronic Counters", *RCA Review*, Vol. XII, No. 3, p. 438, September, 1946.

- (c) The conducting section is rapidly cut off and the plate rises toward a more positive value determined by the resistance divider from B+. Assuming a driving pulse of negligible width, the rate of rise is determined by the value of the resistance divider and the stray capacity to ground.
- (d) The grid of the previously cut-off section rises and causes conduction of plate current and a corresponding plate voltage drop. This completes the action.

ELECTRONIC COUNTERS

Binary counters can be arranged in cascade, so that the system will count to any integral power of two. In such service each binary will be used to drive the following binary through a differentiating circuit. For example, if it is desired that the system be capable of counting to 128, or any number between 64 and 128, seven binaries could be arranged in cascade. If it is not desired to count to a full 128, the system could either be reset when the desired count is reached, by suitable circuitry, or the chain could be reset to an advance number (i.e., other than 0), so that the additional number of desired counts would complete the counter cycle.

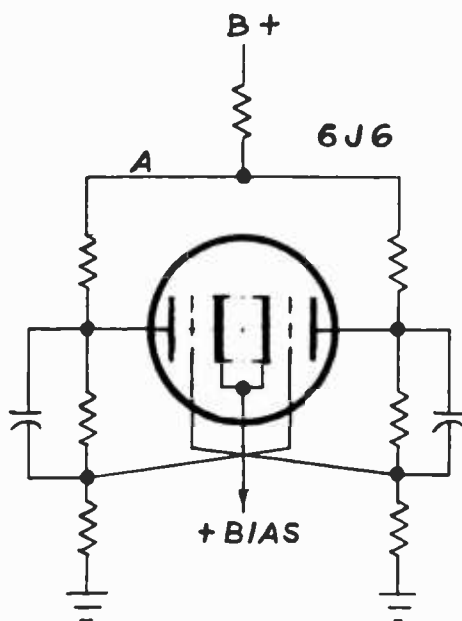


Fig. 1—Binary schematic.

Four binary counters may be arranged in cascade to count to ten by using feedback. Feedback effectively introduces extra driving pulses to the binary counters during the normal cycle, thereby acting as the equivalent of various numbers of input pulses. For example, suppose four binaries are arranged in cascade. Feedback is applied so that every time the third stage turns over in a certain direction, a driving pulse will be applied to the second stage. This feedback pulse would be the equivalent of two input pulses to the first stage. This would decrease the normal count by two each cycle, or would make three stages count to six instead of eight. Similarly, if feedback is utilized between the fourth and third stages, the feedback pulse to the third stage would be the equivalent of four pulses to the first stage. If both

feedbacks are used, the count for one cycle will be ten instead of sixteen for the four cascade stages, by virtue of the fact that the first feedback pulse is the equivalent of two input pulses, and the second feedback pulse is the equivalent of four input pulses. This subtracts six pulses from the required sixteen to complete the cycle.

The arrangement just described is typical, but not the only feedback arrangement that is feasible to reduce the normal count of a series of binary stages. By using the same principle, virtually any count may be achieved.

The binary arrangement is the simplest from a standpoint of construction, stability of operation and efficiency of circuits. As we are not used to counting in binary numbers, however, it is sometimes difficult to adapt such a counter to read in the system of numbers with which we are familiar; i.e., the decade system. The advantage of the decade counter is that it is directly adaptable to an indicating device which will read in the decade system. Such a counter, however, presents additional circuit problems from a standpoint of stability and is necessarily more complex for counting to a given number than a binary system would be.

An electronic timer is of little use if it cannot be depended upon for continuous accurate counting. An unstable counter may divide erratically or divide by the wrong number; the result in either case being an improper count. Fortunately, it is possible to design this type of counter circuit in such a way that a high order of reliability may be secured from either decade or binary counters.

The driving pulse supplied to the first stage of a counter chain from the oscillator or other driving source is exceedingly important in the stability of the chain. As a rule, an ordinary sine wave oscillator is seldom suitable as a driving source directly. Suitable circuits must be utilized to provide a short, sharp driving pulse. See Figure 2. One such circuit utilizes a tuned-plate, tuned-grid, crystal controlled sine wave oscillator whose output is fed to a self biased amplifier. The amplifier's plate load includes a ringing inductance which will ring at its natural frequency and produce one wave train for each cycle from the oscillator. The output of this ringing coil is damped with a suitable resistor, and this succession of damped wave trains is then fed to another self biased amplifier. The most positive portion of the first cycle of the wave train sets the bias on the self-biased amplifier and causes conduction of plate current at that amplifier. The output of the amplifier is a short sharp pulse of negative polarity and great amplitude which is essentially independent of slight changes of wave

form on the crystal oscillator. This pulse is well suited to the task of driving a counter.

If the optimum in wave shape is not required for purposes of coincidence indication, each stage may be used as a source of driving pulses for the following stage. This is true in either the binary or the decade system. The differentiating circuit used by the stages to transform the square wave of the driver to a pulse for the driven stage should be capable of producing a sharp, short pulse in each case. The driving pulses to each stage should be as nearly identical as possible if the maximum stability is to be secured. Under such conditions the timer

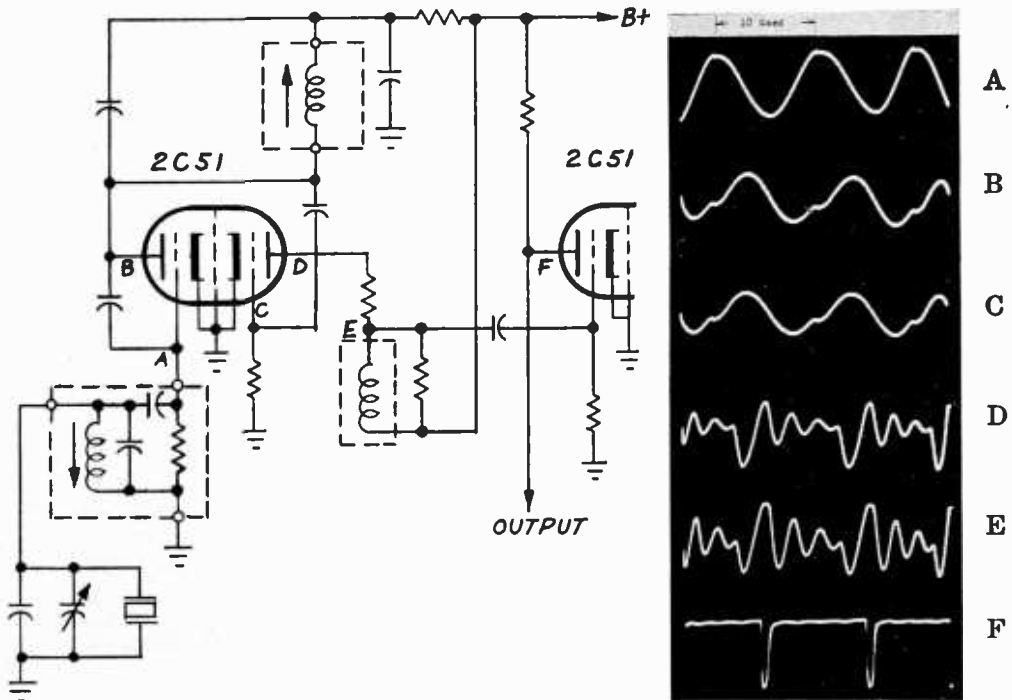


Fig. 2—Oscillator-pulse former.

will not be critical to reasonable changes in B+ voltage, filament voltage, tubes, or normal variations in other circuit components.

If sharp rise and fall times are required on the output wave form of the counter stages, it will be necessary to minimize the loading on these stages. In order to accomplish this; interstage amplifiers must be employed to drive the counter stages, as in the typical decade shown schematically in Figure 3. A differentiating circuit is still used to drive the amplifier, but its input impedance is much higher than the input impedance of a counter stage. It is obvious that the opposite side of a counter stage must be employed to drive the amplifier, due to phase reversal of the latter. The plate load resistor for the amplifier may be the common plate resistor of the driven counter stage, as in Figure 3.

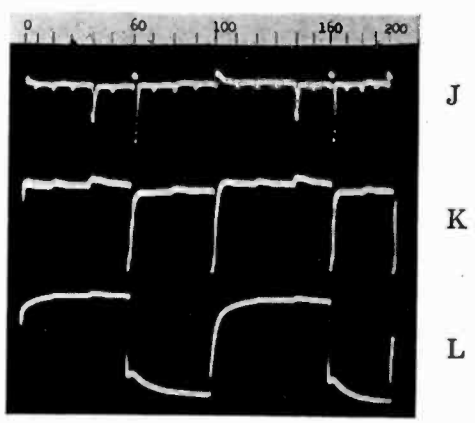
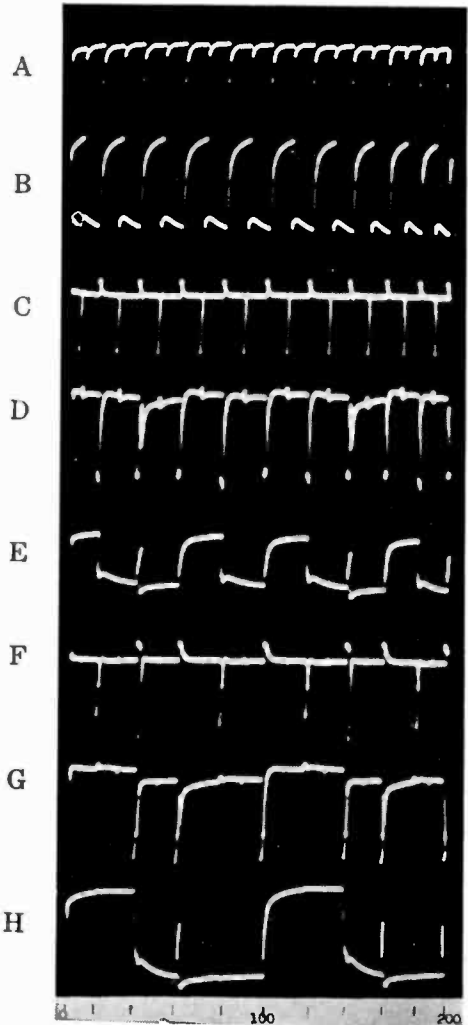
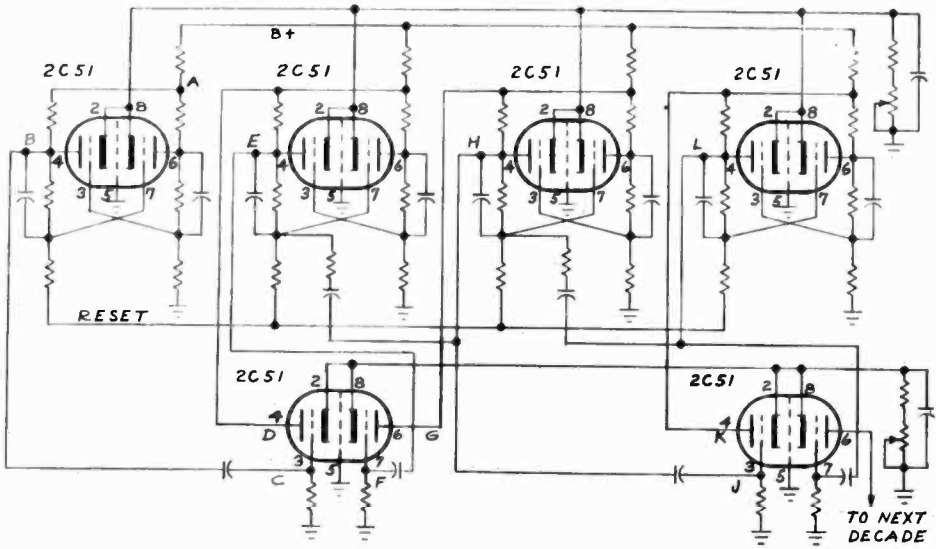


Fig. 3—Decade counter with inter-stage amplifiers, pulse shaping circuit and wave forms.

In some instances it has been found necessary to use special circuits in order to sharpen the pulses used for driving counter stages part of the way down the timer chain. A typical circuit, see Figure 3, might include a clipping amplifier whose output would be a steep-sided square wave, a suitable differentiating circuit, and a self-biased pulse amplifier. The use of such circuits may greatly add to the reliability of a counter system.

METHOD FOR CHOOSING SIGNALS FOR A DESIRED COUNT

An electronic timer, composed of a series of cascaded counters and a coincidence indicator, may be used to provide an output pulse after any given number of input pulses. Assume that at the start of a counter cycle the multivibrators each start out with a given half of the multivibrator conducting. Let us call this "Plate B". The other plate will be designated as "A". It is possible to show that after the application of any given number of input pulses, the counter plates will have a pattern unique to that count. This assumes, of course, that the given number of input pulses does not cause the counter to go through one or more complete cycles. For example, assume we have a two-stage counter, as shown in Figure 4. At the start of the counter cycle, before the application of the first input pulse, the "A" sides of each stage are cut off and therefore are at a higher voltage than the "B" sides. Let us designate the higher voltage plates as plus and the lower voltage plates as minus. Now assume three input pulses have been applied. It is obvious that both of the "B" plates are now plus. If it were desired to indicate the count of three when a coincidence indicator would be connected to each of the "B" plates, the indicator would be so arranged as to provide an output each time both of its input signals were positive simultaneously.

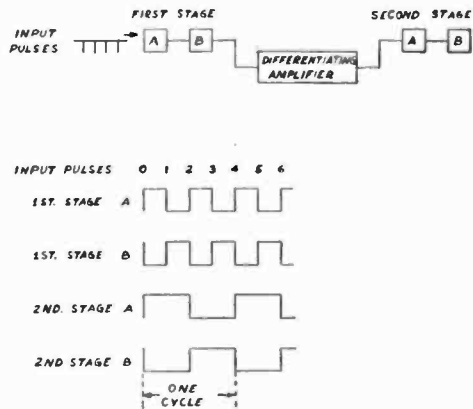


Fig. 4 — Two-stage counter and wave form.

It will be noted that having both "B" plates plus is unique to the count of three, and that this condition will last until the count of four, therefore providing an output equal in duration to the spacing between the input pulses. The principle illustrated by this simple example may be utilized to indicate practically any count, however large. With a

sufficiently long chain of multivibrators, the maximum count is limited only by the complexity of the coincidence indicator.

In the case of a binary counter chain, it is necessary to use the signal at each plate in the chain for coincidence indication. However, when four counter stages are arranged with feedback so as to count to ten, it is not necessary to use all four stages to feed the coincidence

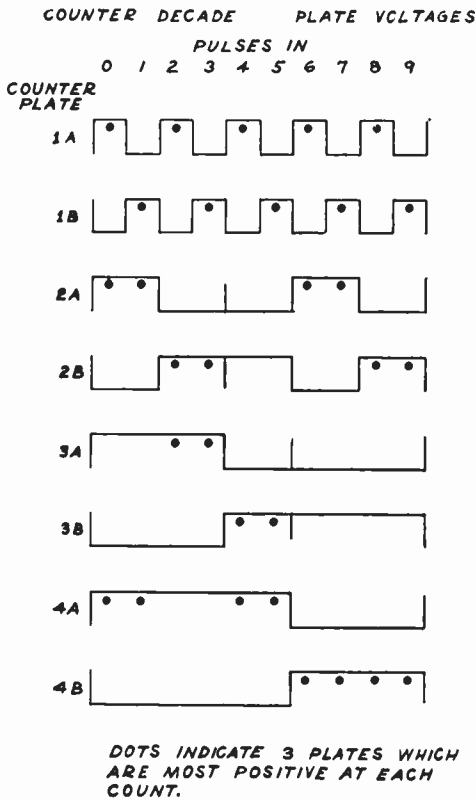


Fig. 5—Counter decade plate signals selected for coincidence indication.

indicator. For example, if a decade system with feedback from the fourth stage to the third stage and from the third stage to the second stage is employed, a unique combination of plus plates may be achieved by using only three plates. This is true for every count — 0 through 9. While all the plates are used for one count or another, it is necessary to select only three for each particular count. The method of doing this may be seen from Figure 5. The dots on the wave form under each number indicate the plates that are selected to indicate the count for that number of input pulses. The above-mentioned figure assumes that the coincidence indicator operates on positive signals. If an indicator operating on negative signals is used, the plates selected would be the opposite to those indicated in Figure 5.

COINCIDENCE INDICATORS FOR ELECTRONIC COUNTERS

Coincidence indicators may be divided into two groups; namely, those which produce a pulse output and those which produce a pedestal output. In the former type the output of several counter stages may be fed to as many triode grids, and the plates connected to a common load resistor. See Figure 6. The grids are so biased as to cause continuous conduction of plate current, except at the time when all grid signals are negative simultaneously. The output of the common plate resistor is a positive square wave, which will have the same width as that of the shortest square wave applied to the grid. It is easily possible to combine four or five signals in this manner. As a rather high value of plate resistor must be used, the output is not generally a good

square wave, but will be somewhat rounded, especially on the positive going side where the stray capacity must be charged through the plate resistor. The negative going side, where the tubes again start to draw current and discharge the stray capacity is somewhat sharper, and differentiating this output will give a negative pulse which is suitable for driving an amplifier which has slight positive bias. The output of this amplifier will be a sharp positive pulse, which will coincide with the end of the highest frequency square wave impressed on the control grid which has been selected for coincidence indication.

This type of coincidence indicator has been found to be especially stable. Because the tubes are operated from grid current to cutoff, it is essentially independent of reasonable variations in tube characteristics, component values, or B+ voltage. The grid wave form need not be especially good in order to provide a good pulse output. In general, no adjustments are required.

A type of coincidence indicator for producing positive pedestal output which has been found quite satisfactory employs a pentode with dual control grids, such as the 6AS6. In this tube the suppressor may be used as a control grid with about half the G_m of the standard control grid. This tube may be operated with, for example, a combination of two superimposed counter square waves impressed on the control grid, and one counter square wave impressed on the suppressor grid. In this case, the control grid would be operated with a negative bias to select the proper operating point. A negative output pedestal would be obtained from the plate at the time when all three signals at the two grids became positive simultaneously. If the wave form at the grid has good frequency response, and if a low value of plate resistor is

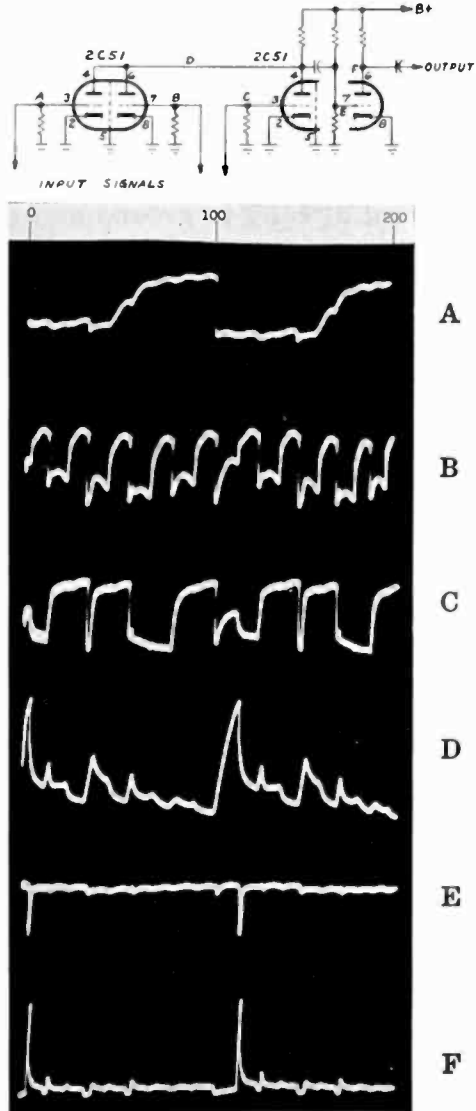
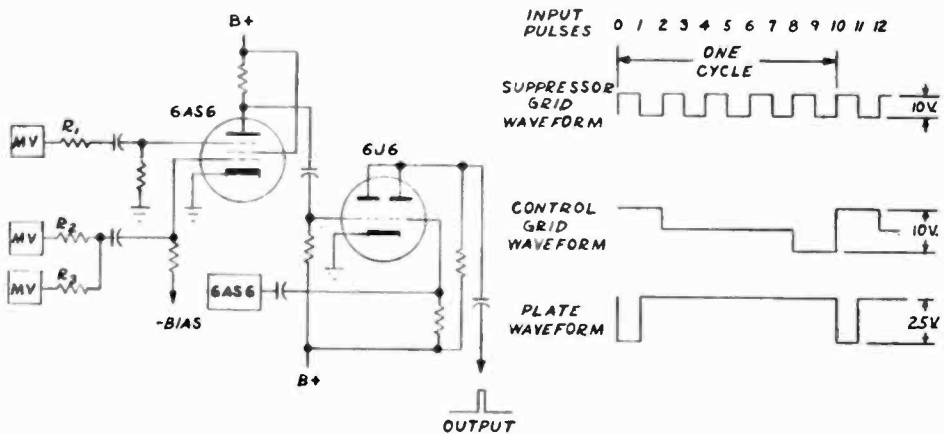


Fig. 6—High frequency coincidence indicator.

operated with a negative bias to select the proper operating point. A negative output pedestal would be obtained from the plate at the time when all three signals at the two grids became positive simultaneously. If the wave form at the grid has good frequency response, and if a low value of plate resistor is

employed, the output pedestal may have good high-frequency response. This produces a steep-sided square wave. The duration of the output pulse will be exactly equal to the duration of the shortest square wave at either grid.

It is possible to operate this circuit with more signals on the control grid and suppressor grid if some stability in operation can be sacrificed. As the number of signals increases, the bias setting for a clean output becomes more and more critical. However, it is entirely feasible to operate with three signals at the control grid, and one signal on the suppressor grid. In this case the suppressor grid resistor may be returned directly to ground and the negative side of its signal will be used to bias off the pentode. See Figure 7. The control grid is so operated as to cause plate current conduction only on the most positive



NOTE: SUPPRESSOR WAVEFORM — BINARY COUNTER;
CONTROL WAVEFORM — DECADE COUNTER, COMBINED OUTPUT,
STAGES 2A & 4A.
 R_1, R_2, R_3 ARE ISOLATING RESISTORS.

Fig. 7—Pentode coincidence circuit.

part of the impressed signal, together with the positive suppressor signal.

If it is decided to combine the output from several such pentodes, a series of triodes may be fed from the negative plate signals of the pentodes with the plates of the triodes connected to a common load resistor. The triodes are so arranged as to be normally conducting in the absence of signal. The output of the common plate resistor will be a positive pedestal, whose duration will be equal to that of the shortest square wave at the pentode plates. As the grid driving signals can be very large, a small plate load resistance may be employed to provide good high frequency response. See Figure 7.

An entire coincidence indicator system may consist of a combination of both the pulse type and the pedestal type indicators. In this case,

the pulse type coincidence indicator is operated from the highest frequency stages of the counter, and the pentodes are operated from the lower frequency stages. One complete cycle of selected counts from the high frequency coincidence indicator will equal in time the pedestal produced by the pentode with the shortest output pedestal. If the pulse and pedestal are combined in a common impedance mixer, the pulse may be selected by a biased amplifier if a rather high impedance output is desired, or the combination may be impressed on the grid of a thyatron, which will produce an output pulse of great amplitude across a very low impedance. See Figure 8. Thyratrons operated in this service obtain their plate current from a storage capacitor, which is fed slowly from B+ through a large resistor. A very small resistor in the cathode of the thyatron may be used to develop the output pulse and quickly discharge the capacitor at conduction, thus extinguishing the thyatron.

The combination of pedestal and pulses would result in only one pulse being elevated by the pedestal, and this pulse could be selected to occur at the desired count. Therefore the firing of the thyatron by this pulse would indicate the desired count.

The signals to operate the coincidence indicators are supplied from the multivibrator plates. Due to the fact that several plate wave forms may be combined at one grid of the coincidence indicator, it is necessary to have some mixing network between the counter plate and indicator grid in order to avoid tying the counter plates together. An isolating impedance from each plate, consisting of a large resistance in parallel with a low value capacitor may be used for this purpose. The other end of these impedances may be connected together and to the grid of the coincidence indicator. A normal grid return resistor is used in addition.

It is the purpose of the capacitor in the isolating impedance to maintain the same rate of rise of the square wave at the coincidence indicator grid as was obtained at the counter plate. The combination may be thought of as an impedance divider; one leg being the grid leak

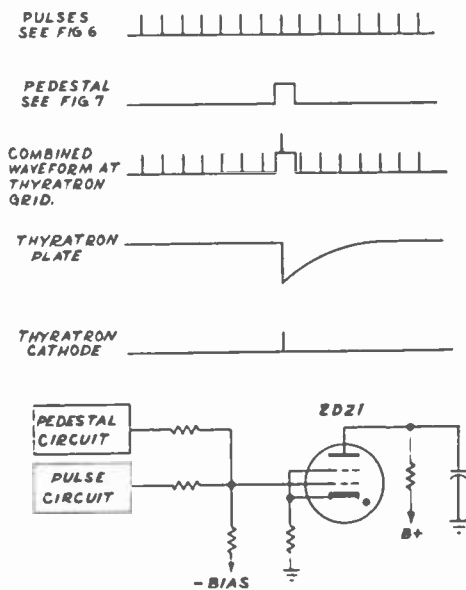


Fig. 8 — Thyatron indicator circuit.

resistor and the stray wiring capacity to ground. The other leg is the isolating impedance. The ratio of reactance to resistance should be the same for each leg if the wave form is to be reproduced faithfully.

The need for faithful reproduction arises when it is desired to obtain coincidence indication near the start of a square wave. It is obvious that the rise time of the square wave at the coincidence indicator grid will determine how closely the coincidence indication may occur to the start of the changeover of the square wave.

Generally all isolating impedances are the same value in order that they may be interchanged by switches and supplied to the coincidence indicator grid. If this is the case then it is necessary that all counter stages be identical. Switching from one isolating impedance to another should then necessitate no adjustment of coincidence indicator bias whatever.

If the isolating impedances are of a high enough value, many isolating impedances may be connected to one counter plate. Therefore, more than one count may be selected from a timer chain by having more than one coincidence indicator. The only limit to the number of coincidence indicators that may be attached to an electronic counter is the ability of the counter to operate under load. As many as three coincidence indicators are entirely practical and it is reasonable to assume that double or triple this number could be used without difficulty if desired. Of course, each coincidence indicator is entirely independent. The setting of one will have no influence on the setting of any other.

RESET MECHANISM

It is frequently desirable to interrupt a counter chain before it has reached its full count. At the time of interruption the counter chain may be reset to 0 or some other definite number. The coincidence indicator may be simplified (because it always selects one definite count) by arranging the counter chain to run to the completion of its count and reset to a definite number other than 0. If the reset can be switched from one number to another, the counter cycle duration will be varied in exactly the same way as it would have been if the chain had been reset to 0 and interrupted before the finish of its cycle. A satisfactory reset device would feed a pulse into the grid of the multivibrator stage in such a way that the multivibrator would assume a definite polarity every time the reset pulse was applied, regardless of whether or not it was in that position at the time of application of the pulse.

It is desirable to maintain as much symmetry as possible between

the two sides of the multivibrator. Therefore, as the reset pulse affects only one side, it should be developed either across a low resistance placed in series with one grid resistor, or should be applied through loose capacity coupling to the grid.

For some applications the thyatron makes an admirable reset tube. If its plate is fed from a storage capacitor which is slowly charged from B+ during the timer cycle, and if the cathode resistor is small, a short sharp pulse of great intensity is available for use as a reset pulse. The thyatron may be easily triggered by the coincidence indicator as its grid circuit is high impedance. The cathode resistor may be so low as to be the grid return for each multivibrator stage in common. The small value of resistor results in a negligible amount of coupling among stages.

The time required for reset is very short. A pulse on the order of one microsecond, for example, will give reliable triggering if the amplitude is great enough. The width of the pulse depends upon the time constant of the thyatron circuit, which is composed of the storage capacitor, the tube itself, and the cathode resistor. The plate resistor is generally made so large that its effect will be negligible.

It is occasionally desirable to broaden the reset pulse to prevent unusual effects within the counter chain. For example, it has been found that a very narrow reset pulse will allow a stage which is being reset to complete its action shortly after the reset pulse has died away. The stage in turn may then trigger the following stage.

In the case of a counter where the reset must be less than a microsecond, it is generally advisable to use a hard tube as the reset tube. The pulse output from such a tube may be much shorter than that of the thyatron although, of course, the impedance across which the pulse is developed must be much higher. If a chain of counters is operated so that some multivibrators operate at a high frequency and others at low frequency, the high frequency stages may be reset by a hard tube and the others reset by a thyatron.

APPLICATIONS

The requirements of timers for Loran receivers are ideally met by this type of electronic counter and coincidence indicator.²

A Loran timer must be capable of counting to sixteen basic repetition periods. Any of the sixteen may be selected by means of a switch. It is a further requirement that the timer must produce an output pulse whose spacing from the start of the counter cycle is variable in

² F. E. Spaulding, Jr. and R. L. Rod, "A New Direct-Reading Loran Indicator for Marine Service", p. 567 of this issue.

one microsecond steps over most of the counter cycle. It is advantageous to provide a mechanical counter which will display the count being selected directly on a dial. Other previous systems have resorted to pulse counting on a cathode ray tube in order to measure the selected time.

In the application of these timers to Loran the highest input frequency was 100 kilocycles, and the division was done by three decades and two binary stages. In order to interpolate between the pulses selected by the coincidence indicator in steps of ten microseconds, a delay line composed of nine one-microsecond sections was

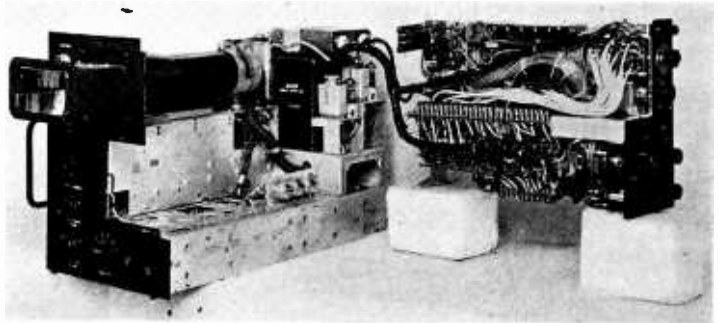


Fig. 9 — Experimental loran timer.

employed. Each of the decades had a knob on the front panel which determined the count which would be selected from that decade by the coincidence indicator. The knob also controlled the corresponding digit on the dial. A special mechanism provided carry-over from units to tens, etc. Figure 9 shows a preliminary Loran timer for airborne use.

Another application of this type of counter is in relation to control of a great many closely-spaced frequencies from a single crystal controlled oscillator. To achieve this the crystal frequency is divided down to a low audio frequency by means of fixed dividers. The output of the variable oscillator, controlled by a reactance tube, is divided down by a chain of variable dividers to approximately the same frequency. If the two audio frequencies are compared in a phase detector, and the output of the detector is used to control the reactance tube, the division ratio of the variable divider will determine the frequency of the variable oscillator. This frequency will be held with the same accuracy as that of the crystal oscillator. The channels may be as closely spaced as the audio frequency which is used at the phase detector.

ACKNOWLEDGMENT

Credit is given to J. D. Woodward for his work in applying the circuits herein described to Loran receivers. Other important contributors were H. C. Lawrence, J. P. Eugley, A. L. Consalvi, and G. H. Webber.

A NEW DIRECT-READING LORAN INDICATOR FOR MARINE SERVICE*

BY

FRANK E. SPAULDING, JR. AND ROBERT L. ROD

Engineering Department, Radiomarine Corporation of America,
New York, N. Y.

Editors note: It is with deep regret that we must inform our readers that Mr. Spaulding lost his life in the tragic airline crash at Washington, D. C., November 1, 1949.

Summary—This paper describes in detail a new Loran indicator especially designed for shipboard use. The discussion treats many of the more recent improvements, including a direct-reading feature, pulse rate automatic frequency control and others. Block diagrams are shown to help explain the operation of various circuits and a summary of performance characteristics is given.

INTRODUCTION

BEFORE entering into a discussion of the technical aspects of the new Loran marine receiving equipment, it is felt that a brief historical resume would be of value. Like Radar, the Loran System of Long Range Navigation was a wartime development which proved to have definite peacetime value. Through use of pulsed radio signals, synchronously transmitted from pairs of shore based transmitters, navigators aboard ships and aircraft are able to determine their positions accurately and at great distances.

Since the time of its inception in the early years of the war, the shore based Loran transmitters have been operated under the jurisdiction of the United States Coast Guard. Initially covering only the North Atlantic area, the Loran system has been extended to the Pacific Coast and serves large portions of the Pacific Ocean. Further extension to areas of the globe not presently served is now under serious consideration.

For many years the Coast Guard has maintained active leadership in improving and extending the Loran system as an aid to mariners and has done much to encourage advances in equipment design. They are now preparing minimum advisory standards for the receiver-indicator units as a guide to those concerned with development and use of this instrument.

* Decimal Classification: R512.2.

During the war, many thousands of Loran indicators were produced and installed on ships and aircraft in military service. Many of these are still in service and will continue so for some time.

Since the war, active development has continued in commercial and government laboratories to devise simpler, more reliable and accurate, as well as less expensive indicating equipment for utilization of Loran signals. RCA has been notably active in this respect. Continued research in the field of electronic timing by members of the RCA Laboratories Division at Princeton resulted in new and more stable methods of using binary and decade multivibrator circuits for frequency division.¹

These techniques were extended and applied to the problem of Loran timing by members of the RCA Victor Aviation Engineering Section at Camden.² Their efforts led to a unique electromechanical design which greatly simplified the task of determining time difference intervals on the Loran indicator. Older methods required the Loran operator to first superimpose the two received pulses and then operate a switch and count a series of markers on the scope to ascertain the correct time difference. With this new direct-reading system, the time-difference reading is continuously and automatically registered on a dial while the pulses are being matched, with the result that readings may be obtained more quickly and with considerably less possibility of error.

Another recent improvement has been the perfecting of automatic frequency control circuits which correct the drift inherently present due to slight differences between transmitter and indicator pulse repetition rates. With automatic frequency control, the pulses of the desired stations are automatically made to stand still on the desired portions of the cathode-ray tube sweeps so that they can be readily matched.

These features are incorporated in a new direct-reading Loran instrument recently introduced by Radiomarine Corporation of America. This new indicator is designed to meet the rigorous requirements of marine service with a minimum of maintenance. Performance of this instrument meets all requirements of the latest Coast Guard specification for equipment of this type.

It also includes a new "S" rate for reception of 20-cycle pulses in addition to the standard "L" (25-cycle) and "H" ($33\frac{1}{3}$ -cycle) basic rates.

¹ I. E. Grosdoff, "Electronic Counters", *RCA Review*, Vol. VII, No. 3, pp. 438-447, September, 1946.

² R. R. Freas, "Direct-Reading Electronic Timer", *RCA Review*, pp. 554-566 of this issue.

Another advance in the design of this indicator is its ability to handle stronger signals than earlier models. This is in keeping with the trend toward use of higher power Loran transmitters, necessitating greater receiver capabilities.

To meet operational requirements, it was apparent that the equipment should have extremely stable timing circuits. From experience with older Loran indicators, it was obvious that substantial efforts should be made to reduce the number of field adjustments. One of the outstanding handicaps of Loran indicators has been the great dependence of their performance on tube parameters. Changing of tubes usually had a large effect on the counting; and thus, auxiliary controls usually required readjustment at such times. By utilizing the more stable binary and decade counters in place of blocking oscillator and thyatron frequency dividers formerly used, the influence of tube constants was minimized, and the auxiliary non-operating controls were reduced substantially.

Receiver circuits have been modified to enable reception of master and slave signals differing in amplitude by as much as 1000:1 with one of the signals being as large as ten volts peak at the receiver input terminals. Over this wide range of signal inputs, the allowable time difference error introduced by receiver distortion is kept below 0.5 microsecond.

Miniaturization techniques have been used throughout the equipment to reduce weight and space. For example, forty-four small printed circuits replace 256 individual resistors and capacitors. Ceramic disc type capacitors used in coupling and by-pass circuits further reduce the space requirements.

THE LORAN SYSTEM

The capabilities of a Loran receiver-indicator may best be understood by reviewing the requirements imposed upon it by the overall Loran system.³ Basically, this consists of two or more pairs of pulsed transmitters at fixed locations supplying navigational information to Loran-equipped vehicles. If, for a moment, a pair of widely separated transmitters on the same frequency is considered to be emitting pulses simultaneously, it is clear that a receiver located half-way between them will receive both pulses at the same instant. Moving the receiver closer to one station results in one pulse being received before the other. The time difference in microseconds, between pulse arrivals

³ LORAN—LONG RANGE NAVIGATION, M. I. T. Radiation Laboratory Series, Vol. 4, Chapter 3, McGraw-Hill Book Co., New York, N. Y., 1948.

may be observed and measured on the Loran indicator. If both transmitters pulsed simultaneously, similar time differences would exist on either side of the imaginary line half-way between the stations. Thus, a certain time difference would not represent a point in space but rather an infinite number of points along two *hyperbolas*, one on either side of the dividing line between transmitters. In practice, one hyperbola is eliminated, thus removing the ambiguity existing as to which is the nearest station. This is accomplished by first pulsing one

transmitter, then later the second, instead of two simultaneously. One station, known as the "master", transmits 40-microsecond wide pulses at rather low pulse repetition rates (PRR) ranging from 20 to $33\frac{1}{3}$ cycles per second. A second station, known as the "slave", located several hundred miles from the master, receives the master pulse and retransmits it after waiting a precise interval of time always exceeding one half the pulse repetition period, the latter being called the "L/2 interval".

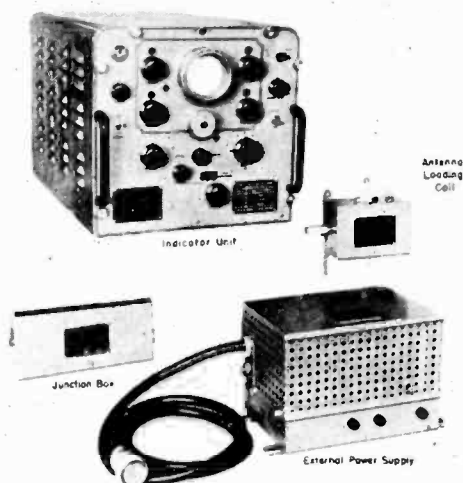


Fig. 1—Direct reading Loran indicator.

A simple example would be on the so-called "S-rate", wherein the PRR is 20 cycles, corresponding to a 50,000-microsecond period. Both stations transmit at 20 cycles, however the slave does so at least $L/2$ (or more than 25,000 microseconds) later than the master. A receiver located within the service area of these two stations, correctly designed to measure only the time difference between arrival of the slave and master pulses respectively, will place the vehicle somewhere along only one hyperbola or "line of position". Then by repeating the process using another pair of stations, a fix may be obtained where the two lines intersect. In practice, the two pairs usually consist of three stations, one of which serves as the master for the other two slaves. Identification between pairs is accomplished by slight differences in PRR between the two pairs or by changes of radio frequency.

Suitable navigational charts have been prepared by the United States Hydrographic Office on which accurate Loran lines of position have been overprinted. Hyperbolas corresponding to each service pair are similarly colored to permit easy identification and also bear the necessary receiver tuning information. Once a time difference from a particular pair has been measured and noted and the correct hyper-

bola charted, a second hyperbola is then found by selection of another pair. The crossing point of the two lines is the desired fix. A simplified Loran chart is illustrated in Figure 2.

USE OF THE LORAN INDICATOR

In obtaining a time-difference reading, the Loran operator first notes his general location with respect to known Loran transmitter sites. Reference to the Loran charts identifies existing stations within the usable range of some 600 miles during daylight and about 1,200 miles at night. The correct receiver radio-frequency channel is selected, followed by choice of both the basic PRR of the desired pair and the "station rate", or small incremental differences about the basic PRR.

Observation of the cathode-ray tube indicator then should show a pair of stationary pulses located somewhere along either the upper or lower traces, or both. Each trace length is nearly $\frac{1}{2}$ the pulse repetition period being transmitted by the pair, thus causing the desired station pulses to stand still, while those on other rates will travel rapidly by. Figure 3 illustrates this presentation.

In addition, a pedestal is provided for each of the sweeps. The one at the left of the upper trace (called the master pedestal) is fixed in position 1,010 microseconds from the left edge while the pedestal on the lower trace moves along as determined by the "time difference" controls of the receiver-indicator. The lower pedestal is called the "delay" or "slave" pedestal.

By altering the synchronism between the transmitter pair and the receiver-indicator slightly, using the "left-right" switch, the pulses are "drifted" across the trace until the master pulse sits atop the master pedestal. The slave pulse thereby automatically appears on the lower trace, since the interval between master and slave exceeds $L/2$, or $\frac{1}{2}$ the pulse repetition period, as mentioned earlier. The operator then moves the slave or delay pedestal under the slave pulse. The

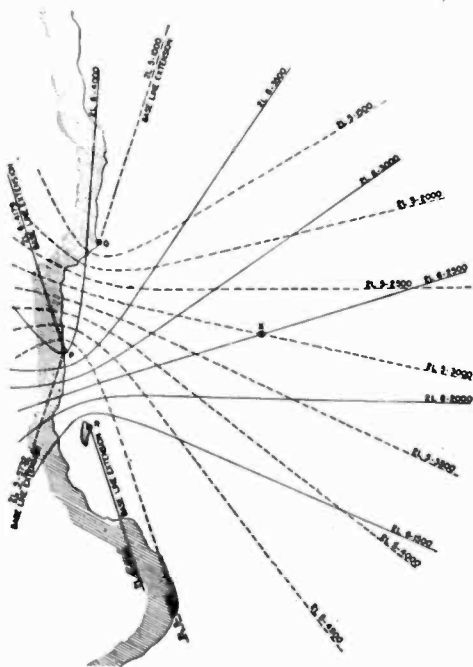


Fig. 2 — Simplified Loran chart—2L5—3500 indicates radio-frequency channel 2, basic rate L, station 5 and 3500 microseconds time difference.

measured time difference is the horizontal distance between the master and slave pedestals with the received pulses in corresponding positions atop the pedestals. For accuracy, the operator switches to another presentation showing the pulses expanded on the tops of the pedestals only, as shown in Figure 3, whereupon he slightly readjusts the time difference controls for a closer match, one pulse above the other. The final step is accomplished by superimposing the two received pulses atop one another so that they may be accurately matched by a final time-difference adjustment using 1-microsecond steps. When this is done, the time-difference dial shows the reading for the correct Loran line of position.

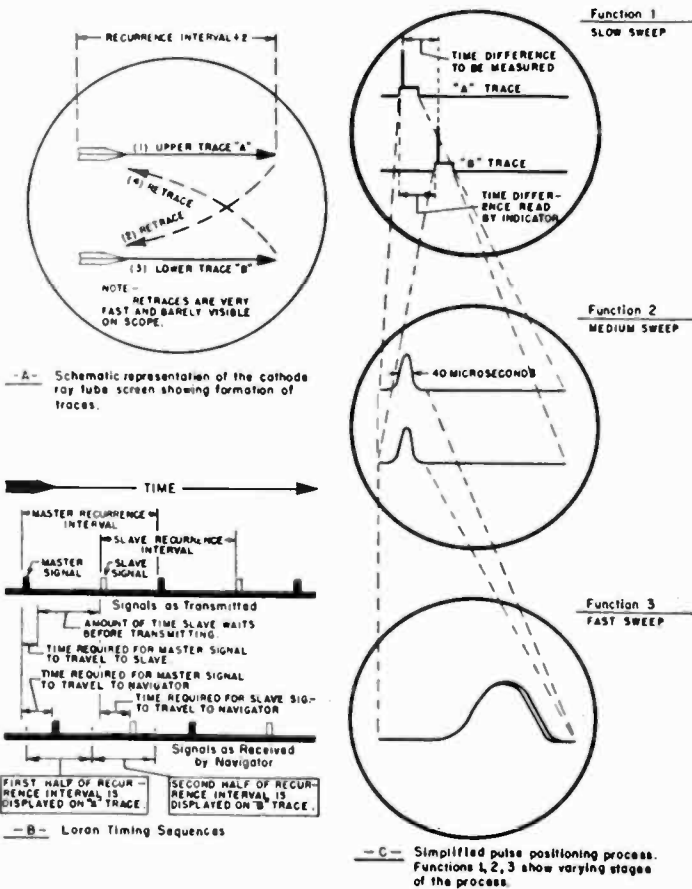


Fig. 3—Loran signal presentations.

TIMER CIRCUITS

In addition to receiving the pulses and displaying them on the cathode-ray tube, the Loran receiver-indicator must be capable of locking itself in step with the transmitter pair at any one of the 24 different combinations of PRR and station rates. Synchronism must be precise, otherwise the received pulses will drift across the sweeps rendering them useless for measurement purposes. The receiver-

indicator also must measure the displacement of the slave pedestal from the master pedestal with an accuracy of one microsecond.

The synchronization and time-difference measurements are functions of the "timer" portion of the apparatus. Referring to the block diagram, Figure 4, it can be seen that sharp pulses derived from a 100-kilocycle crystal oscillator drive three decade and two binary multivibrators in cascade. Each decade itself consists of four binaries in cascade modified by intra-feedback to divide by a factor of 10 rather than 16 which would otherwise be produced by the four binaries.⁴ The unsymmetrical plate waveforms at each of the individual binary multivibrators are fed through appropriate selector switches to separate PRR and delay coincidence amplifier systems. Operation of these circuits is described in detail in an accompanying paper in this issue.² A series of pulses spaced $L/2$ microseconds for each of the 24 different PRR's is generated by these circuits. For the L-0 Rate and Station, for example, the PRR coincidence amplifier system produces pulses spaced 15,000 microseconds, while for S-7, the spacing changes to 24,650 microseconds. Each $L/2$ pulse synchronizes a trace on the CRT and also resets the entire series of multivibrators to zero so that a new count is immediately initiated.

The delay coincidence amplifier system produces an output pulse every other $L/2$ pulse which may be adjustably delayed from the reset interval or zero time anywhere to a maximum of 20,000 microseconds. The maximum delay can be obtained only when the $L/2$ interval exceeds 20,000 microseconds; however, this is clearly no operational barrier inasmuch as a measured time difference can never exceed the $L/2$ interval. With the new 20 cycle S rate, the full 20,000 microsecond capabilities of the delay system may be realized, because the $L/2$ interval itself varies from 24,650 to 25,000 microseconds. This extremely long interval makes the S rate suitable for locations where the two stations constituting a pair must be very widely separated due to terrain considerations.

INDICATOR CATHODE-RAY TUBE DISPLAY CIRCUITS

Each output pulse of the delay coincidence system is fed to the indicator where it initiates the lower movable pedestal by triggering the pedestal generator multivibrator, V-112. The pedestal generator also receives a trigger pulse 1,010 microseconds after every other $L/2$ pulse to create the master (upper) pedestal which appears indented on the upper trace in the Function 1, or slow sweep operation. Each

⁴Reference (1), p. 444.

pedestal is approximately 1,200 microseconds wide except for Function 3, or the fast sweep operation, where the multivibrator output is reduced to 200 microseconds.

Since the measured time-difference is taken as the horizontal distance along the slow sweep between the leading edges of the master and slaves pulses, a correction of 1,010 microseconds must be inserted into the timing system to overcome the error caused by the delay coincidence system as it starts counting from the $L/2$ instant rather than from the start of the master pedestal. One thousand microseconds is accounted for by rotating the scale on the 1,000s place of the time-difference dial back one digit. The additional 10 microseconds is made up with a 10-microsecond delay line in the circuit driving the slave pedestal generator. This fixed amount of delay is purposely introduced to overcome an inherent "system time delay" which accumulates in the timer circuits.

Sweep and sweep intensifier circuits are shown on the block diagram, Figure 4. The Function 1 slow sweep generator produces a continuous series of linear sawtooth sweeps having a length a few microseconds shorter than the $L/2$ interval. At the onset of the next $L/2$ pulse, the generator resets itself in a few microseconds and resumes the production of another sweep. This sweep voltage is fed to the horizontal deflection plates of the 3KP1 oscilloscope in the usual manner at the same time a voltage square wave is being applied to one of the vertical deflection plates to effect trace separation. This square wave is the output of an extra binary that is being triggered by the PRR coincidence amplifier $L/2$ output pulses; and thus each half-period part of the square wave is also $L/2$ microseconds long. The net result is the shifting of every other sweep so that the observer sees two sweeps, one above the other, and each of $L/2$ microseconds duration. At the correct instant, and on alternate sweeps, the master and slave pedestal voltages are injected on a vertical deflection plate.

For the two faster sweeps, an aperiodic sweep generator is utilized. Gating pulses applied to the grid of this "fast" sweep generator are derived from the two pedestals produced by the pedestal multivibrator. The sweeps thus developed are as long as the pedestals or 1200 microseconds for Function 2 and 200 microseconds for Function 3. Received pulses which have been correctly positioned atop the pedestals within the first 200 microseconds from the left edges may then be matched.

Sweep intensification is used on Functions 2, 3 and 4 to achieve a constant trace intensity. These three Functions have their traces automatically intensified by positive grid modulation to the level of the

slow sweep Function 1 presentation, and thus, the conventional intensity control may be eliminated from the front panel of the instrument.

SELF-CHECKING FEATURE

The complex nature of Loran indicators makes it almost mandatory that the technically unskilled operator be furnished some indication of equipment performance and accuracy. Consideration was given to the problem of devising a single-scope presentation which would immediately self-check the entire equipment in a simple, reliable manner. A solution was devised which proves extremely useful and which self-checks the entire Loran instrument in a matter of seconds.

It will be recalled that the time interval measured between the slave and the master pulses is always less than the $L/2$ interval. This fact makes it feasible to trigger the special Function 4 self-checking

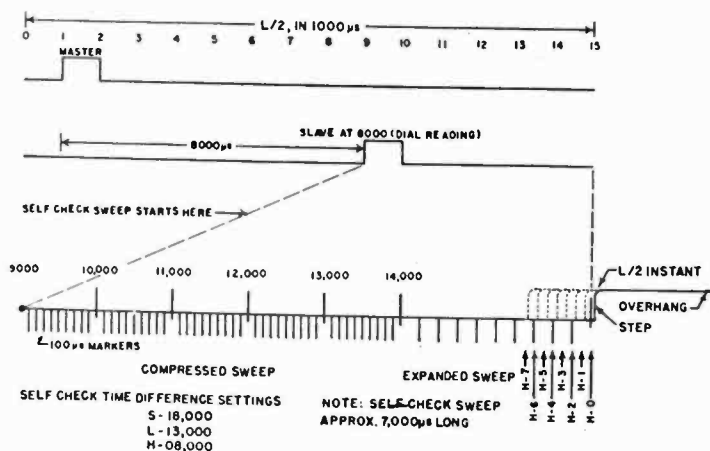


Fig. 5—Self-check presentation.

sweep with the leading edge of the slave pedestal. The resulting aperiodic sweep of approximately 7,000 microseconds has presented upon itself a notch corresponding to the onset of the next $L/2$ pulse. The procedure used merely requires the operator to set his time-difference controls to either 8,000, 13,000 or 18,000 microseconds on Function position 4, when checking the H, L and S rates respectively. When the equipment is operating properly, the time interval between the start of the sweep (or slave pulse) and the notch (or $L/2$ pulse) is then always a constant 6,000 microseconds on the zero station rates, as shown in Figure 5. Thus the notch appears near the end of the 7,000-microsecond sweep. For station rate 1, the interval is reduced by 50 microseconds, 100 microseconds for 2, etc.

A series of 100- and 1,000-microsecond calibration marks is fed to the scope to assist the operator in measuring the sweep length from the left starting end to the onset of the notch. For convenience, the

first 5,000 microseconds of the sweep is compressed, and the last 1,000 microseconds expanded by a dual slope sweep generator circuit which abruptly changes the sweep linearity to a steeper waveform at the right hand portion of the trace. The operator merely selects the basic rate to be checked, sets the corresponding time-difference reading noted from a convenient plate on the front panel, and switches through all 8 station rates while observing that the notch jumps 50 microseconds to the left or one-half a division between 100-microsecond marks, for each successive station. Any circuit faults will prevent this operation from being performed, either by removing the trace or altering the 6,000-microsecond figure sufficiently to indicate that the instrument readings are questionable.

LEFT-RIGHT POSITIONING

As mentioned in the previous section on the method of making a Loran reading, the synchronism between the transmitters and the receiver-indicator is slightly altered in order to drift the received pulses along the sweeps when positioning them atop their respective pedestals. One method, frequently used, achieves this change in synchronism by detuning the 100-kilocycle frequency standard crystal with lumped capacity as required. In this instrument, decreasing changes in synchronism of 100 microseconds per $L/2$ interval for the slow sweep are achieved by zero resetting one of the binaries in the counter chain 100 microseconds earlier, causing the received pulses to drift to the right. The left drifting action is obtained by increasing the $L/2$ interval by 100 microseconds. This is accomplished by gating out ten successive 10-microsecond driver pulses to the counter chain every $L/2$ interval. For the fast sweeps, the drift speed is reduced to 10 microseconds change per $L/2$ interval by either resetting one of the binaries to zero 10 microseconds earlier than normal for right action or by gating out only one 10-microsecond driver pulse for the left action.

AUTOMATIC FREQUENCY CONTROL

It is convenient in a Loran receiver-indicator to incorporate provisions to "lock" the received Loran pulses atop their respective pedestals once they have been correctly positioned. To do this, means must be provided to synchronize the 100-kilocycle crystals in both the Loran shore transmitters and the receiver-indicator to precisely the same frequency. The apparatus incorporates an automatic frequency control circuit to make slight changes in frequency of its own 100-kilocycle

with the automatic frequency control switched on. Sufficient automatic frequency control action is then available to immediately stop any pulse drift until the slave pedestal can be moved under the slave pulse, whereupon additional automatic frequency control "pull in" is provided. This 200-microsecond "gating" action is secured by the use of a "one shot" multivibrator (V-245) triggered by the master and delay trigger pulses.

Receiver video output is fed to the signal grid of the coincidence amplifier (V-241) through cathode follower (V-239B), while the suppressor grid of this same tube is fed positive 200-microsecond "gate" pulses from V-245. The coincidence amplifier delivers output only when both inputs occur simultaneously, or during the 200-microsecond "gate" interval. Thus, only the Loran pulses atop the 1,200-microsecond pedestals and within the first 200 microseconds are fed to the discriminator (V-243) in the form of equal and opposite sets of "gated" video pulses.

The discriminator receives, in addition to the video pulses, a 200-microsecond sawtooth waveform starting at both master and delay trigger instants. The sawtooth generator (V-239A and V-240B) is also started and stopped by the automatic frequency control multivibrator to keep the circuit synchronized. With the video pulses superimposed on the sawtooth, the discriminator develops a negative 3-volt direct-current potential when the positive and negative video pulses are approximately half way up the sawtooth. Assuming the Loran shore transmitter drifts *lower* in frequency, the pulses will tend to drift *up* the sawtooth causing one of the discriminator diodes to conduct more heavily, thereby decreasing the bias on the reactance tube. Conversely, a transmitter drift *higher* in frequency will shift the video pulses *down* the sawtooth (to the left) and thus cause the other diode to conduct and raise the reactance tube bias.

Manual Drift Control is also provided for use under adverse conditions such as when skywaves are present or under excessively noisy conditions. The drift control manually varies the reactance tube (V-244) bias voltage over a range sufficient to permit the stopping of any normal pulse drift.

AMPLITUDE BALANCE

One of the requirements for new Loran receiver-indicators is the ability to furnish differential gain control to received master and slave signals differing in amplitude by as much as 1000 to 1. To accomplish this without introducing distortion in the pulse wave shape requires

careful design of receiver circuits. Time-difference errors due to this cause are held to less than $\frac{1}{2}$ microsecond for signals differing by 1000 to 1 and with the stronger signal equaling 10 volts peak value.

Amplitude or gain balancing is accomplished by the application of a variable amplitude reversible polarity square wave to two vacuum tube suppressor elements in the Loran receiver. The same square wave is used for this application as that mentioned previously for the cathode-ray tube trace separation function. Its period equals the Loran pulse repetition period, and therefore, each half of the square wave is $L/2$ microseconds long. Referring to Figure 7, a simplified diagram of the amplitude balancing and receiver gain system, the "balance" control selects either one or the other of two identical but opposite polarity square waves which are fed to the receiver as variable bias. In the center of its range, this potentiometer will have zero output, while all other positions will allow the selection of either polarity square wave at any desired amplitude up to that existing at the ends of the potentiometer.

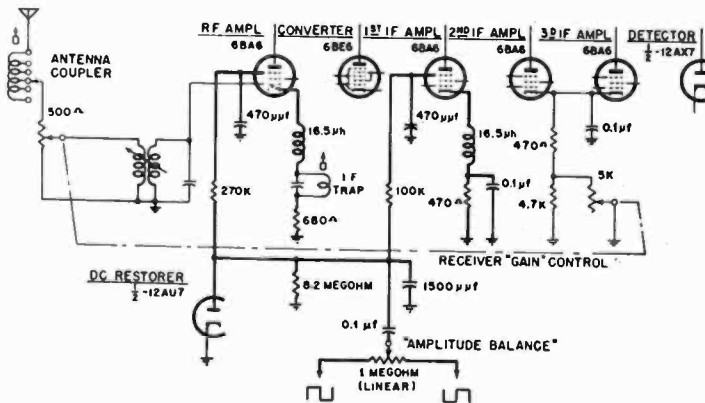


Fig. 7 — Receiver amplitude balance circuits in bold lines. Gain circuits are drawn in light lines.

Assuming for example that at the receiver antenna input, the slave pulse is 1000 times weaker than the master, the amplitude balancing system is capable of equalizing both pulses by the application of less bias to the receiver during the lower trace interval and more bias during the upper trace period. Over the whole operating range from 1:1 to 1000:1 difference in pulse amplitudes, errors introduced by leading edge distortion of the received pulses are kept exceedingly low by using two control tubes rather than one in the manner shown by the heavy lines in the diagram. Before deciding upon this particular grouping of controlling elements for amplitude balance, several other combinations were tried resulting in greater distortion to the pulse envelopes. This distortion is the result of varying input capacities with changing RF grid bias and nonlinearity of tube characteristics. The

system as applied in this instrument makes best use of the linear portions of the characteristics of the selected tubes, so that the output pulse shapes suffer a minimum of clipping and leading-edge distortion.

MECHANICAL DESIGN

Figure 8 shows the front panel layout of the instrument. Controls for channel, function, station and rate are grouped around the cathode-ray tube on the upper portion. These dials, plus the time-difference dial below, are indirectly illuminated from behind the panel, with a dimmer rheostat, mounted at the upper left, to provide continuous control of brightness. In addition, a hooded panel lamp at the center, also controlled by the dimmer, furnishes a proper amount of external

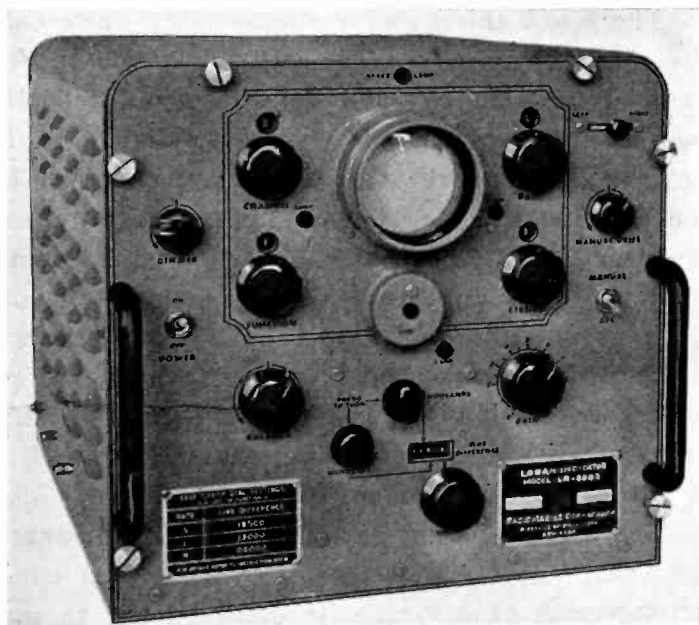


Fig. 8—Front panel view.

illumination for night time use. The left-right and drift controls are at the upper right with the automatic frequency control on-off switch below them. Receiver gain and amplitude balance knobs are symmetrically positioned above the time-difference controls. There are three time-difference knobs, providing coarse, medium and fine adjustment for this important item. Each may be used independently of the others with the lower order controls (units and hundreds) effecting "carryover" of the higher ones. Depressing the "thousands" or "hundreds" knobs disengages them from the mechanism so that the units knob does not have to spin rapidly when the former are rotated.

The main power switch is located on the left side of the front panel. This switch additionally serves to turn on or off auxiliary rotary power

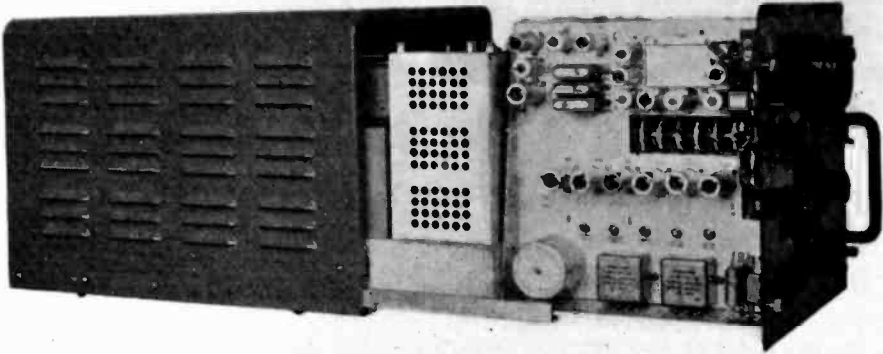


Fig. 9—Left side view. Indicator rolled out of cabinet for inspection.

conversion equipment when the equipment is being operated from other than 115-volt alternating current.

There are three major subassembly units combining to make up the receiver-indicator. The left side, seen in Figure 9, contains the receiver near the top and the sweep and deflection circuits near the bottom. The right side, seen best in Figure 10, is the complete timer unit, beginning with the 100-kilocycle crystal at the top rear, and concluding with the 25-cycle multivibrator circuits. The automatic frequency control circuit is also found on this unit. All tubes on these chassis are miniature seven- and nine-pin types. The third section at the rear is the power supply unit which generates high voltage for the cathode-ray tube and furnishes filament power for all tubes in the indicator. A small blower unit, mounted in the right rear corner, draws in cool air from beneath the cabinet, and, after filtering, blows it into the central area within the indicator.

The direct-reading switch mechanism mounts immediately behind the front panel and wires into the various timer circuits using an arrangement of low-capacity spaced leads to insure rapid rise time of the many and complex waveforms present.

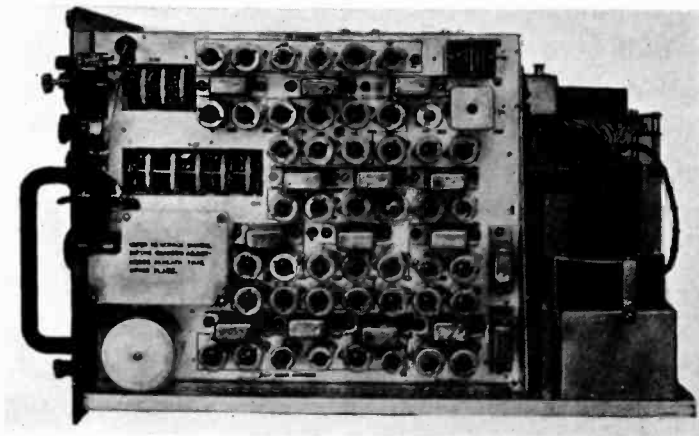


Fig. 10—Right side view showing timer chassis.

To facilitate service and preventative maintenance operations, the equipment is track mounted and may be withdrawn giving easy access to tubes and adjustments.

An external power supply is furnished. It provides regulated plate voltage for the entire equipment and contains line filter units for interference suppression as well as the necessary protective fuses.

Every effort has been made to effect a sturdy, dependable instrument in as compact a unit as possible.

GENERAL CHARACTERISTICS OF DIRECT-READING LORAN INDICATOR,
MODEL LR-8802

Receiver Tuning

Channel 1	1950 kilocycles
Channel 2	1850 kilocycles
Channel 3	1900 kilocycles
Channel 4	1750 kilocycles

Basic Pulse Rates

S	20 cycles
L	25 cycles
H	33 $\frac{1}{3}$ cycles

Station Pulse Recurrence Rates 24 (8 on each basic rate)

Time-Difference Measuring Range

S rate	100 to over 17,000 microseconds
L rate	100 to over 15,000 microseconds
H rate	100 to over 11,000 microseconds

Time-Difference Presentation—Readings directly displayed on simple five-digit dial. No interpolation necessary. Error due to signals differing in amplitude by as much as 1000:1, with 10 volts maximum peak signal, will not exceed 0.5 microsecond. Overall time difference reading accurate within one microsecond.

Power Requirements—115 volts \pm 10 per cent, 50-60 cycles, approximately 3 amperes at 0.9 power factor (310 watts). Direct-current operation is possible using auxiliary conversion equipment.

Automatic Frequency Control—Includes circuits to automatically stabilize drift, and make the received pulses stationary on the working portions of the traces. Locks on either or both the master and slave pulses. When locked on both pulses, one pulse may fade out without destroying the stabilization. Operates on signal-to-noise ratio of

1:1 with pulse amplitude as low as one-fourth inch on the cathode-ray tube.

Timer and Counter Circuits—Binary and decade counters actuated by stable 100-kilocycle crystal oscillator.

Receiver Sensitivity—8 microvolts peak input signal gives 1-inch deflection on 3-inch scope with at least 3:1 signal-to-noise ratio. Ten decibels additional gain is provided.

Receiver Selectivity—Within the following limits:

Decibels	Band Width in Kilocycles
6	40 to 50
20	90 maximum
40	130 maximum
60	180 maximum
80	250 maximum

Intermediate Frequency—1100 kilocycles.

Radio Frequency Oscillator—Crystal controlled.

Spurious Responses—More than 80 decibels down.

Antenna—Single vertical wire 35 to 125 feet long is suitable.

Indicator Controls—Power switch, dimmer, channel, rate, station, function, left-right, automatic frequency control-manual, manual drift, delay controls (thousands-hundreds-units). (Display presentation shown on 3-inch scope and time-difference shown in microseconds on direct-reading illuminated dial).

Unit	Height	Width	Depth	Weight
Indicator	14 $\frac{1}{4}$ "	15"	22 $\frac{5}{8}$ "	93 lbs.
Power Supply	8 $\frac{15}{16}$ "	14 $\frac{3}{16}$ "	8 $\frac{9}{16}$ "	33 lbs.
Antenna Coil				
Unit	7 $\frac{1}{16}$ "	8 $\frac{1}{16}$ "	3 $\frac{3}{8}$ "	8 lbs. 2 oz.
Junction Box	5"	11 $\frac{1}{2}$ "	3"	2 lbs. 3 oz.

Mounting

Indicator—Table or shelf-mounted

External Power Supply—Table or shelf-mounted

Antenna Loading Coil—Interior or exterior bulkhead mounted.

Accessory Equipment—RM-89A Junction Box, provides means for cable connection when indicator is more than 10 feet from external power supply.

ACKNOWLEDGMENTS

The writers acknowledge with thanks the technical cooperation and assistance offered to them by members of the Aviation Engineering Section of the RCA Victor Division. Development of the LR-8802 was greatly facilitated by their efforts.

Edward Oschmann contributed substantially toward refinement of the automatic frequency control, amplitude balance and receiver circuits. Joseph F. Trupiano planned the mechanical layout of the instrument, and numerous other Radiomarine personnel assisted in the completion of the project.

A NEW IMAGE ORTHICON*†

By

R. B. JANES, R. E. JOHNSON AND R. R. HANDEL

Tube Department, RCA Victor Division,
Lancaster, Pa.

Summary—The design of a new panchromatic high-sensitivity photosurface has resulted in the development of a new image orthicon, RCA-5820, which permits the televising of low-level illuminated scenes with a faithful gray-scale rendition of colors. Performance results of this new tube in comparison with other types for both remote and studio pickup are given.

INTRODUCTION

IN 1946 the 2P23 image orthicon was introduced for remote pickup use.¹ In spite of drawbacks such as a rather low signal-to-noise ratio and unfaithful gray-scale color rendition because of its infra-red sensitivity, the versatility of the 2P23 in picking up scenes having wide ranges of illumination quickly led to its nearly universal adoption for remote pickups. Further development² brought about a considerable improvement in its signal-to-noise ratio and resolution, but the color rendition still presented difficulties, especially for studio use. In 1947, the 5655 was brought out to fill the urgent need for a studio tube.² The use of a different photosurface with no infra-red response gave a considerably better color rendition. The signal-to-noise ratio was also improved by a change in the target structure which raised the target capacitance. The photosurface of the 5655, however, had a lower sensitivity, particularly to incandescent light, than that of the 2P23. Because of the lower sensitivity and the greater capacitance of the target, the 5655 requires the use of more light. Studio lighting levels of 200 to 300 foot-candles of incandescent light or 150 to 200 foot-candles of fluorescent light have been needed for use with this tube in order to obtain good depth of focus. The better color rendition, however, was so advantageous that in 1948 the 5769, which has the same target structure as the 2P23 but with the photosurface of the

* Decimal Classification: R583.6.

† Presented at the Nat'l Electronics Conf., Chicago, September 26, 1949.

¹ A. Rose, P. K. Weimer and H. B. Law, "The Image Orthicon — A Sensitive Television Pickup Tube", *Proc. I.R.E.*, Vol. 34, No. 7, pp. 424-432, July 1946.

² R. B. Janes, R. E. Johnson and R. S. Moore, "Development and Performance of Television Camera Tubes", *RCA Review*, Vol. X, No. 2, pp. 191-223, June 1949.

5655, was introduced. The 5769 has found wide use in both remote pickups and studio use. In the studio, it has been preferred by many over the 5655 because it requires less light and because of its ability to handle a wide range of illumination.

Although the 5655 and 5769 have better color rendition than the 2P23, they have two shortcomings. First, their over-all sensitivity is only about one-third that of the 2P23 for incandescent lighting. For fluorescent lighting and daylight, the tubes are more comparable partly because the sensitivity of the 2P23 falls off for this type of lighting. Second, the spectral response of the 5655 and 5769 is largely in the blue end of the spectrum. Unless a considerable amount of incandescent "modeling" lighting is used, facial tones which are largely in the yellow and red come out too dark. For example, light beards when televised would appear almost black.

Experience with these three image orthicons has pointed to the need for a high-sensitivity photosurface which more closely matches the response of the eye. Such a surface has now been incorporated in a new image orthicon, the RCA-5820. The 5820, which uses the wider-spaced, lower-capacitance target structure of the 2P23 and 5769, is especially useful for remote pickups. In addition, it may be preferred by many for studio use because of its ability to handle wide ranges of illumination.

SPECTRAL SENSITIVITY CHARACTERISTICS OF IMAGE ORTHICONS

Curves comparing the spectral sensitivity characteristics of all the image orthicons are given in Figure 1. The curves are plotted on an absolute scale, i.e., for any given wavelength of light the response is given in microamperes of photo current for one microwatt of light energy falling on the photo cathode. The over-all response of the different surfaces to incandescent light of 2870 degrees Kelvin is also given. This figure must be used with care because incandescent light, which contains a good deal of red and infra-red, makes the response of a tube with infra-red sensitivity higher than it would be for sources with less red.

Two curves (C and D) are given for the 2P23 to show the wide range of response that may be encountered in different tubes of this type. The higher-sensitivity tubes (curve C) have a high infra-red sensitivity resulting in a high sensitivity to tungsten illumination (20 microamperes per lumen). These tubes have been useful in the past for picking up scenes illuminated with low-level incandescent light. The infra-red response, however, causes peculiar color renditions.

Reds appear almost white and objects which reflect infra-reds such as green grass appear a light gray. Tubes of lower sensitivity (curve D) have a smaller response to infra-red, but also lack high sensitivity to incandescent light. Because of the wide range in spectral response, it is difficult to obtain two matched 2P23's. In one tube grass might appear gray and in another nearly white. Usually, in operation, a higher-sensitivity tube tends to lose infra-red response and sensitivity so that its characteristics gradually shift towards those of the lower-sensitivity tube.

The 5769 and 5655 make use of a photosurface that has a fairly good blue response but is deficient in the yellow and red compared to the response of the human eye. Curve B of Figure 1 is a typical curve for these two tube types. The sensitivity to 2870 degrees Kelvin

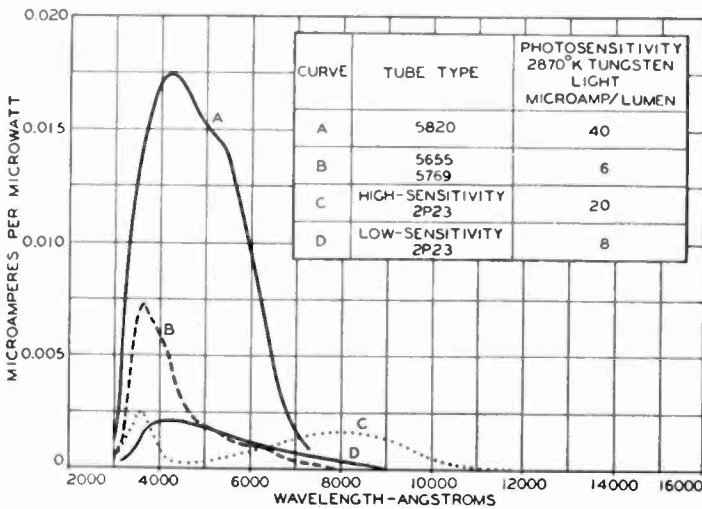


Fig. 1—Spectral sensitivity characteristics of image orthicons.

incandescent sources is much lower than that of the higher 2P23. For blue-rich sources such as fluorescent lights or blue skylight, however, the sensitivity of the 5769 or 5655 may be actually higher. In the studio, the use of a proper balance of fluorescent base lighting and incandescent "modeling" leads to a fairly good color rendition with the 5655 or 5769, but the lack of good yellow and red response tends to give flat facial appearances.

CHARACTERISTICS OF THE 5820

Curve A of Figure 1 shows the spectral sensitivity characteristic of the new photosurface incorporated in the 5820. The surface has a high sensitivity to 2870 degrees Kelvin incandescent sources—on the average 40 microamperes per lumen. Because its spectral response is fairly close to that of the eye, the total response does not depend greatly on the type of light source. For incandescent, fluorescent, and

daylight sources, the response of the surface will average about the same. The curves of Figure 2 show how the spectral response of the 5820 compares with that of the eye. Curve A of Figure 2 gives the uncorrected response of the tube, Curve B the response when a Wratten No. 6 filter is used, and Curve C gives the eye response. If a picture of various colored objects is observed critically on a 5820 without a filter, it can be noted that although the reds and yellows give about the same response as the eye, the blues and greens appear to be somewhat lighter to the tube than to the eye. This characteristic, however, will be objectionable only under special conditions. The use of a Wratten No. 6 filter drops the blue and green response to nearly the eye value with a loss of sensitivity of only about one lens stop. The closeness of the response to that of the eye makes the problem of proper scenery and makeup a much simpler one. In general, if lighting and makeup look satisfactory to the eye, the camera will also give a good color rendition. Any further changes that are made can be checked with the eye without the need of televising the scene.

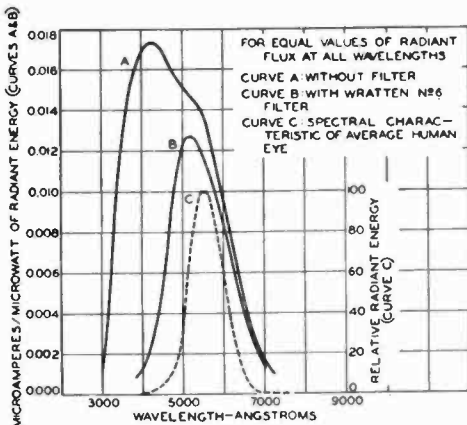


Fig. 2—Comparison of spectral sensitivity characteristic of type 5820, with and without a filter, with that of the average human eye.

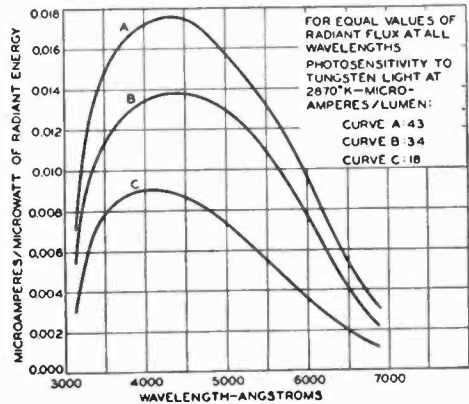


Fig. 3—Spectral sensitivity characteristic of three different 5820's.

Figure 3 gives the spectral response characteristic of three different 5820's all with the new photosurface. As these curves indicate, there is some variation in spectral response from tube to tube, especially in the region of 5000 to 6000 angstrom units. This variation is much less than that encountered among 2P23's and, under normal use, is not noticeable.

OPERATING CONSIDERATIONS

The much higher sensitivities of the 5820 poses some problems in its use. With a lens aperture of $f:2.8$ it is possible to obtain a usable

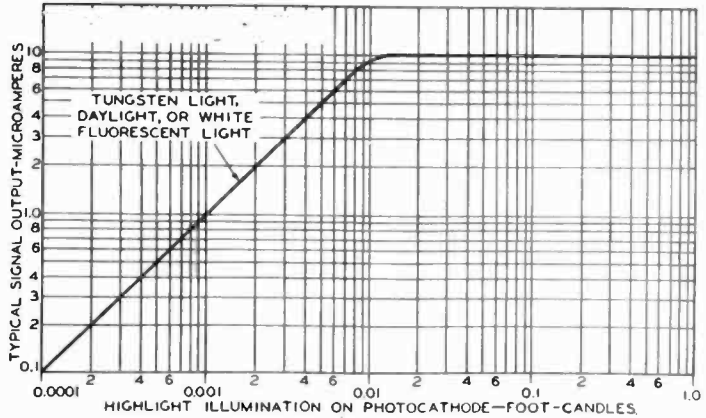
picture with only 1 or 2 foot-candles of illumination. Such low light levels, however, should be used only when there is no other way of obtaining a picture. To obtain good depth of focus and to pick up the grays near black, a light level of 20 to 30 foot-candles should be used. In the studio, it is very seldom worthwhile to drop below about 100 foot-candles. With too low a light level, modeling lights will give too sharp contrasts which are undesirable unless special effects are wanted. It is better to use a base lighting of perhaps 50 to 60 foot-candles of fluorescent light and to use modeling lights to build up the total illumination to approximately 100 foot-candles. In the studio, slim-line instant-start white fluorescent lights of 3500 to 4500 degrees Kelvin are satisfactory for base lighting.

When the 5820 is used for outdoor pickup, operators will encounter a problem of too much light on very bright days. In this case, the use of neutral filters is helpful. When the illumination is of the order of several thousand foot-candles, as is obtained with bright sunshine, a Wratten neutral filter with a transmission of 5 per cent can be used. For slightly cloudy days with an illumination of 500 to 1000 foot-candles, a filter with a transmission of 10 per cent should be satisfactory. Because of the higher sensitivity of the 5820, stray light also will be troublesome. Wherever the possibility of stray light entering the lens exists, a lens shield should be used.

FEATURES OF PHOTOSURFACE

In addition to the gain in sensitivity and the improvement in spectral response, the use of the new photosurface has led to other desirable characteristics. In the 5769 and 5655 the photosurface is quite transparent so that a good deal of light passes through it. This light may be reflected from different parts of the image section and return to the photocathode where it will cause unwanted photo emission. Also, because all of the targets are somewhat photosensitive, light passing through the photosurface can cause trouble in the darker parts of the picture. The lower degree of transparency of the new surface reduces both of these effects. In addition, the much higher photosensitivity of the new surface will in itself cause a reduction in the amount of light reaching the target and, therefore, reduce the emission of unwanted electrons from the target. Because of these features, the 5820 gives a picture with a better gray scale and more "snap". The new tube also has, on the average, better resolution than its predecessors although all the reasons for this improvement have not as yet been fully determined.

Fig. 4—Typical signal output of type 5820.



ILLUMINATION AND CAMERA REQUIREMENTS

Figure 4 is a simplified curve of the signal output of the 5820. This curve is for a small white object on a black background, but it holds reasonably well for a more complicated picture. Photocathode illumination at the knee of the curve averages about 0.01 foot-candle. The curves of Figures 5a and 5b show how much illumination is needed for a given angle of view and for a lens with a given f: number. Two sets of curves are given—one for black-and-white rendition and one for better half-tone rendition. These curves are calculated from the simple formula,

$$I_s = \frac{4f^2 I_{pc} (m + 1)^2}{TR}$$

where

I_s = scene illumination in foot-candles. This value is the illumina-

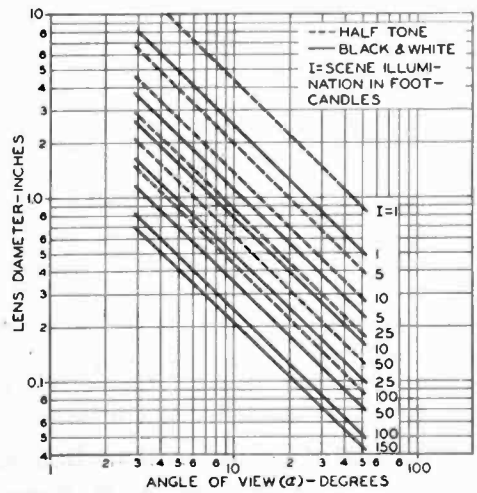
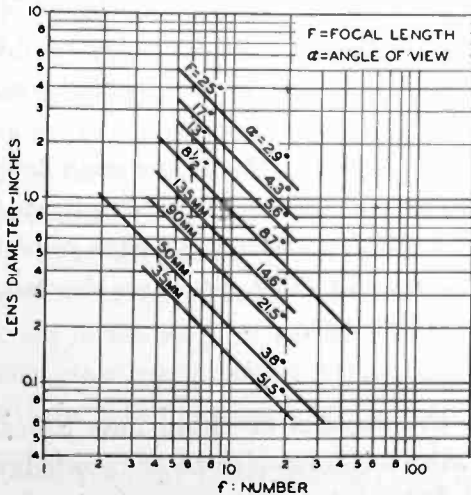


Fig. 5—Illumination requirements for various lens diameters, f: numbers, and angles of view.

tion on the scene measured with a light meter positioned towards the lens of the camera,

$f = f$: number of lens,

I_{pc} = photocathode illumination in foot-candles,

m = linear magnification of scene to target,

T = total transmission of lens,

R = reflectance of principal subject in scene.

For black-and-white rendition, the conditions are set up for a barely acceptable picture, i.e., one in which the high lights just reach the knee of the curve. The reflectance R for these high lights is taken as 0.5, the lens transmission as 75 per cent (there will be some error here as not all the lenses will have this transmission), I_{pc} is taken as 0.01 foot-candle, and m can be neglected. For half-tone rendition, the conditions are the same as for black and white except it is assumed that the reflectance of the object when the high lights just reach the knee of the curve is 0.16. Figure 5a shows the effective lens diameter or opening in inches plotted against the f : number of the lens. Curves are given for many of the lenses used with television cameras along with their respective angle of view. Figure 5b gives the lens diameter plotted against angle of view for different values of scene illumination for both black-and-white and half-tone rendition. The following examples illustrate how these curves can be used. In the studio, a scene has an illumination of 100 foot-candles. For half-tone rendition and an angle of view of 8.7 degrees, the required lens diameter of 0.5 inch is determined from Figure 5b. In Figure 5a, it can be seen that for an 8.7-degree lens with a diameter of 0.5 inch, an f : number of 17 is satisfactory. For an outdoor shot with a scene illumination of only 10 foot-candles where black and white may be useful, Figure 5b shows that a 2.9-degree angle of view calls for a lens diameter of 2.6 inches. In Figure 5a this value of lens diameter corresponds to an f : number of 10.

For complete information, curves of depth of focus for each lens should be included. These curves, however, would be very complicated because a separate curve is needed for each f : number and each object distance. This information, in most cases, is either given on the lens or can be obtained from the lens manufacturer.

ACKNOWLEDGMENT

Many groups have contributed to the success of these new tubes. In the Tube Department at Lancaster, the authors wish to acknowledge the help of L. Young, A. D. Cope and J. K. Johnson in the fabrication and processing of the tubes, and A. A. Rotow for his extensive testing.

THE EVALUATION OF CHROMIUM-IRON ALLOYS FOR METAL KINESCOPE CONES*

By

ARNOLD S. ROSE AND JOHN C. TURNBULL

Tube Department, RCA Victor Division,
Lancaster, Pa.

Summary—A series of tests on chromium-iron alloys is described which establishes the suitability of each of the alloys for sealing to the glasses used in the manufacture of metal-cone kinescopes.

These tests are based upon the behavior of the alloy as it is heated to the sealing temperature of 1200 degrees centigrade and include microscopic examination of the structure of the alloy, a thermal expansion test, and a seal test. The tests provide quantitative data which may be used to evaluate the alloy.

INTRODUCTION

THE materials of construction used for the popular 16AP4 metal-cone kinescope are standard, readily available metals and glasses, concerning which a considerable technology has been established. Thorough utilization of this fund of engineering data has contributed materially to the successful solution of the many problems encountered and has permitted the establishment of a series of standard test procedures which ensure control of the properties of the materials involved. It is the purpose of this paper to review some fundamental metallurgical principles and to describe how they are used to evaluate the chromium-iron alloys used for metal kinescope cones.

The metal cone of the 16AP4 kinescope, shown in the outline drawing (Figure 1), is fabricated by a spinning process¹ from a 28 per cent chromium-iron alloy known commercially as AISI Type 446 modified. The large end of this cone is sealed to a circular face plate of 3/16-inch high-quality window glass which is formed to a uniform radius of curvature from center to edge. The small end of the metal cone is sealed to a pressed lead-glass cone. When the metal cone and the glass components are sealed by heating them with gas fires, they attain a temperature of close to 1200°C in the immediate vicinity of

* Decimal Classification: R331.

¹ A. Hildebrandt, "Automatic Spinning of Stainless Steel", *The Tool Engineer*, Vol. XXI, p. 21, 1948.

the sealing surfaces. It is the effect of this high temperature on the thermal expansion characteristics of the 28 per cent chromium-iron which constitutes the basis for these evaluation tests.

EFFECTS OF TEMPERATURE ON CHROMIUM-IRON ALLOYS

The phase relationships that prevail in the chromium-iron alloys at various temperatures have been investigated thoroughly by Bain.² Figure 2 is adapted from curves in this reference to show the relationships graphically. Reference to it will help to clarify the problems involved in the use of the alloys. Figure 2 shows that when an alloy containing 28 per cent chromium is heated to a temperature of 1200°C it will retain without change its predominantly ferritic (+ carbides) crystalline structure. A photomicrograph of such an alloy, water-quenched after heating at 1200°C for 15 minutes, is shown in Figure

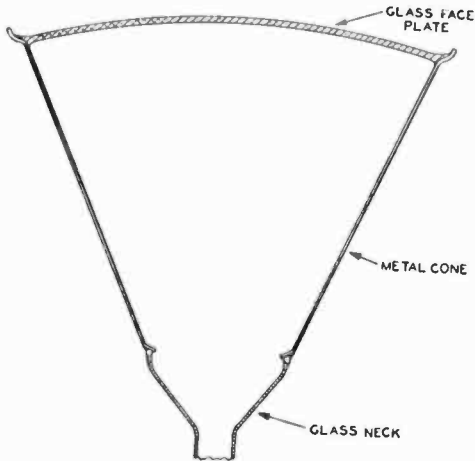


Fig. 1 — Metal cone—glass assembly.

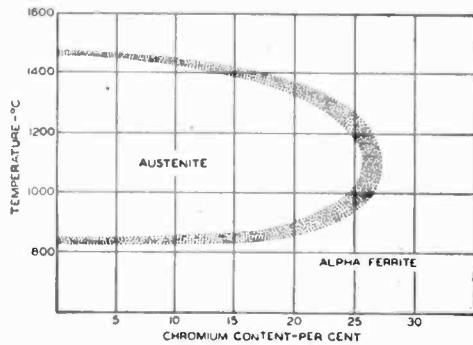


Fig. 2—Effect of temperature on structure of various quenched chromium-iron alloys. Adapted from information given in Reference (2).

3a. In terms of thermal expansion, since no change in structure has been experienced, the slope of the expansion curve will remain uniform and without discontinuity as the alloy is heated to and cooled from the 1200°C temperature. Curve A of Figure 4 illustrates the typical expansion characteristics of a chromium-iron alloy containing 28 per cent chromium. Because the value of the expansion coefficient generally obtained for this type of alloy ranges from 108 to 110×10^{-7} per degree centigrade between 25°C and 500°C, no difficulty is experienced when glass seals are made during the tube manufacturing processes.

As a contrast to the behavior of this 28 per cent alloy, which does

² E. C. Bain, "The Nature of the Alloys of Iron and Chromium", *Trans. Amer. Soc. Steel Treeters*, Vol. 9, 1926.

not undergo any transformation with heating, compare the behavior of a chromium-iron alloy containing 17 per cent chromium. Figure 2 shows that a typical commercial alloy containing 17 per cent chromium undergoes a transformation at the 1200°C temperature from a predominantly ferritic crystalline structure to one which is partially austenitic. A photomicrograph showing such a structure is given in Figure 3b. The expansion curve of this alloy heated to 1200°C and subsequently cooled will, of course, be changed by the transformation.

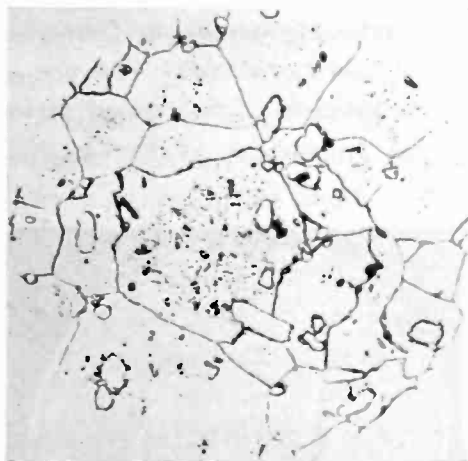


Fig. 3a—Photomicrograph at 500 \times of a chromium-iron alloy containing 28 per cent of chromium and quenched after heating to 1200°C. The structure shows only the ferrite phase plus scattered carbides.

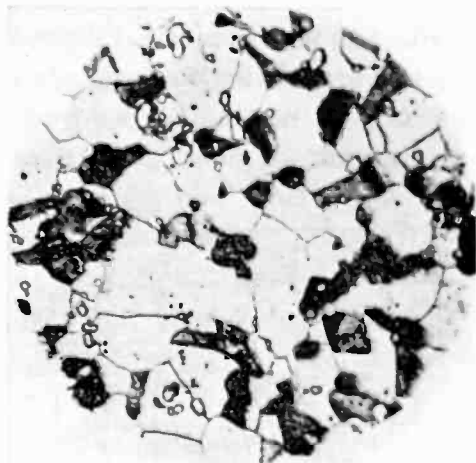


Fig. 3b—Photomicrograph at 500 \times of a chromium-iron alloy containing 17 per cent of chromium and quenched after heating to 1200°C. The structure shows clearly the presence of transformed austenite in the predominant field of ferrite.

Curve B of Figure 4 shows that the alloy containing 17 per cent chromium expands from room temperature at a constant rate until a temperature of approximately 800°C is attained. At this point the alloy undergoes a transformation to the gamma austenite phase. The rate of thermal expansion of the alloy is increased by the formation of this high-expansion constituent and on cooling remains high. Because the chromium content of the alloy renders the reverse (gamma-alpha) transformation sluggish, the reverse transformation will generally not occur until the alloy has cooled to a temperature of approximately 200-300°C. Inasmuch as this reverse transformation is below the setting point of the glass (530°C) and is accompanied by a sudden expansion, the seal between metal and glass fails as a result of the increased tensile stresses. The radial cracks observed in the face-plate seal of Figure 5 clearly illustrate this type of failure. Obviously an alloy which undergoes such a transformation is not suited for tube manufacture.

Some lots of the 28 per cent alloy show a variation from the general behavior which merits description. Such alloy lots when heated to 1200°C are subject to a transformation in the neighborhood of 1150°C. The resultant austenite, however, is an extremely stable phase which does not undergo the reverse transformation to the alpha-ferrite state even when the alloy is held at temperatures as low as that of liquid air (-185°C). Moreover, holding the alloy at 350°C for 48 hours has failed to cause the gamma-to-alpha transformation to take place. The thermal-expansion curve of this material, Curve B, Figure 4, shows a slight although definite increase in the rate of expansion following the transformation to austenite at elevated temperatures. The use of this type of material is not recommended because of increased stress in the glass-to-metal seal caused by the formation of the higher-

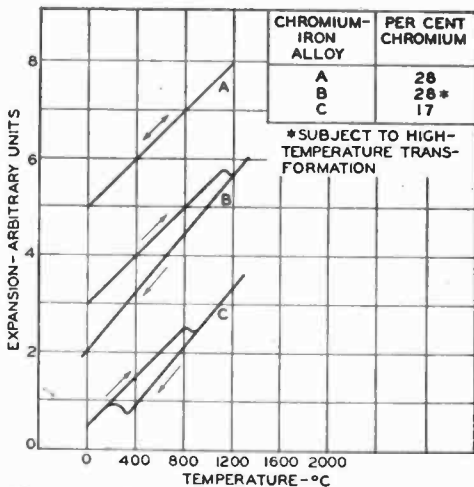


Fig. 4—Idealized expansion curves of chromium-iron alloys.

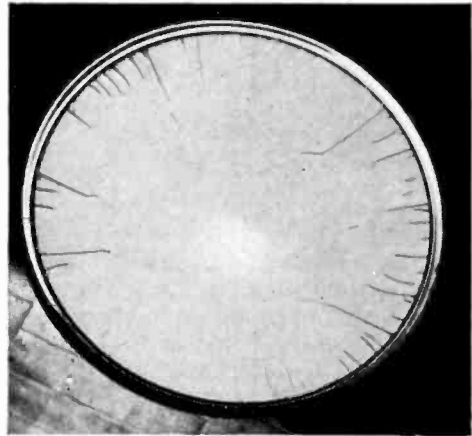


Fig. 5—Face-plate cracks in a 16-inch kinescope made with a chromium-iron alloy cone containing 17 per cent of chromium.

expansion phase which in some instances has increased the thermal expansion coefficient between 25°C and 500°C to a value of 120×10^{-7} per degree centigrade.

As a result of these considerations, an evaluation of the acceptability of the chromium-iron alloy for use in metal-cone kinescopes may be written, based upon the appearance of the microstructure of the alloy after it is heated to 1200°C. When a sample of the alloy to be tested is heated to 1200°C ($\pm 10^\circ\text{C}$) for 15 minutes, water quenched, and then examined microscopically at a magnification of $500\times$, the sample should exhibit no evidence that any transformation has occurred, i.e., the field should consist essentially of ferrite and carbides. Should any austenite or other transformation product be present, the value for thermal expansion coefficient of the alloy, which is given

below and which actually allows for the appearance of a small amount of austenite, will govern the acceptability of the alloy.

THERMAL EXPANSION

The effects of high glass-sealing temperature on glass strains can be investigated directly, as noted above, by measurements of the thermal contraction curve of the metal. The sealing schedule used in the manufacture of the metal-cone kinescope is approximately the following: (1) heat to 1200°C for 3 minutes (glass sealing), (2) transfer to an oven at 550°C and hold for 8 minutes (glass annealing), and (3) remove from the oven and cool in air to room temperature. The cooling rates in this schedule are too rapid for accurate dilatometric measurements, but, since only that portion of the contraction curve between the setting point of the glass (530°C) and room temperature is significant in determining glass strains, the required change in test procedure affects only step 3. The test procedure follows: (1) heat a pointed specimen 4 inches long by placing it in a furnace at 1200°C for 15 minutes, (2) transfer the specimen rapidly to the dilatometer and insert specimen and dilatometer promptly into the dilatometer furnace (held at 550°C) before the sample temperature drops below 550°C, and (3) measure the contraction curve by lowering the temperature of the dilatometer furnace at a slow rate (two degrees centigrade per minute to 40°C). The measurement is made on a recording instrument³ consisting of a quartz tube dilatometer with an electrical strain gauge for measuring sample expansion or contraction.

In order to establish a factor of safety for the test, the metal is heated at 1200°C for a somewhat longer time than would actually be used for glass sealing. As an acceptance specification for the alloy, it is required that after the specimen is heated to 1200°C there be no sudden change in length between 530°C and -40°C, and that the average coefficient of expansion between 500°C and 30°C be less than 114×10^{-7} per degree centigrade.

GLASS-SEALING TEST

A rapid check of the thermal expansion of metals can be made with a glass-sealing test, in which a glass of known physical properties is sealed to the metal and then annealed. Strains which depend on the difference between the contraction curve of the glass and the metal

³ J. C. Turnbull, "A Recording Dilatometer for Measurement of Thermal Expansion", *Bulletin of the American Ceramic Society*, Vol. 28, p. 121, March 15, 1949.

will be developed in the glass. Because the expansion of the glass can be maintained as a constant factor, the glass strain can be taken as an indication of the over-all contraction of the metal for the approximate temperature range of 500°C to 30°C. It is necessary in this test, to standardize the composition of the glass, the dimensions of the seal, and the sealing and annealing conditions.

A lot of drawn sheet glass, which is the same as that used for the face plate of the metal-cone kinescope, is used for this test. This glass has a thermal expansion coefficient between 30°C and 300°C, of 91×10^{-7} per degree centigrade. The dimensions of the metal strip used for the seal are $\frac{1}{8} \times 1\frac{1}{2} \times 4$ inches, and of the glass strip $\frac{3}{16} \times \frac{3}{4} \times 3$ inches (Figure 6). The metal strip is prepared for

sealing by cleaning one of the $1\frac{1}{2} \times 4$ -inch surfaces by sandblasting. The sealing procedure follows:

(1) the metal strip is placed in an air-atmosphere furnace at 1200°C for 15 minutes, (2) the glass is placed in the furnace on top of the metal strip, (3) the sealed sample is removed after the glass has melted and fused to the metal but before the edges of the glass strip flow out over the metal appreciably, (4) the seal is cooled rapidly to about 600°C and placed in an

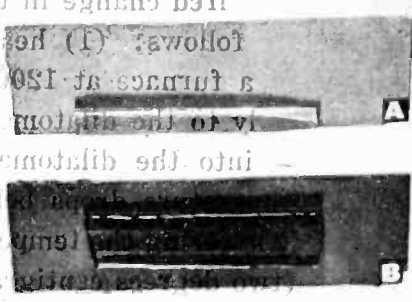


Fig. 6—Glass-sealing test sample: (A) Metal and glass strips prior to sealing; (B) Sample after sealing.

annealing furnace held at 525°C for at least 30 minutes to allow the glass and metal to come to an equilibrium temperature, and (5) the furnace is cooled slowly (1 degree centigrade per minute) to a temperature of 400°C, after which the seal can be cooled rapidly to room temperature.

After the glass is cooled, it is examined by means of a polariscope parallel to the plane of the seal to determine the amount of residual strain in the glass. The Goranson-Adams arrangement⁴ in which a $\frac{1}{4}$ -wavelength plate is used gives good results when these strain measurements are made on a polariscope. As an acceptance specification for the material, it is required that the seal strain, measured under the above conditions, should be less than 700 millimicrons per centimeter.

⁴R. W. Goranson and L. H. Adams, "A Method for the Precise Measurement of Optical Path Differences, Especially in Stressed Glass", *Jour. Frank. Inst.*, Vol. 216, p. 475, 1933.

CONCLUSION

The tests described above establish the criteria which may be used to evaluate the suitability of a particular chromium-iron alloy for use as the cone of a kinescope. Inasmuch as each of these tests is based upon the reaction of the alloy to the thermal treatment imposed upon it during the glass sealing operations incurred in the actual manufacture of the tube, the data obtained may be utilized with complete assurance. Confidence in the validity of the test procedures arises from a background of experience in testing 28 per cent chromium-iron alloys for kinescope use and from the successful utilization of several hundred approved alloys in the manufacture of many thousands of 16-inch metal-cone kinescopes.

THE PROVISIONAL FREQUENCY BOARD*

BY PHILIP F. SILING

Engineer-in-Charge, RCA Frequency Bureau,
RCA Laboratories Division, New York, N. Y.

Summary—The Provisional Frequency Board was created at the International Radio Conference which met at Atlantic City in 1947. Its purpose is to prepare a master list of frequency requirements for international communications. The functioning of the Board and its progress to date are described.

INTRODUCTION

THE Provisional Frequency Board, which has been continuously in session in Geneva since January 8, 1948, has been engaged in the monumental task of endeavoring to formulate, on the basis of sound engineering principles, a master frequency assignment plan for the radio stations of the world. Subdivisions of the overall task have been undertaken by the International Aeronautical Administrative Radio Conference¹, the International High Frequency Broadcasting Conference², and by a marine group of the Provisional Frequency Board membership. Upon the success of these negotiations depend the fulfillment of the Atlantic City radio agreements and the coming into force of the Atlantic City frequency allocations table which is the heart of the Atlantic City agreements³. The impact of the radio frequency allocations problem upon all usage, present and contemplated, of the frequency spectrum, makes a review of the history and accomplishments of the Board to date of general interest throughout the radio industry.

Due to traditional random and haphazard methods of international frequency selection, the added chaos in international registration produced by World War II, and the new developments in radio since the Cairo Conference of 1938, it was found necessary at the Atlantic City Conference of 1947 to make a fresh start in the formulation of a frequency allocations table and in the setting up of the world's radio stations on a new and orderly basis of radio frequency listing. Since,

* Decimal Classification: R007.1 × R084.

¹ Geneva, April 19-October 1, 1948; sessions resumed, Geneva, August 1, 1949.

² Mexico City, October 22, 1948-April 9, 1949.

³ P. F. Siling, "Frequency Allocations", *RCA Review*, Vol. VIII, No. 4, p. 737, December, 1947.

in the Atlantic City allocations table, frequency space now used was withdrawn from certain services, primarily the fixed services, in order to make provision for the expanded services of aviation and broadcasting, it was recognized that planned frequency assignments would have to be prepared as a point of beginning before there could be implementation of the Atlantic City agreements. It was for the purpose of formulating an initial master list meeting these needs that the Provisional Frequency Board was created.

FUNCTIONS OF THE PROVISIONAL FREQUENCY BOARD

The Provisional Frequency Board was given responsibility for listing all classes of stations on frequencies between 10 and 30,000 kilocycles. The critical problems of the Board, however, have been those relating to international point-to-point stations in the fixed service bands between 4 megacycles and 27.5 megacycles.

A detailed resolution creating the Provisional Frequency Board was adopted at Atlantic City. This resolution includes, in summary, the following directives to the Board governing its work:

- (a) To compile the technical principles to become the basis for forming the new international frequency list.
- (b) To compile a list of the requirements for communications circuits from the statements filed with it by the various governments.
- (c) To prepare a frequency list by the application of the principles referred to in (a) above to the requirements referred to in (b).

Into this list would be integrated the assignment plans prepared by the aeronautical and broadcasting groups (hereafter discussed). The resulting master plan would not only permit the coming into effect of the Atlantic City allocations table but also serve as the starting point for future international frequency selection and registration.

It was agreed at Atlantic City that, at the conclusion of the work of the Provisional Frequency Board, a Special Administrative Radio Conference would be convened to review the actions of the Provisional Frequency Board, finalize them, and take appropriate action for implementation.

At the initial meeting of the Board in Geneva, 17 nations were represented directly or by proxy and this representation was augmented so that by August 1, 1949 fifty-nine countries were represented, (nine by proxy), and there were also nine members of the International Frequency Registration Board taking part in the Provisional Frequency Board work.

During the first eight months of the existence of the Board, its

substantive work was divided between the preparation of a list of circuits, or requirements list (Committee 3), and the preparation of engineering and technical principles to guide the preparation of the new master frequency list, (Committee 4).

A Committee 5 was later established whose functions were to coordinate the work of Committees 3 and 4 and prepare a list of circuits with proposed complements of frequencies (by megacycle band order only) which would satisfy the needs of the circuits accepted under the rules of the Board. Finally a Committee 6 was created whose functions were to take the lists prepared by Committee 5 and assign specific frequencies to each circuit as close as possible to the megacycle orders proposed.

The Board has fallen far behind its schedule of completion dates for its tasks. This has been due in part to the lack of adequate cooperation on the part of a certain few countries. A further reason for the long period of time which has been consumed in the work of the Board has been the complexity and magnitude of its undertaking.

With the exception of the data applicable to these few countries, the work of Committee 3 has now been completed. There has been compiled a list of the radio communications circuits of the world, with the data regarding each circuit required in the work of assigning frequencies. The list includes presently operated circuits and those expected to be operated according to the filings of the respective countries. The claim of the non-cooperating countries has been that the Board should not approach the problem on the basis of frequency assignments necessary to satisfy specific circuit requirements but on the basis of assignments to the particular radio transmitting station; and that the committee should have used the data as published in the 1939 Berne List of Frequency Registrations.

Regardless of the final result of the Provisional Frequency Board's effort — and this will not be known for several months — the achievement of its Committee 4 in securing the establishment and acceptance of sound technical engineering principles is of far reaching significance and value. These principles, it is believed, will necessarily be utilized as the basis for frequency assignments by the nations in the years to come.

Committee 4 has established rules for determination of maximum, minimum and interposed working frequencies for typical transmission paths. It has determined the appropriate channel spacing between frequency assignments and determined the rules for channel sharing on both a simultaneous and non-simultaneous basis. There have also been prepared circuit data such as maximum-usable-frequency charts,

radio path propagational studies for all regions, a study of the regional density of circuits in operation, an assessment of minimum frequency requirements of typical circuits having varying operational characteristics, calculation of the megacycle band loadings for each transmitting area, aggregating a very large mass of technical studies and data. One of the principal contributions to the science of frequency utilization has been the obtaining of agreement almost universally among the radio technicians of the world, on the application and use of ionospheric prediction data. The Provisional Frequency Board has adopted the technical principles as a guide to its future work.⁴

By the middle of June, 1949, the work of the circuit planning groups constituting Committee 5, in allocating megacycle orders of frequencies to the list prepared by Committee 3, had been completed except for gaps due to declinations by the certain few countries to furnish information.

The Board has made limited progress on the final task of formulating actual frequency assignments. The situation encountered is well indicated by the following remarks quoted from the report of the Chairman of the Board of August 15, 1949, applicable to the 4-7 megacycle frequency bands:

"There is no possibility of a plan being prepared for many areas of the world which will provide for all frequency requirements. This is particularly so in the higher bands where the overload varies from about four hundred per cent to about eighteen hundred per cent in extreme cases."

This report was prepared for consideration by the Administrative Council of the International Telecommunications Union which began its sessions August 17, 1949. By this time the Provisional Frequency Board had reached a critical point with regard to most of the bands allocated to the fixed and land mobile services. A number of alternative proposals as to whether or not the Board should continue its work and as to the basis for continuation were presented to the Administrative Council by various countries. It was apparent from the proposals offered by a majority of the delegations that the prospect of ultimate success still existed; however, there was implied recognition that further progress could be made only by a new approach to the problem.

The direction of the new approach will be determined early in the future proceedings of the Board. The indicated direction of attack is

⁴ The RCA Frequency Bureau maintains a complete file of the many hundreds of conference documents for reference regarding the proceedings of the Board.

to arrive, on a country-by-country basis, at the order of priorities in which the particular country desires fulfilment of its requirements in terms of frequencies which are to acquire international protection through registration. It will be borne in mind that while the objective is to acquire international protection of as many frequency assignments as possible through registration, failure of registration does not preclude frequency utilization on the basis of non-interference to international services.

In the United States itself the reduction of requirements, or re-assessment of proposals on a priority or other acceptable basis, continued to present grave difficulties. One of the reasons why the United States had not by September 1949 been able to present to the Board a realistic proposal applicable to its own services was that the military services of the United States had not agreed to return to a peace-time basis in stating frequency requirements. At the highest levels within our government, actions were being taken for the review of the United States international registration requirements.

SERVICE CONFERENCES

Concurrently with the work of the Provisional Frequency Board, aeronautical, international broadcasting and marine meetings have been held for the framing of assignment plans in the frequency bands allocated to these services.

Broadcasting. The International High Frequency Broadcasting Conference, which remained in session for six months at Mexico City, found itself confronted initially with the same basic difficulty, i.e., the listed requirements far exceeded the total frequency space available. A Planning Committee of the Conference had held previous meetings at Geneva and Mexico City which had indicated that the High Frequency Broadcast Plan would have to make provision for the use of frequencies on an hour-by-hour basis, even though this type of planning was extremely difficult. The complete loading of the high frequency broadcast bands was expected to yield about 6,000 broadcast hours per day whereas the requirements filed by the various countries totaled 15,000 channel hours.

The program of specifying for each country the frequency to be used, power, direction of transmission and exact hours, necessarily involved preparation of several plans in order to take account of variations in propagation due to sunspot activity and seasonal changes. However, it was finally realized that there was no other feasible alternative. Even on this basis, concessions were required by the vari-

ous countries as to shifting hours of broadcasting and in making other changes in requirements. The first of the several necessary plans, that covering the No. 70 or June median sunspot phase, was finally prepared by the Mexico City Conference. Insufficient time remained to prepare the additional plans for the other seasons and the other phases of the sunspot cycle, and a Technical Planning Committee was established to carry out the principle of the June median plan in establishing the remainder of the high frequency broadcasting assignments.

Most of the countries parties to the Mexico City Conference signed the resulting agreement. Among the countries not signing were two major powers. Both countries had succeeded in obtaining, in the final agreement, all the frequency hours that they had requested or the use of which was contemplated. It can only be deduced, therefore, that the refusal of the two governments to sign rested on political grounds. One factor which undoubtedly had an effect on this situation was the matter of numbers; one of the countries had been allocated three times as many frequency hours as had the other. While analysis shows that these numbers are without true significance, considering the requirements and geographical situations of the two countries, the fact standing alone of the disparity in numbers was apparently deemed to have political significance. In the statement on refusal to sign by the delegate of one power, reference was also made to the program of "jamming" its international broadcasting which had by that time (April 1949) been launched by the other.

The effect of these actions is that neither country is able to participate as members in the further work of the Technical Planning Committee; and there will remain for resolution, at the time of the final integration of all services by the Special Administrative Radio Conference, the problem of adoption or rejection of the High Frequency Broadcasting Plan.

Aeronautical. The first sessions of the International Aeronautical Administrative Radio Conference at Geneva occupied more than five months and were characterized throughout by the non-cooperative actions of certain countries. The work of the Conference was further complicated by the existence in certain European countries, notably France, of a basis of assignment of frequencies for aeronautical mobile purposes which visualized CW telegraphy as the exclusive method of working. It was desired by other countries, led by the United States, to formulate a plan based on the band widths required for radio-telephone so that maximum advantage could be taken, in the future,

of developments in the art, employing CW where that was necessary, by subdivision of the telephone channels and at the same time permitting telephony, high speed radioteletype or other high capacity means of communication.

The Aeronautical Conference began its work, much as the Provisional Frequency Board had done, by endeavoring to list requirements and by establishing technical principles and standards of good engineering practice. Furthermore, the Aeronautical Conference worked out a formula for assessing load factors to serve as a starting point for the final task of reducing requirements to the supply level.

After the adoption of technical principles with regard to channel widths, protection ratios, power and other factors, the Conference undertook without success the final stage of its activities. As has invariably been the case, the requirements exceeded the frequency supply. The principal reason for the inability of the Conference to complete its task was the necessity of going back to the respective administrations for re-assessment and drastic reduction of the stated requirements. The Conference adjourned at the end of September with an agreement to reconvene August 1, 1949 and with the setting up of detailed arrangements for review of requirements by individual administrations and for the holding of several regional conferences in the interval. The Conference did accomplish the allotment of frequencies in the aeronautical mobile "OR" bands, of chief concern to the military and to off-route operators.

Among the countries which had found themselves unable to make the necessary concessions at the first Geneva meetings were a number of the Latin American nations. Accordingly a Region 2 Conference was held in Washington March-June, 1949, the result of which was to resolve the difficulties in the Western Hemisphere and secure the adoption of a Western Hemisphere frequency allotment plan.

The sessions of the Aeronautical Conference were resumed in August and October of 1949. The Conference achieved final success, adopting by a vote of 32-10 a world-wide allotment plan for the aeronautical mobile "R" frequencies. Under the plan, complements of frequencies are made available for the various major world air routes and for regional and subregional areas, thus establishing the frequencies which may be assigned by the particular governments concerned to the aviation services. It is believed this success will furnish psychological as well as practical stimulation to the work of the Frequency Board as a whole.

Marine. A group of representatives of those countries having primary interest in the maritime mobile frequency bands held informal meet-

ings at Geneva concurrently with the proceedings of the Provisional Frequency Board. As a result of this effort, a plan had been formulated, by the spring of 1949, which was agreed to be circulated by correspondence to the nations of the world for concurrence. In the United States and in most other countries concerned, the marine plan is still being made the subject of detailed study as this article is being written.

PRESENT STATUS AND FUTURE OF PROVISIONAL FREQUENCY BOARD

Perhaps the best indication of the extremely critical point which had been reached in the work of the Board was the temporary withdrawal in the late summer of 1949 of the delegation of the United Kingdom from its proceedings. In its report to the Administrative Council, the Provisional Frequency Board recommended that it be allowed to continue its work. By a substantial majority, the Administrative Council agreed to extend the life of the Board to February 28, 1950, looking forward to the holding of the Special Administrative Radio Conference to finalize the work and accomplish integration of the service plans on or about September 1, 1950. As a result of this action, the United Kingdom delegation returned to active participation in the work of the Board. The U.S.S.R., however, withdrew its delegation, stating that further work along the lines being pursued by the Provisional Frequency Board was impracticable.

In the United States there has been recognition of the existence of the crisis in the work of the Board, with the implications of threatened loss by the United States of prestige and leadership in the communications field, and recognition of the disastrous consequences of failure to reach agreement and of the necessity for urgent and drastic action. The obligation of the United States to furnish leadership in solving problems of the Board has been recognized among the responsible authorities in our government.

The majority of the foreign administrations have indicated cooperative attitudes and desires. Although it has taken much longer than anticipated, the problem has now been solved of bringing about realization by most governments of the necessity for agreement, realization of the concessions which must be made in order to make agreement possible, and acceptance of the technical principles which will furnish the basis for agreement. Whether the countries, following the example expected to be set by the United States will respond with sufficient concessions to produce agreement cannot, of course, be predicted with certainty. However, it can be said that without question the Provisional Frequency Board has made substantial progress and that the next five months may very well see the successful termination of its labors.

RCA TECHNICAL PAPERS†

Third Quarter, 1949

Any request for copies of papers listed herein should be
addressed to the publication to which credited

"Admittance of the 1B25 Microwave Switching Tube", R. W. Engstrom (Coauthor), <i>Proc. I.R.E.</i> (August)	1949
"Baseball Television", J. P. Taylor, <i>Broadcast News</i> (September)	1949
"Broad-Band Power-Measuring Methods at Microwave Frequencies", L. E. Norton, <i>Proc. I.R.E.</i> (July)	1949
"Comments of Radio Corporation of America", C. B. Jolliffe, Letter concerning color television (August 25)	1949
"Correlation between Cathodoluminescence Efficiency and Decay as a Function of Temperature", R. H. Bube, <i>Jour. Opt. Soc. Amer.</i> (August)	1949
"Directional Microphone", H. F. Olson and J. Preston, <i>RCA Review</i> (September)	1949
"Electrical Shock Versus the Broadcast Engineer", F. W. Smith, <i>Broad. Eng. Jour.</i> (August)	1949
"Electromechanical Phase Indicator", Sidney Wald, <i>Rad. and Tele. News</i> (July)	1949
"Engineering Statement Supplemental to Comments of Radio Corporation of America", E. W. Engstrom, Letter concerning color television (September 6)	1949
"Engineering Techniques in Motion Pictures and Television", A. N. Goldsmith, <i>Jour. Soc. Mot. Pic. Eng.</i> (August)	1949
"Engineer's Role in the Progress of Science", V. K. Zworykin, <i>Elec. Eng.</i> (August)	1949
"A Fluosilicic Acid Solution Process for Producing Low-Reflection Films on Glass", R. F. Leinhos, <i>RCA Licensee Bulletin LB-782</i> (August 20)	1949
"The Illuminating System of the Electron Microscope", J. Hillier and S. G. Ellis, <i>Jour. Appl. Phys.</i> (July)	1949
"Illumination for Television Studios—Part I", H. M. Gurin, <i>Tele-Tech</i> (September)	1949
"The Image Isocon—An Experimental Television Pickup Tube Based on the Scattering of Low Velocity Electrons", P. K. Weimer, <i>RCA Review</i> (September)	1949
"Importance of Groove Fit in Lateral Recordings", D. R. Andrews, <i>Audio Eng.</i> (July)	1949
"An Improved Method of Testing for Residual Gas in Electron Tubes and Vacuum Systems", E. W. Herold, <i>RCA Licensee Bulletin LB-783</i> (August 20)	1949
"An Improved Method of Testing for Residual Gas in Electron Tubes and Vacuum Systems", E. W. Herold, <i>RCA Review</i> (September)	1949
"Influence of Fluxes on the Cathodoluminescence of Zinc Sulfide Phosphors", A. L. Smith, <i>Jour. Electrochemical Society</i> (August)	1949
"Low Reflection Films on Glass by an Improved Chemical Method", F. H. Nicoll, <i>RCA Review</i> (September)	1949
"Mechanical Filters for Radio Frequencies", W. van B. Roberts and L. L. Burns, Jr., <i>RCA Review</i> (September)	1949
"The Medalist's Career", David Sarnoff, <i>Elec. Eng.</i> (August) .	1949

† Report all corrections or additions to RCA Review, Radio Corporation of America, RCA Laboratories Division, Princeton, N. J.

- "Method of Determining the Dielectric Constant and Power Factor of Ceramics at 100 Megacycles as a Function of Temperature", H. J. Evans, *American Ceramic Society Journal* (August 1) 1949
- "Modern Television Producing Plant", M. M. Ellwell, *Televiser* (July) 1949
- "A Network Bisection Theorem", V. D. Landon, *RCA Review* (September) 1949
- "New TV Studio Relay Switching System", W. E. Tucker and C. R. Monro, *Tele-Tech* (August) 1949
- "New Worlds for Study", J. Hillier, *Scientific Monthly* (September) 1949
- "Operational Features of a New Electron Diffraction Unit", R. G. Picard, P. C. Smith and J. H. Reisner, *Rev. Sci. Instr.* (August) 1949
- "Pencil-Type UHF Triodes", G. M. Rose, D. W. Power and W. A. Harris, *RCA Review* (September) 1949
- "Picture Storage Tube", L. Pensak, *Electronics* (July) 1949
- "A Power-Equalizing Network for Antennas", R. W. Masters, *Proc. I.R.E.* (July) 1949
- "Problems of Television Deflection and High-Voltage Supply", A. A. Barco, *RCA Licensee Bulletin LB-781* (August 10) . 1949
- "Progress Report—Theater Television", B. Kreuzer, *Jour. Soc. Mot. Pic. Eng.* (August) 1949
- "Receiving Tubes Employing Secondary Electron Emitting Surfaces Exposed to the Evaporation from Oxide Cathodes", C. W. Mueller, *RCA Licensee Bulletin LB-784* (September 1) 1949
- "A Six-Megacycle Compatible High-Definition Color Television System", Pamphlet (September 26) 1949
- "Television Photometry and Optical Background", R. L. Kuehn, *Tele-Tech* (July) 1949
- "Television Service. Part VII—Vertical Deflection Troubles", J. R. Meagher, *RCA Rad. Serv. News* (September-October) 1949
- "Temperature-Dependent Structure of the Emission Spectra of Two Crystalline Forms of the Zinc Silicate: Mn Phosphor", R. E. Shrader, *Jour. Opt. Soc. Amer.* (August) 1949
- "Theory and Application of Electronic Meters", R. G. Middleton, *RCA Rad. Serv. News* (September-October) 1949
- "Transient Response of Filters", M. S. Corrington, *RCA Review* (September) 1949
- "The Use of Ferrite-Cored Coils as Converters, Amplifiers and Oscillators", V. D. Landon, *RCA Review* (September) 1949
- "Use of VHF Beam Power Amplifier RCA-5763 as Frequency Multiplier up to 175 Megacycles", *RCA Application Note AN-141*, RCA Tube Department, Harrison, N. J. (September 1) 1949
- "The Valuable By-Product", V. K. Zworykin, *Proc. I.R.E.* (Editorial) (August) 1949

NOTE—Omissions or errors in these listings will be corrected in the yearly index.

AUTHORS



DAVID H. CUNNINGHAM received the B.S. degree in Electrical Engineering from the University of Missouri in 1927. From 1927 to 1930, he was with the Westinghouse Company at Pittsburgh, Pennsylvania, in the Radio Receiver Engineering Department. In 1930, he transferred to the RCA Manufacturing Company at Camden, New Jersey where he was engaged principally in the development and design of loudspeakers. At present, he is Group Manager of Loudspeaker Development in the Parts Engineering Department at Camden. Mr. Cunningham is a member of Tau Beta Pi, Eta Kappa Nu, Pi Mu Epsilon,

Sigma Xi, and an associate member of the Acoustical Society of America.

RICHARD O. ENDRES studied engineering at Tulsa University and majored in communications at Purdue University, receiving the B.S. degree in Electrical Engineering in 1948. He joined the Engineering Products Department of the RCA Victor Division at Camden, N. J. in the same year. His work in the Advanced Development Section since that time has been on applied research. Mr. Endres is presently doing graduate study at Pennsylvania University, and is an associate member of the Institute of Radio Engineers.



EVERETT EBERHARD—(See *RCA Review*, Volume X, No. 1, March 1949, page 154)



ROBERT R. FREAS graduated from Drexel Institute where he studied Electrical Engineering. In 1942 he entered the employ of the RCA Victor Division, and in 1945 he joined the staff of the Aviation Engineering Section of the Engineering Products Department.

RICHARD R. HANDEL received the B.S. degree in Mechanical Engineering from Stevens Institute of Technology in 1942, and is presently engaged in part-time graduate study at Franklin and Marshall College, Lancaster, Pa. Upon graduation from Stevens he joined the Tube Department of the RCA Victor Division at Lancaster, Pa. where he is now located. Since 1946 Mr. Handel has specialized in the development of new television pickup tubes and their manufacturing problems.



ROBERT B. JANES—(See *RCA Review*, Volume X, No. 2, June 1949, page 317)

RALPH E. JOHNSON—(See *RCA Review*, Volume X, No. 2, June 1949, page 317)



GEORGE A. MORTON received the B.S. in Electrical Engineering in 1926; the M.S. in 1928 and the Ph.D. in Physics in 1932 from Massachusetts Institute of Technology. From 1927 to 1933 he was research associate and instructor at Massachusetts Institute of Technology. In 1933 he became a Member of the research division of RCA Manufacturing Co., and from 1941 to the present time has been with RCA Laboratories Division. In 1946-7 he was at Oak Ridge, Tennessee on a year's leave of absence working in the field of nuclear physics. He is active in the fields of television, special electron tubes, and the application of electronics to nuclear problems. During the war he served as Section Member of the National Defense Research Committee and is a member of the AAF Scientific Advisory Board. Dr. Morton is a member of Sigma Xi, the American Physical Society and the American Institute of Electrical Engineers and a Senior Member of the Institute of Radio Engineers.

HARRY F. OLSON—(See *RCA Review*, Volume X, No. 3, September 1949, page 455)

JOHN PRESTON—(See *RCA Review*, Volume X, No. 3, September 1949, page 456)

ROBERT L. ROD received the B.S. degree in E.E. from the Georgia Institute of Technology in 1942. Immediately thereafter, he joined the U.S. Army Signal Corps Electronics Training Group, studying UHF at the British Military College of Science and serving as a radar maintenance officer with the Royal Artillery Anti-Aircraft Command. After transferring to the Air Force in 1943, he engaged in operational testing of new radar and racon equipment installed in the South Pacific area. Since 1945, Mr. Rod has been a member of the Engineering Department of the Radiomarine Corporation of America where he has been engaged in the design of radar and loran equipment. Mr. Rod is a Member of the Institute of Radio Engineers, the American Association for the Advancement of Science and the American Radio Relay League.



PHILIP F. SILING received the Ph.D. degree in E.E., from Yale University in 1917. He was employed by the American Telephone and Telegraph Company from 1917 to 1929, International Telephone and Telegraph Corporation until 1933, and as Assistant Deputy Administrator of the National Recovery Administration, in charge of codes of the electrical manufacturing industry until 1935. From 1935 until 1945 he served in the Federal Communications Commission. During World War II he was active in the work of the Board of War Communications. In 1945 he joined RCA as Engineer-in-Charge of the RCA Frequency Bureau. He is a member, and past chairman, of the Joint Technical Advisory Committee. Dr. Siling is a Senior Member of the Institute of Radio Engineers, and a Member of Sigma Xi.



RAYMOND P. MOORE, JR. received the B.S. degree in Physics from Rensselaer Polytechnic Institute, in 1948. In the same year, he joined the RCA Victor Division at Camden, N. J. At present Mr. Moore is working in the Advanced Development Section of the Engineering Products Department on problems in applied research.

ARNOLD S. ROSE received the B.S. degree in 1935 and the M.S. degree in Chemical Engineering in 1939 from New York University. From 1939 to 1940, he was engaged in metallurgy research for the National Bureau of Standards, Washington, D. C. From 1940 to 1942, he was associated with the Williams Gold Refining Company as a metallurgical engineer. Since 1942, he has been a metallurgist with the Tube Department of the RCA Victor Division at Lancaster, Pa. Mr. Rose is a member of the American Society for Metals and the American Institute of Mining and Metallurgical Engineers.



The late FRANK E. SPAULDING, JR. studied electrical engineering at Yale University and Worcester Polytechnic Institute, receiving the degree of B.S. in E.E. in 1933. He was associated with the General Electric Company from 1935 to 1938, at the Radio Receiver Engineering Department at Bridgeport, Conn. In 1938 he joined Radiomarine Corporation of America at New York, N. Y., where he was concerned with the design and development of marine radio apparatus, in the capacity of Supervisory Engineer. At the end of the war he became active in the development of commercial marine radar

equipment. He was a Senior Member of the Institute of Radio Engineers. Mr. Spaulding was killed in the tragic airline crash at Washington, D.C., November 1, 1949.

ALFRED H. TURNER received the B.S. degree in Electrical Engineering from the University of Delaware in 1925. From 1925 to 1927 he was employed in the general engineering laboratory of the General Electric Company to study long and short wave radio propagation. From 1927 to date he has been employed by the Victor Talking Machine Company and the Radio Corporation of America. Since 1930 Mr. Turner has been engaged in work on ultra-high-frequency and microwave receivers and television receivers and terminal equipment.



JOHN C. TURNBULL received the B.S. degree from the Massachusetts Institute of Technology in 1934 and the Ph.D. degree in Physics from Brown University in 1938. From 1939 to 1941, he was engaged in research on glass problems for Glass Container Association. From 1942 to 1945, he was associated with the M.I.T. Radiation Laboratory and the Radio Research Laboratory in Cambridge, Mass. Since 1945, he has been with the Tube Department of the RCA Victor Division at Lancaster, Pa. engaged in glass technology. Dr. Turnbull is a member of the American Ceramic Society and the American

Physical Society.

RCA REVIEW

a technical journal

RADIO AND ELECTRONICS
RESEARCH • ENGINEERING

INDEX — Volume X, 1949

TABLE OF CONTENTS

March

	Page
"Some Novel Circuits for the Three-Terminal Semiconductor Amplifier," W. M. Webster, E. Eberhard, and L. E. Barton.....	5
"Standardization of the Transient Response of Television Transmitters," R. D. Kell and G. L. Fredendall.....	17
"Phase and Amplitude Equalizer for Television Use," E. Dudley Goodale and Ralph C. Kennedy.....	35
"Development of a Large Metal Kinescope for Television," H. P. Steier, J. Kelar, C. T. Lattimer and R. D. Faulkner.....	43
"The Graphophon—A Picture Storage Tube," L. Pensak.....	50
"Certain Aspects of Triode Reactance-Tube Performance for Frequency Modulation at Ultra-High Frequencies," C. L. Cuccia.....	74
"Ultrafax," Donald S. Bond and Vernon J. Duke.....	99
"Thyratrons in Radar Modulator Service," H. H. Wittenberg.....	116
"Some Characteristics of Diodes with Oxide-Coated Cathodes," W. R. Ferris.....	134

June

"Method of Multiple Operation of Transmitter Tubes Particularly Adapted for Television Transmission in the Ultra-High-Frequency Band," G. H. Brown, W. C. Morrison, W. L. Behrend and J. G. Reddeck.....	161
"A Record Changer and Record of Complementary Design," B. R. Carson, A. D. Burt and H. I. Reiskind.....	173
"Development and Performance of Television Camera Tubes," R. B. Janes, R. E. Johnson and R. S. Moore.....	191
"Reversible-Beam Antenna for Twelve-Channel Television Reception," O. M. Woodward, Jr.	224
"Tracing Distortion in Phonograph Records," M. S. Corrington.....	241
"Analysis by the Two-Frequency Intermodulation Method of Tracing Distortion Encountered in Phonograph Reproduction," H. E. Roys.....	254
"The Electron Coupler—A Developmental Tube for Amplitude Modulation and Power Control at Ultra-High Frequencies," C. L. Cuccia.....	270
"Video Announcer," E. P. Bertero.....	304

September

"Pencil-Type UHF Triodes," G. M. Rose, D. W. Power and W. A. Harris....	321
"Directional Microphone," H. F. Olson and J. Preston.....	339
"Mechanical Filters for Radio Frequencies," W. van B. Roberts and L. L. Burns, Jr.	348
"The Image Isocon—An Experimental Television Pickup Tube Based on the Scattering of Low Velocity Electrons," P. K. Welmer.....	366
"The Use of Ferrite-Cored Coils as Converters, Amplifiers, and Oscillators," V. D. Landon.....	387
"Transient Response of Filters," M. S. Corrington.....	397
"An Improved Method of Testing for Residual Gas in Electron Tubes and Vacuum Systems," E. W. Herold.....	430
"Low Reflection Films on Glass by an Improved Chemical Method," F. H. Nicoll.....	440
"A Network Bisection Theorem," V. D. Landon.....	448

December

	Page
"Counter Circuits Using Transistors," E. Eberhard, R. O. Endres and R. P. Moore	459
"Artificial Lines for Video Distribution and Delay," A. H. Turner	477
"Duo-Cone Loud Speaker," H. F. Olson, J. Preston and D. H. Cunningham ..	490
"A Six-Megacycle Compatible High-Definition Color Television System	504
"Photomultipliers for Scintillation Counting," G. A. Morton	525
"Direct-Reading Electronic Timer," R. R. Freas	554
"A New Direct-Reading Loran Indicator for Marine Service," F. E. Spaulding, Jr. and R. L. Rod	567
"A New Image Orthicon," R. B. Janes, R. E. Johnson and R. R. Handel	586
"The Evaluation of Chromium-Iron Alloys for Metal Kinescope Cones," A. S. Rose and J. C. Turnbull	593
"The Provisional Frequency Board," P. F. Siling	600

INDEX, VOLUME X

	Issue	Page
"Analysis by the Two-Frequency Intermodulation Method of Tracing Distortion Encountered in Phonograph Reproduction," H. E. Roys	June	254
"Artificial Lines for Video Distribution and Delay," A. H. Turner ..	Dec.	477
"Certain Aspects of Triode Reactance-Tube Performance for Frequency Modulation at Ultra-High Frequencies," C. L. Cuccia ..	Mar.	74
"Counter Circuits Using Transistors," E. Eberhard, R. O. Endres and R. P. Moore	Dec.	459
"Development and Performance of Television Camera Tubes," R. B. Janes, R. E. Johnson and R. S. Moore	June	191
"Development of a Large Metal Kinescope for Television," H. P. Steier, J. Kelar, C. T. Lattimer and R. D. Faulkner	Mar.	43
"Directional Microphone," H. F. Olson and J. Preston	Sept.	339
"Direct-Reading Electronic Timer," R. R. Freas	Dec.	554
"Duo-Cone Loud Speaker," H. F. Olson, J. Preston and D. H. Cunningham	Dec.	490
"The Electron Coupler—A Developmental Tube for Amplitude Modulation and Power Control at Ultra-High Frequencies," C. L. Cuccia	June	270
"The Evaluation of Chromium-Iron Alloys for Metal Kinescope Cones," A. S. Rose and J. C. Turnbull	Dec.	593
"The Graphicon—A Picture Storage Tube," L. Pensak	Mar.	59
"The Image Isocon—An Experimental Television Pickup Tube Based on the Scattering of Low Velocity Electrons," P. K. Weimer	Sept.	366
"An Improved Method of Testing for Residual Gas in Electron Tubes and Vacuum Systems," E. W. Herold	Sept.	430
"Low Reflection Films on Glass by an Improved Chemical Method," F. H. Nicoll	Sept.	440
"Mechanical Filters for Radio Frequencies," W. van B. Roberts and L. L. Burns, Jr.	Sept.	348
"Method of Multiple Operation of Transmitter Tubes Particularly Adapted for Television Transmission in the Ultra-High Frequency Band," G. H. Brown, W. C. Morrison, W. L. Behrend and J. G. Reddeck	June	161
"A Network Bisection Theorem," V. D. Landon	Sept.	448
"A New Direct Reading Loran Indicator for Marine Service," F. E. Spaulding, Jr. and R. L. Rod	Dec.	567
"A New Image Orthicon," R. B. Janes, R. E. Johnson and R. R. Handel	Dec.	586
"Pencil-Type UHF Triodes," G. M. Rose, D. W. Power and W. A. Harris	Sept.	321
"Phase and Amplitude Equalizer for Television Use," E. Dudley Goodale and R. C. Kennedy	Mar.	35
"Photomultipliers for Scintillation Counting," G. A. Morton	Dec.	525
"The Provisional Frequency Board," P. F. Siling	Dec.	600
"A Record Changer and Record of Complementary Design," B. R. Carson, A. D. Burt and H. I. Reiskind	June	173

	Issue	Page
"Reversible-Beam Antenna for Twelve-Channel Television Reception," O. M. Woodward, Jr.....	June	224
"A Six-Megacycle Compatible High-Definition Color Television System"	Dec.	504
"Some Characteristics of Diodes with Oxide-Coated Cathodes," W. R. Ferris	Mar.	134
"Some Novel Circuits for the Three-Terminal Semiconductor Amplifier," W. M. Webster, E. Eberhard and L. E. Barton.....	Mar.	5
"Standardization of the Transient Response of Television Transmitters," R. D. Kell and G. L. Fredendall.....	Mar.	17
"Thyratrons in Radar Modulator Service," H. H. Wittenberg....	Mar.	116
"Tracing Distortion in Phonograph Records," M. S. Corrington..	June	241
"Transient Response of Filters," M. S. Corrington.....	Sept.	397
"Ultrafax," D. S. Bond and V. J. Duke.....	Mar.	99
"The Use of Ferrite-Cored Coils as Converters, Amplifiers and Oscillators," V. D. Landon.....	Sept.	387
"Video Announcer," E. P. Bertero.....	June	304

AUTHORS, VOLUME X

	Issue	Page
Barton, L. E. (Coauthor)—"Some Novel Circuits for the Three-Terminal Semiconductor Amplifier"	Mar.	5
Behrend, W. L. (Coauthor)—"Method of Multiple Operation of Transmitter Tubes Particularly Adapted for Television Transmission in the Ultra-High-Frequency Band".....	June	161
Bertero, E. P.—"Video Announcer".....	June	304
Bond, D. S. (Coauthor)—"Ultrafax"	Mar.	99
Brown, G. H. (Coauthor)—"Method of Multiple Operation of Transmitter Tubes Particularly Adapted for Television Transmission in the Ultra-High-Frequency Band"	June	161
Burns, L. L., Jr. (Coauthor)—"Mechanical Filters for Radio Frequencies"	Sept.	348
Burt, A. D. (Coauthor)—"A Record Changer and Record of Complementary Design"	June	173
Carson, B. R. (Coauthor)—"A Record Changer and Record of Complementary Design"	June	173
Corrington, M. S.—"Tracing Distortion in Phonograph Records" ..	June	241
"Transient Response of Filters"	Sept.	397
Cuccia, C. L.—"Certain Aspects of Triode Reactance-Tube Performance for Frequency Modulation at Ultra-High Frequencies"....	Mar.	74
"The Electron Coupler—A Developmental Tube for Amplitude Modulation and Power Control at Ultra-High Frequencies"....	June	270
Cunningham, D. H. (Coauthor)—"Duo-Cone Loud Speaker".....	Dec.	490
Duke, V. J. (Coauthor)—"Ultrafax"	Mar.	99
Eberhard, E. (Coauthor)—"Some Novel Circuits for the Three-Terminal Semiconductor Amplifier"	Mar.	5
(Coauthor)—"Counter Circuits Using Transistors".....	Dec.	459
Endres, R. O. (Coauthor)—"Counter Circuits Using Transistors" ..	Dec.	459
Faulkner, R. D. (Coauthor)—"Development of a Large Metal Kinescope for Television"	Mar.	43
Ferris, W. R.—"Some Characteristics of Diodes with Oxide-Coated Cathodes"	Mar.	134
Freas, R. R.—"Direct-Reading Electronic Timer".....	Dec.	554
Fredendall, G. L. (Coauthor)—"Standardization of the Transient Response of Television Transmitters".....	Mar.	17
Goodale, E. D. (Coauthor)—"Phase and Amplitude Equalizer for Television Use"	Mar.	35
Handel, R. R. (Coauthor)—"A New Image Orthicon".....	Dec.	586
Harris, W. A. (Coauthor)—"Pencil-Type UHF Triodes".....	Sept.	321
Herold, E. W.—"An Improved Method of Testing for Residual Gas in Electron Tubes and Vacuum Systems.....	Sept.	430
Janes, R. B. (Coauthor)—"Development and Performance of Television Camera Tubes"	June	191
(Coauthor)—"A New Image Orthicon".....	Dec.	586
Johnson, R. E. (Coauthor)—"Development and Performance of Television Camera Tubes"	June	191
(Coauthor)—"A New Image Orthicon".....	Dec.	586

	Issue	Page
Kelar, J. (Coauthor)—"Development of a Large Metal Kinescope for Television"	Mar.	43
Kell, R. D. (Coauthor)—"Standardization of the Transient Response of Television Transmitters"	Mar.	17
Kennedy, R. C. (Coauthor)—"Phase and Amplitude Equalizer for Television Use"	Mar.	35
Landon, V. D.—"A Network Bisection Theorem"	Sept.	448
"The Use of Ferrite-Cored Coils as Converters, Amplifiers, and Oscillators"	Sept.	387
Lattimer, C. T. (Coauthor)—"Development of a Large Metal Kinescope for Television"	Mar.	43
Moore, R. S. (Coauthor)—"Development and Performance of Television Camera Tubes"	June	191
Moore, R. P. (Coauthor)—"Counter Circuits Using Transistors"	Dec.	459
Morrison, W. C. (Coauthor)—"Method of Multiple Operation of Transmitter Tubes Particularly Adapted for Television Transmission in the Ultra-High-Frequency Band"	June	161
Morton, G. A.—"Photomultipliers for Scintillation Counting"	Dec.	525
Nicoll, F. H.—"Low Reflection Films on Glass by an Improved Chemical Method"	Sept.	440
Olson, H. F. (Coauthor)—"Directional Microphone"	Sept.	339
(Coauthor)—"Duo-Cone Loud Speaker"	Dec.	490
Pensak, L.—"The Graphochon—A Picture Storage Tube"	Mar.	59
Power, D. W. (Coauthor)—"Pencil-Type UHF Triodes"	Sept.	321
Preston, J. (Coauthor)—"Directional Microphone"	Sept.	339
(Coauthor)—"Duo-Cone Loud Speaker"	Dec.	490
Reddeck, J. G. (Coauthor)—"Method of Multiple Operation of Transmitter Tubes Particularly Adapted for Television Transmission in the Ultra-High-Frequency Band"	June	161
Reiskind, H. I. (Coauthor)—"A Record Changer and Record of Complementary Design"	June	173
Roberts, W. v. B. (Coauthor)—"Mechanical Filters for Radio Frequencies"	Sept.	348
Rod, R. L. (Coauthor)—"A New Direct-Reading Loran Indicator for Marine Service"	Dec.	567
Rose, A. S. (Coauthor)—"The Evaluation of Chromium-Iron Alloys for Metal Kinescope Cones"	Dec.	593
Rose, G. M. (Coauthor)—"Pencil-Type UHF Triodes"	Sept.	321
Roys, H. E.—"Analysis by the Two-Frequency Intermodulation Method of Tracing Distortion Encountered in Phonograph Reproduction"	June	254
Siling, P. F.—"The Provisional Frequency Board"	Dec.	600
Spaulding, F. E., Jr. (Coauthor)—"A New Direct-Reading Loran Indicator for Marine Service"	Dec.	567
Steier, H. P. (Coauthor) "Development of a Large Metal Kinescope for Television"	Mar.	43
Turnbull, J. C. (Coauthor)—"The Evaluation of Chromium-Iron Alloys for Metal Kinescope Cones"	Dec.	593
Turner, A. H.—"Artificial Lines for Video Distribution and Delay"	Dec.	477
Webster, W. M. (Coauthor)—"Some Novel Circuits for the Three-Terminal Semiconductor Amplifier"	Mar.	5
Weimer, P. K.—"The Image Isocon—An Experimental Television Pickup Tube Based on the Scattering of Low Velocity Electrons"	Sept.	366
Wittenberg, H. H.—"Thyratrons in Radar Modulator Service"	Mar.	116
Woodward, O. M.—"Reversible-Beam Antenna for Twelve-Channel Television Reception"	June	224